TECHNICAL BULLETIN

Vol. 2

ECONOMIC COMMISSION FOR ASIA AND THE FAR EAST COMMITTEE FOR CO-ORDINATION OF JOINT PROSPECTING FOR MINERAL RESOURCES IN ASIAN OFFSHORE AREAS

May, 1 9 6 9

The authors of the papers alone are responsible for the statements and opinions contained in their respective papers. All communications relating to this Bulletin should be addressed to the Editor-in-Chief, Technical Bulletin of CCOP. c/o Geological Survey of Japan.

Geological Survey of Japan
Address:
135, Hisamoto-cho, Kawasaki-shi, Japan
Cable: GEOLSURV TOKYO
Printed by the Geological Survey of Japan,
as a contribution to the work of the Committee.

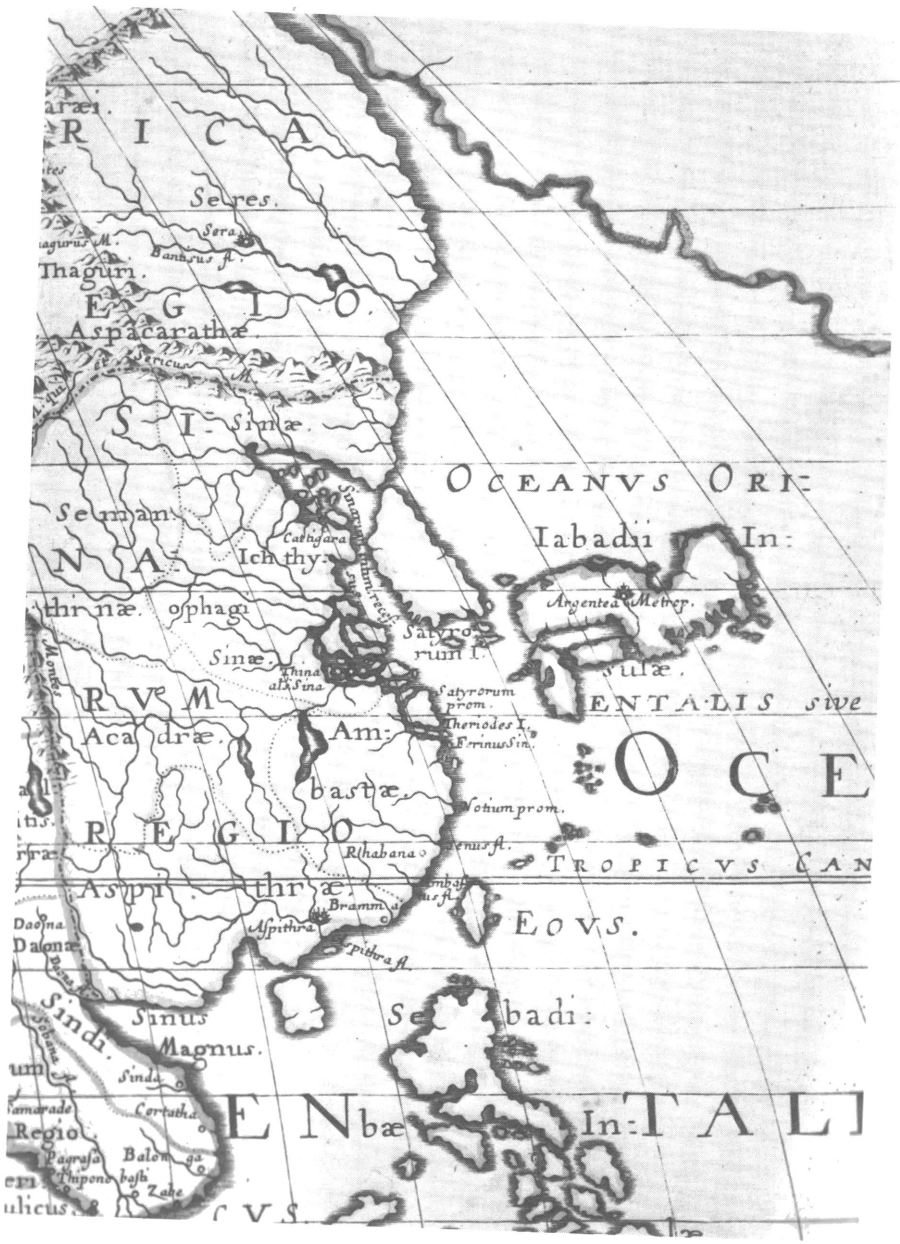

By the kindness of Dr. K. O. Emery

TECHNICAL BULLETIN

Vol. 2

ECONOMIC COMMISSION FOR ASIA AND THE FAR EAST COMMITTEE FOR CO-ORDINATION OF JOINT PROSPECTING FOR MINERAL RESOURCES IN ASIAN OFFSHORE AREAS

May, 1 9 6 9

ECONOMIC COMMISSION FOR ASIA AND THE FAR EAST

COMMITTEE FOR CO-ORDINATION OF JOINT PROSPECTING FOR MINERAL RESOURCES IN ASIAN OFFSHORE AREAS (C.C.O.P.)

TECHNICAL BULLETIN Vol. 2

This second issue of C.C.O.P.'s technical bulletins was printed by the Geological Survey of Japan, as a contribution to the work of the Committee.

PREFACE

The Committee for Co-ordination of Joint Prospecting for Mineral Resources in Asian Offshore Areas (referred to briefly as the Co-ordinating Committee for Offshore Prospecting, and abbreviated to CCOP) is an inter-governmental body established under the sponsorship of the United Nations Economic Commission for Asia and the Far East (ECAFE). The steps leading to its establishment are outlined in the reports of its first session (paragraphs 1–5) and second session (paragraphs 1,2); its terms of reference are contained in appendix 11 of the report of its first session.

At the eighteenth session of the ECAFE Committee on Industry and Natural Resources, held at Bangkok in February 1966, the Governments of the Republic of China, Japan, the Republic of Korea and the Philippines affirmed their readiness to join in the establishment of the Co-ordinating Committee. At the invitation of the Government of the Philippines, the first session of CCOP, attended by representatives of the Governments of those countries, and professional staff of the ECAFE secretariat, was held at the University of the Philippines, Quezon City, from 27 May to 2 June 1966.

Since that time, four more sessions of CCOP have been held (second session at Tokyo, 29 October to 7 Nobember 1966; third at Seoul, 24 June to 4 July 1967; fourth at Taipei, 6 to 16 November 1967; fifth at Tokyo, 10–19 June 1968), together with meetings of its Technical Advisory Group at each of these sessions; the sixth session of CCOP is planned to be held at Bangkok from 13–27 May 1969. At its fourth session, the Governments of Thailand and the Republic of Viet-Nam were welcomed to the Committee as full members and Malaysia was represented by an observer. At the fifth session, both Indonesia and Malaysia were represented by observers and, at meetings sponsored by ECAFE since that time, both Cambodia and Malaysia have signified their intention to join CCOP as full members.

During the course of these meetings the Committee decided that technical studies relating to marine geology and offshore prospecting for mineral resources, particularly in the offshore areas of the member countries of CCOP, should be published in a special series of Technical Bulletins, separately from the reports of the Committee's sessions. The Committee was pleased to accept the offer of the Government of Japan to print one number of the Technical Bulletin annually; this second volume of the series, also printed by the Geological Survey of Japan, contains papers and documents that were recommended to be included in Technical Bulletin, volume 2, at the fifth session of CCOP, together with others subsequently submitted.

The Technical Bulletins and the printed reports of the sessions of CCOP, including technical documentation, are distributed to the appropriate organizations and authorities concerned in the member countries of CCOP. Enquiries as to their availability to institutions and organizations in other countries may be directed to: The Technical Secretariat of CCOP, United Nations ECAFE, Sala Santitham, Bangkok–2, Thailand.

FOREWORD

Scientific investigation of the oceans is now very actively pursued by many countries of the world and the activities of CCOP is one of the most significant as the basis for the economic development of the ECAFE region.

The first volume of the Technical Bulletin was published last year and it is a great pleasure to be able to present the second volume. This volume includes the results of the scientific work carried out during the last year and I deeply appreciate the authors of the articles, members of the ECAFE Secretariat, and all the personnel concerned whose efforts contributed to the publication of this Bulletin.

Konosuke Sato
Director,
Geological Survey of Japan

PREFACE

It is our great pleasure to be able to see the second volume of this Technical Bulletin in time of the sixth session of CCOP at Bangkok. I believe that all the scientists who sent their manuscripts for this publication have made great contributions in spite of the change of dead line for acceptance of manuscripts, whom I would like to express our best thanks for their kind co-operations on behalf of the co-editors in member countries concerned. And also same thanks are due to ECAFE technical advisors and to ECAFE secretariats for their valuable suggestions.

During the last one year since the fifth session of CCOP at Tokyo, many valuable scientific and technological investigations on offshore and marine fields related to earth science have been made in the ECAFE region and the countries of technical advisors concerned.

We are happy to know that some of these investigations have been included in this second volume. The contents of the first half of this volume are for geophysical papers, while the latter half are for mostly geological ones.

The dead line for the next issue-third volume of this issue-will be in the end of January 1970, so if all the contributors, who will give their drafts, could try to send them before this time, the editors will be obliged to them. Finally, on behalf of the co-editors, I would like to convey our gratitudes for the kindness of the Geological Survey of Japan for their good service for this printing.

February, 1969
Masami Hayakawa,
Editor-in-chief

CONTENTS

REGIONAL GRAVITY SURVEY OF LUZON ISLAND, PHILIPPINES

Prepared by
Bureau of Mines, Department of Agriculture and Natural Resources, the Philippines
(with two maps, in pocket on back cover)

Note: The text of this document (I&NR/R.83) has been included as No. 5 in Part 2 (Documentation) of the report of the fifth session of CCOP. The maps submitted with this document are enclosed in the pocket on the back cover of this publication; they consist of:

Plate 1. Simple Bouguer gravity map, Central Luzon, Philippines.

Plate 2. Simple Bouguer gravity map, Southern Luzon, Philippines.

Blank page

Page blanche

GEOLOGICAL STRUCTURE AND SOME WATER CHARACTERISTICS OF THE EAST CHINA SEA AND THE YELLOW SEA

By

K. O. Emery[1], Yoshikazu Hayashi[2], Thomas W. C. Hilde[3], Kazuo Kobayashi[2], Ja Hak Koo[4], C. Y. Meng[5], Hiroshi Niino[6], J. H. Osterhagen[3], L. M. Reynolds[3], John M. Wageman[3], C. S. Wang[7], and Sung Jin Yang[4].

ABSTRACT

A geophysical survey was conducted in the East China Sea and the Yellow Sea between 12 October and 29 November 1968 aboard R/V F. V. HUNT. Joint participation of scientists from the Republic of China, the Republic of Korea, and Japan with American scientists was provided through ECAFE (Committee for Co-Ordination of Joint Prospecting for Mineral Resources in Asian Offshore Areas). The survey covered a region that is about equal to the combined areas of Texas, Oklahoma, and New Mexico or of Southeast Asia (Vietnam, Laos, Cambodia, and Thailand).

During the cruise more than 12,000 line km of continuous seismic reflection profiles were run with a 30,000-joule sparker. A continuous geomagnetic profile was made simultaneously. At two-hour intervals the following oceanographic data were measured for surface waters: color, transparency, quantity of suspended sediment, temperature, salinity, direction and size of waves, direction and speed of surface winds. Some of the oceanographic observations were, of course, restricted to daylight hours, and some (suspended sediment and salinity) required later laboratory analyses. Preliminary analyses of data were made aboard ship, and charts of each kind of measurement were kept up-to-date in order to guide the planning. Final analyses, compilations, and illustrations were completed ashore in the United States.

Most important for offshore mineral (oil and gas) exploration are the geophysical results. These show that the region is underlain by a series of nearly parallel ridges, each of which has served as a dam to trap sediments that have been derived mostly from the large area of China that is drained by the Yellow and the Yangtze rivers. The northermost ridge consists of Precambrian igneous and metamorphic rocks that crop out along the Shantung Peninsula. Sediments from the Yellow River have been trapped in the Gulf of Pohai by this ridge. The next ridge consists of Mesozoic-to-Precambrian rocks that were uplifted during the Mesozoic as the Fukien-Reinan Massif that crosses the mouth of the present Yellow Sea. Within the Yellow Sea the massif trapped a volume of at least 200,000 cu. km

1) Woods Hole Oceanographic Institution, Woods Hole, Mass., U.S.A., Contribution No. 2300.
2) Japan Petroleum Development Corporation, Tokyo, Japan
3) Pacific Support Group, U.S. Naval Oceanographic Office, San Diego, California, U.S.A.
4) Geological Survey of Korea, Republic of Korea (South Korea).
5) Chinese Petroleum Corporation, Taipei, Republic of China (Taiwan).
6) Tokyo University of Fisheries, Tokyo, Japan
7) National Taiwan University, Taipei, Republic of China (Taiwan).

of sediments mostly of Neogene age. Next seaward is a ridge of igneous and folded sedimentary rock that is located near the edge of the continental shelf between Japan and Taiwan. This is the Taiwan-Sinzi Folded Zone. Landward of it are perhaps 1 million cu. km of sediments believed to be mostly Neogene in age, on the basis of seismic characteristics, outcrops and wells on land, and dredgings from the sea floor. Beyond the continental shelf the Ryukyu Ridge, composed of volcanic rocks and folded Neogene and older sedimentary strata, has dammed a belt of sediment in the Okinawa Trough. A smaller ridge probably of similar composition and origin half way down the eastern slope of the Ryukyu Ridge has trapped a similar belt of sediment whose surface is a broad terrace at depths of several thousand meters. A portion of this feature off Japan is known as the Tosa Terrace. Lastly, at the base of the slope from the Ryukyu Ridge is the Ryukyu Trench that contains zero to only a few hundred meters of sediment.

Sediments beneath the continental shelf and in the Yellow Sea are believed to have great potential as oil and gas reservoirs. An area several times larger than Taiwan lies north of that island with sediment thicknesses exceeding 2 km, and perhaps reaching the 9 km thickness that underlies Taiwan. Most of these sediments are believed to be Neogene in age, the same as the oil-producing strata on the island. Anticlines, faults, and unconformities were encountered in these strata during the survey, and the character of the seismic reflections indicate that both shales and sandstones are included. Neogene sediments in two large basins beneath the Yellow Sea are less than 2 km thick, but the shales probably have a higher content of organic matter than do those of the continental shelf owing to the high organic productivity that is permitted by the nutrients in the rivers that debouch into the sea.

The shallow sea floor between Japan and Taiwan appears to have great promise as a future oil province of the world, but detailed seismic studies are now required. Afterward, the final test must be made by offshore drilling.

황해와 동지나해의 지질구조 및 해수특성

케이. 오. 에머리(1), 요시가즈 하야시(2), 토마스 다부류. 시. 힐드 (3),
사스오 고바야시 (2), 구자학 (4), 시. 와이. 멩(5), 히토시 니노(6),
제이. 에취. 오스터하겐(3), 엘. 엠. 레이놀드 (3), 존 엠. 왜그만(3),
시. 에스. 왕 (7), 양승진(4)

요 약

동지나해와 황해에 대한 물리탐사가 1968년 10월 12일부터 11월 29일까지 조사선 "알 부이 에푸 부이 헌트"에 의하여 실시되었다.

에카페 (아시아 지역 천해저광물자원 공동탐사 조정위원회)를 통해서 한국 중국 미국 일본의 과학자들이 조사에 공동 참여 하였다.
조사면적은 텍사스 오크라호마 뉴멕시코를 합한 면적또는 동남아시아 (월남 라오스 캄보디아 타이랜드) 의 면적에 상당한다.
12,000 킬로메타 이상의 조사항해를 하는 동안 연속 탄성파반사법이 30,000 줄의 스파카로서 행해졌고 동시에 지자기 연속측정이 행해졌다. 그리고, 해양학적 자료로서 해수의 색 투명도 부유물의 양 해수온도, 염도 파도의 방향과 크기 풍향과 풍속등이 두시간마다 해수면에서 측정되었다.
해양학적 관측 중 몇가지는 낮에만 행해졌고 몇가지 (부유물과 염도)는 차후 실험실 분석이 요망된다.

자료의 일차적인 해석은 배에서 행해졌고 각종 측정도면은 기록을 세우기 위해서 지금까지 보관되었다.

최종적인 해석과 편집및 설명은 미국에서 완성되었다. 천해저광물(석유및 까스) 탐사를 위하여 가장 중요한 것은 지구 물리학적 결과이다.

이 물탐결과에 의하면 조사해역에는 몇줄기의 평행한 구능이 분포하는바, 이 구능들은 황화와 양자강에 의하여 중국의 광범한 지역으로부터 운반된 퇴적물을 집적하는 땅의 역활을 한다.

북쪽 구능은 상동반도에 연하여 노출한 선캠부리아기의 화성암및 변성암으로 되어있다. 황하로 부터의 퇴적물은 이 구능에 의하여 포하이만에 퇴적되었다. 다음구능은 황해입구를 횡단하는 독강-영남 저반대로 중생대에 상승한 중생대및 선캠부리아기에 걸친 암석으로 되어있다. 황해해역내에서 이 저반대는 적어도 200,000 입방 킬로메타의 신제3기 퇴적물을 집적하였다. 다음 바다쪽으로 일본과 대만사이의 대륙붕의 끝 부근에 위치한 화성암및 습곡퇴적암으로된 구능이 있다.

이것이 타이완-신지 습곡대이다. 여기서 육지쪽으로는 탄성파 특성과 육지에서의 노두및 시추공과 해저시료채취 결과에 근거하면 신제3기라 믿어지는 퇴적물이 1백만 입방킬로메타 가량존재한다.

대륙붕바깥쪽으로 멀어진 곳에는 화산암및 습곡된 제3기 및 고기의 퇴적암층으로 되어있는 류구 구능이 있어 오끼나와 해구에 퇴적암대를 집적케 하고 있다.

류규 구능의 동쪽사면 중간쯤에는 흡사한 성분과 근원으로 보이는 더 작은 구능이 유사한 퇴적암대를 집적케하고 있는바 이 퇴적암의 표면은 수천메타의 깊이에서 광범한 테러스로 되어있다.
일본 근해에서 이런 구조의 일부는 도사 테러스라고 알려져있다.
마지막으로 류규 구능의 경사의 저부는 류규 해구로서 O내지 수백메타의 퇴적물을 포함하고 있다.
대륙붕 하부와 황해에 있어서의 퇴적물은 석유및 까스 보유암으로서의 유망성을 많이 갖었다고 믿어진다.
대만 북쪽에는 2킬로메타 이상의 퇴적암 두께를 갖인 지역이 대만의 수배되는 면적에 걸쳐 분포하며 대만 하부에서는 퇴적암 두께가 9 킬로메타에 달할 것이다. 이 퇴적물의 대부분은 육지의 함유층과 같은 신제3기층이라 생각된다. 배사구조 간층및 부정합이 이번조사에서 확인되었으며 탄성파반사파의 특성은 이들 퇴적층이 셰일뿐 아니라 사암도 포함하고 있다는 것을 보여준다. 황해 해저의 두개의 커다란 분지의 퇴적물의 두께는 2킬로메타 이하이나 그 중 셰일은 바다로 유입되는 강물내의 영양분에 의한 유기물 생성능력때문에 대륙붕의 셰일보다 더 많은 유기물을 함유하고 있다.
일본 대만 사이의 얕은 해저는 미래의 세계유전으로서의 전망을 갖었으나 더 세밀한 탄성파적 연구가 요망된다. 차후에 최종적인 탐사는 해상 시추에 의하여 행해져야 한다.

(1) 우드 홀 해양연구소, 미국 마사츄세쓰주 우드 홀

(2) 일본 석유 개발회사, 일본 동경

(3) 미국 해군 해양연구소 태평양 지원반, 미국 캐리포니아주 산디아고

(4) 한국 국립 지질조사소, 대한민국 서울

(5) 중국 석유공사, 중화민국 대북

(6) 동경 수산대학교, 일본 동경

(7) 대만 국립대학교, 중화민국 대북시

東支那海海底の地質構造と，海水に見られるある種の特徴に就いて

摘　　要

東支那海海底の地球物理学的調査は1968年10月12日より同年11月29日の間R/V F.V. HUNTにより行なわれた．この調査にはE.C.A.F.E.の亜細亜海域沿岸海底鉱物資源協同調査委員会を経て中華民国・大韓民国・日本および北米合衆国の科学者が参加したがその調査海域は米国ならばテキサス・オクラホマ・ニューメキシコ州を併せたものか，亜細亜ならばベトナム・ラオス・カムボチャ・タイ国等を併せた広さに相当した．

航跡は12,000 kmにおよび30,000 Joule のスパーカーで反射記録が得られ，また地磁気の継続記録も得た．2時間間隔海洋表層の観測が行なわれた．水色，透明度，浮遊物質量，水温，塩分，波浪の強さと方向，海面風速および方向等であるがこのうちではもちろん昼間に限られる種類も後で研究室での調査が不可欠のものもある．予察的な調査要素の分析は調査進行の一指針として刻々船上で作られた．しかし完全な解析および実状は米国着後に示される予定である．沖合鉱物資源（主として石油および天然ガス）開発にとって地球物理学的調査の結果は重要である．今回の調査の結果この海底にはほとんど平行して発達した一連の海底隆起地形があって，そのそれぞれが，広大な支那大陸から楊子江・黄河等の流れにより運ばれてきた堆積物にとって堰堤の役割を演じて堆積が行なわれた如くである．

このうち最北の隆起は山東半島に沿う前カムブリア紀の変成岩と火成岩である．黄河によって勃海湾に運ばれたものはこの隆起部で捕捉された．次の隆起は黄海を通過する前カムブリア紀から中生代に至る地層で構成される地塊である．この地塊により少くとも 2,000,000 km^3 の堆積物が捕捉されこれは主として新第三紀層に属する．次の海洋側の隆起は火成岩および皺曲している水成岩よりなり台湾と日本とを結ぶ大陸棚の縁辺に沿うものでいわゆる台湾—嶼道皺曲帯に相当する．陸側にある堆積物は百万立方 km，これが新第三紀層に考えられるいわゆるスパーカーの連続記録による特徴，島嶼の露頭陸上および海底からの採取岩石の特徴によるものである．

大陸棚を離れると琉球隆起がある．琉球隆起は古生代，火成岩および皺曲した新第三紀の地層よりなり沖縄海淵中の堆積帯の堰堤を形成している．

琉球隆起の東側の斜面中途に琉球隆起に同一源の構成と考えられる小隆起があり，これによって一連の数千メートルの深さの広い深海段丘面を形成している堆積帯がある，この面は土佐深海段丘として知られているものの一部分と考えられる．最後に琉球隆起の斜面の基部は琉球海溝でありここには0～数百メートルの堆積物があるにすぎない．大陸棚下底と黄海下にある堆積物には石油および天然ガスが保留されている可能性が大きい．台湾島の広さに数倍する広い地域が台湾の北方に広がりそこでの堆積物の厚さは 2 km 以上に達していることが明らかであるが，恐らく台湾で知られている 9 km の厚さにも達するかも知れない．そしてこの堆積物は新第三紀層に属すると考えられている．台湾ではこの地層から石油を産出している．背斜軸，断層等が調査中にこの堆積層中で認められている．地球物理学的（地震反射波）の特徴から推してこの堆積物は頁岩ばかりでなく砂岩を包含している．

黄海海底の堆積物は 2 km 以内ではあるが，ここの頁岩は大陸棚のそれより高い有機物を含んでいるであろう．何故ならば河川が運んだ営養塩により有機質の高い生産があるからである．

台湾と日本との間に横たわる浅海底は将来一つの世界的な産油地域となるであろうと期待される．しかし更めて詳細な地震探査が必要である．最後に，沖合鑿井により最終的な試掘が望まれる．

黃海及中国東海地質構造及海水性質測勘

摘　　要

黃海及中國東海区之地球物理測勘举行於亨特號（R/V F. V. HUNT）研究船上，自1968年十月十二日起至同年十一月廿九日止，共計49日。此行経聯合國亜経會聯合探勘亜洲海底礦産資源協委會方面供中華民國，大韓民國，日本處美國科学家共同参加此頃海上探勘之工作，総計測勘面積，如以東南亜地区相比約相等越南柬埔寨及泰國三國面積之徳和。

本次海上測勘総航程一万二千公里長度中，進行聯續不停之反射震測剖面記録，係以三万 Joule 能力之火花爆震測儀施測者。同時，另一聯續性地磁剖面記録工作亦在進行。有関海洋学方面之各項記録，如近海面水之顔色，透光度，飄懸物含量，水温，塩份，海浪之方向及大小，近海面風之方向及速度等，皆每隔二小時観察一次，其中若干項僅能於日間観察，亦有若干項須戻抵岸後作試験，其初歩記録分析及解釋工作皆於航行中進行，孟対整計劃可有啓発及指導之作用。至於最後之詳細解釋，分析，編綴及製図等工作俟於不久将左美完成之。

海底礦産資源測勘（石油及天然気之探勘佔重要位置）最重要者即穫得地球物理測勘之結果。本次地探記録顕示最明者為本区内有数条幾相平行排列背梁之出現，每一背梁均形成一攔覇，将大部份来自中國大陸黃河及楊子江所携来之沉積物存積其内。本区最北之一背梁為前寒武紀及変質岩所組成，沿山東半島露出，黃河携帯之泥砂即被本背梁所阻，積於渤海湾之内。次一背梁為前寒武紀至中生代之岩石所組成，於中生代末期熱山運動擁起為福建一越南地塊，在本区内乃横跨今日之黃海出口位置。此地塊所形成之背梁乃阻聚至少二十万立方公里体積数量之沉積物於黃海中，年代多半應属新第三紀以後者。

更向海方向歷数，又為一由火成岩及経褶皺之沉積岩所構成之背梁，其位置乃接近本区大陸棚之辺縁，而介於日本及台湾之間。其向陸方向，或可有一百万立方公里体積之沉積物，依震測記録之性質，陸上所見之露頭，鑽井記録以及在海底所採獲之岩様等引証，其年代應當為新第三紀者。

大陸棚以外之琉球背梁，係由火成岩及経褶皺之新第三紀地層組成，応将其西北之沖繩海槽沉積物攔阻背内。另一小背梁或處前者同一組成，位置於琉球背梁向東坡之中途，形成一寛濶面積，日人称此地形特徵為「土佐台地」(Tosa Terrace)，向海之最後特徵為琉球海槽，係位置於琉球背梁東坡之底，最深処達7881公尺。該槽内，僅存留自零至数百公尺厚之之積物而已。

本区大陸棚下之沉積，経本次測勘認為儲集石油及天然気之可能性甚重，居台湾之東北方有面積較其本島達数倍之一處，沉積厚度在二千公尺以上，可能延至台湾達八，九千公尺者。該沉積大部份応属新第三紀，亦即台湾油気之生産地層。本次海上測勘期中曾見於地層剖面中有背斜，断層及不整合等対儲油有利之構造，且於震測反射記録中，応可分辨非僅属頁岩，砂岩更存在不少。黃海海底之両大盆地内之沉積厚度似少於二千公尺，但其頁岩中成可能含有机物質較大陸棚者為豊，因黃河及楊子江所携至海内之營養物較多，易使有机生産率増高也。

日本至台湾間之浅海底似可成為将来世界豊厚希望之産油区，但目前所急需進行者，為進一歩之詳細震測工作及研究，従之必在海上鑽井，以試意究也。

INTRODUCTION

In 1966 the United Nations Economic Commission for Asia and the Far East (ECAFE) set up a Committee for Co-ordination of Joint Prospecting for Mineral Resources in Asian Offshore Areas to aid in the reconnaissance exploration for potential mineral resources from the sea floor off eastern Asia. The initial members of this committee were Japan, the Republic of Korea, the Republic of China, and the Philippines. One of the first acts of the committee was to invite participation of representatives from the Federal Republic of Germany, France, United Kingdom, and the United States as members of a Technical Advisory Group. Meetings of the committee and of the Technical Advisory Group in Tokyo, Seoul, and Taipei indicated a great likelihood of stratigraphy and structure favorable for accumulations of oil and gas in the shallower parts of the East China Sea and vicinity. Evidence was based upon previous studies of about 330 sediment samples from the region (Niino and Emery, 1961), rock dredgings and extrapolation of structures known on land in Japan, Korea, and China (Emery and Niino, 1967), and preliminary results of an airborne geomagnetic survey made by the U.S. Naval Oceanographic Office's Project MAGNET in June 1968 as a United States' contribution to the ECAFE objectives.

The accumulated information indicated that thick Neogene strata, possibly oil-bearing, underlies the Ryukyu Ridge, the outer margin of the continental shelf between Japan and Taiwan, the central part of the Yellow Sea, and the Gulf of Pohai. Geophysical measurements were needed in order to estimate the thickness and attitude of the Neogene sediments and to infer the nature of underlying rocks. Although the airborne geomagnetic profiles provided some information, seismic data were considered more definitive. Several possible sources of ships and equipment were investigated; the most practical source was an offer for joint participation of ECAFE personnel in a study planned by the Pacific Support Group of the U.S. Naval Oceanographic Office to investigate the East China Sea using shipboard reflection seismic and geomagnetic methods. The ship was R/V F. V. HUNT, operated by the Marine Acoustical Services of Miami, Florida, under contract to the Navy's Military Sea Transportation Service and directed by the U.S. Naval Oceanographic Office. She is a 850-ton, 55-meter, dieselelectric converted cable-laying vessel (Fig. 1). The ample laboratory space in the original cable tank and her good sea-keeping ability are ideal for marine geophysical investigations.

Work in the East China Sea occurred during three separate cruise legs: Sasebo (Japan) to Sasebo—12 to 21 October; Sasebo to Chilung (Taiwan)—25 October to 11 November; and Chilung to Sasebo—16 to 29 November 1968. The total distance run was 12,200 km. During all three legs John M. Wageman was chief scientist, assisted by Thomas W. C. Hilde, L. M. Reynolds, and John H. Osterhagen. K. O. Emery served as ECAFE liason scientist. During each of the three legs two or three Asian scientists participated in the work: C. Y. Meng and C. S. Wang from China; Yoshikazu Hayashi, Kazuo Kobayashi, and Hiroshi Niino from Japan, and Ja Hak Koo and Sung Jin Yang from Korea. All contributed heavily to the success of the cruise and are listed in simple alphabetical order as authors of this report.

Appreciation is due Captain Samuel W. Shores and his officers and crew whose ability, good humor, and willingness to work insured the success of the cruise. Special thanks are due Ronald G. Roy, John A. Frank, and Edwin O. Danford for their contributions as electronics technicians and as watch standers. Measurements of chlorinity were made at Nagasaki University, Faculty of Fisheries.

METHODS

Several kinds of geophysical and oceanographic measurements were obtained during the cruise, with geophysical measurements recorded continuously and automatically, and oceanographic data collected at two-hour intervals.

Simplest of the geophysical measurements was bathymetry, measured from a crystal transducer that was towed alongside the ship and that acted as both transmitter and receiver. Echoes from the bottom are filtered (12 kHz), amplified, and recorded with a Gifft recorder on wet paper 49 cm wide. In some areas of acoustically transparent sediment the records revealed subbottom reflections.

A Varian proton precession magnetometer was towed about 200 meters astern in order to be free of the magnetic effects of the steelhulled ship. Results were recorded by ink pen on paper having a 25.5-cm width for 1000 gammas.

Continuous seismic reflection profiles were made with a Geotech (a Teledyne company) system. A condenser bank at 14 kv was discharged at 4-second intervals to release 30,000 joules between electrodes about 50 cm apart that were trailed 50 meters astern of the ship. The hydrophone receiver was a single streamer 50 meters long, containing 100 crystal detectors, and towed with its leading end 135 meters astern; thus the center of the receiving streamer was about 110 meters from the spark sound source. The echoes from bottom and subbottom reflectors were fed through band pass filters between 20 and 100 Hz, amplified, and recorded on a Raytheon unit having a 4-second sweep rate on spark-sensitive dry paper 49 cm wide. The results obtained at the standard cruising speed of 10 knots (18 km/hour) were excellent and far better than those at lower ship speeds.

Oceanographic observations consisted mainly of surface or nearsurface water characteristics. Surface water obtained in a plastic bucket provided temperature, a 100-m*l* sample for chlorinity and a 1000-m*l* sample for suspended sediment. The 1000-m*l* sample was filtered aboard ship through tared 0.45-micron millipore filters. Later, on shore, the filters were dried, weighed, and the concentrations of suspended sediment were calculated. For comparison with the concentration of suspended sediments, the color of the sea was measured during the daytime with standard Forel color vials, and the transparency was measured by Secchi disk at daytime stations where the ship lay stopped. At two-hour intervals the Beaufort wind force, the wind direction, and the height, length, and direction of the two or three distinct wave trains also was obtained visually.

Navigation was based upon RADAR when the ship was within range of the many steep islands off Korea, Japan, and along the Ryukyu Ridge. Positions farther from shore were controlled by LORAN A and star fixes. Positions are considered accurate within 3 km except in the northern part of the Yellow Sea and in Taiwan Strait where some of them may be as much as 6 km in error.

Running plots were kept on ship for all geophysical measurements and for oceanographic observations of the surface waters. These served as the bases for the drawings that accompany this report.

REGIONAL SETTING

This study covers a range of environments that have distinct differences in structure, rocks types, sediments, topography and water properties. The main objective was to

discover and describe the structure; however, a brief description of the region in terms of its other characteristics is desirable. For convenience, the region can be divided into three main topographic units that are nearly equal in area: the Yellow Sea, the continental shelf, and the trough, ridge, and trench province.

YELLOW SEA

The northernmost topographic unit of the region is the Yellow Sea and its adjacent Gulf of Pohai. The area of this unit northwest of a line between southeastern Korea, southeastern Cheju Island, and the south side of the Yangtze River (Fig. 2) is about 0.50 million sq. km. It is a flat region with depths that average about 55 meters and nowhere exceed 125 meters. The western side is bordered by the combined deltas of the Yellow and the Yangtze rivers plus the hilly projection of the Shantung Peninsula that separates the lowland areas through which the Yellow River has alternately debouched in historical time and earlier. The eastern side of the Yellow Sea is hilly and fringed by hundreds of small rocky islands, but lowlands border the mouths of the Han River of South Korea, the Yalu River of North Korea, and the Liao River of China (in the Gulf of Pohai).

Influence of the Yellow and Yangtze rivers extends far beyond the shorelines, so that a smooth gentle slope from the west (1:26,000) meets the steeper and less regular slope from the east (1:6,000) in an axial valley that borders the eastern third of the sea. Sediments as well as topography reflect the work of the rivers, for the eastern third of the Yellow Sea is floored by sands derived from the mountains of Korea, whereas the western two thirds has silt and clay brought by the Yellow and Yangtze rivers (Fig. 3). Echograms made during the survey show that the upper layers of sediment in many parts of the sea are transparent to sound from ordinary echo sounding at 12 kHz, as is typical of fine-grained sediments deposited in low energy environments. In several places along the eastern side large sand waves were discovered, and their steeper slopes suggest a general northward flow of bottom water.

Properties of the water in the Yellow Sea provide information about the sediment sources and the current systems. Temperature and chlorinity of the surface waters, measured during the survey, show that a tongue of warm high-chlorinity water flows northward along the eastern side of the Yellow Sea. It eventually turns southward and returns along the western side much diluted by river effluent as a cool lower-chlorinity current (Figs. 4, 5). Similar results have been found by other workers in other years (Ichiye, 1960; Asaoka and Moriyasu, 1966).

The Yellow River (*Hwang Ho*) takes its name from its load of reworked loess derived from northwestern China. This load plus that of the Yangtze River is distributed throughout the western half of the sea, imparting the color that is the origin of the name for the Yellow Sea (*Hwang Hai*). In terms of Forel standard colors, the water in the western half of the sea contains more than 30 per cent yellow. In contrast, the warm saline water that flows northward in the eastern half contains less than 20 per cent yellow except in shallow depths near shore (Fig. 6). The same concentrations of sediment that produce yellow color also reduce the transparency of the water in the western half to less than 10 meters for the Secchi disk, whereas the transparency in the eastern half is more than 10 meters (Fig. 7) except near shore. The results are similar to those obtained by Nishizawa and Inoue (1958), who used transparency meters in the southern part of the Yellow Sea.

Suspended sediment concentrations are more direct indicators of the influence of the

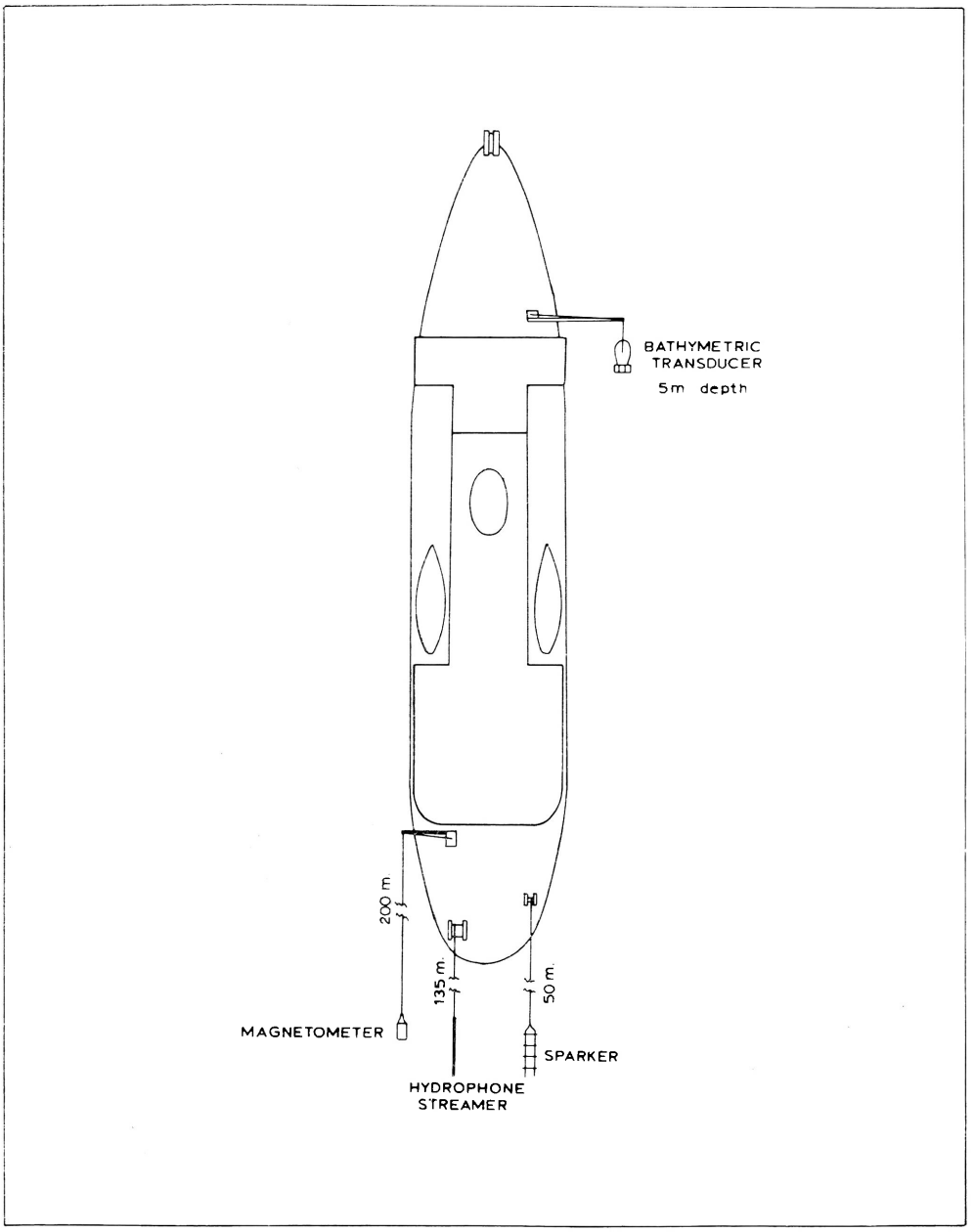

Figure 1. Sketch of R/V F. V. HUNT showing positions of towed sounding fish, spark electrodes, hydrophone streamer, and magnetometer.

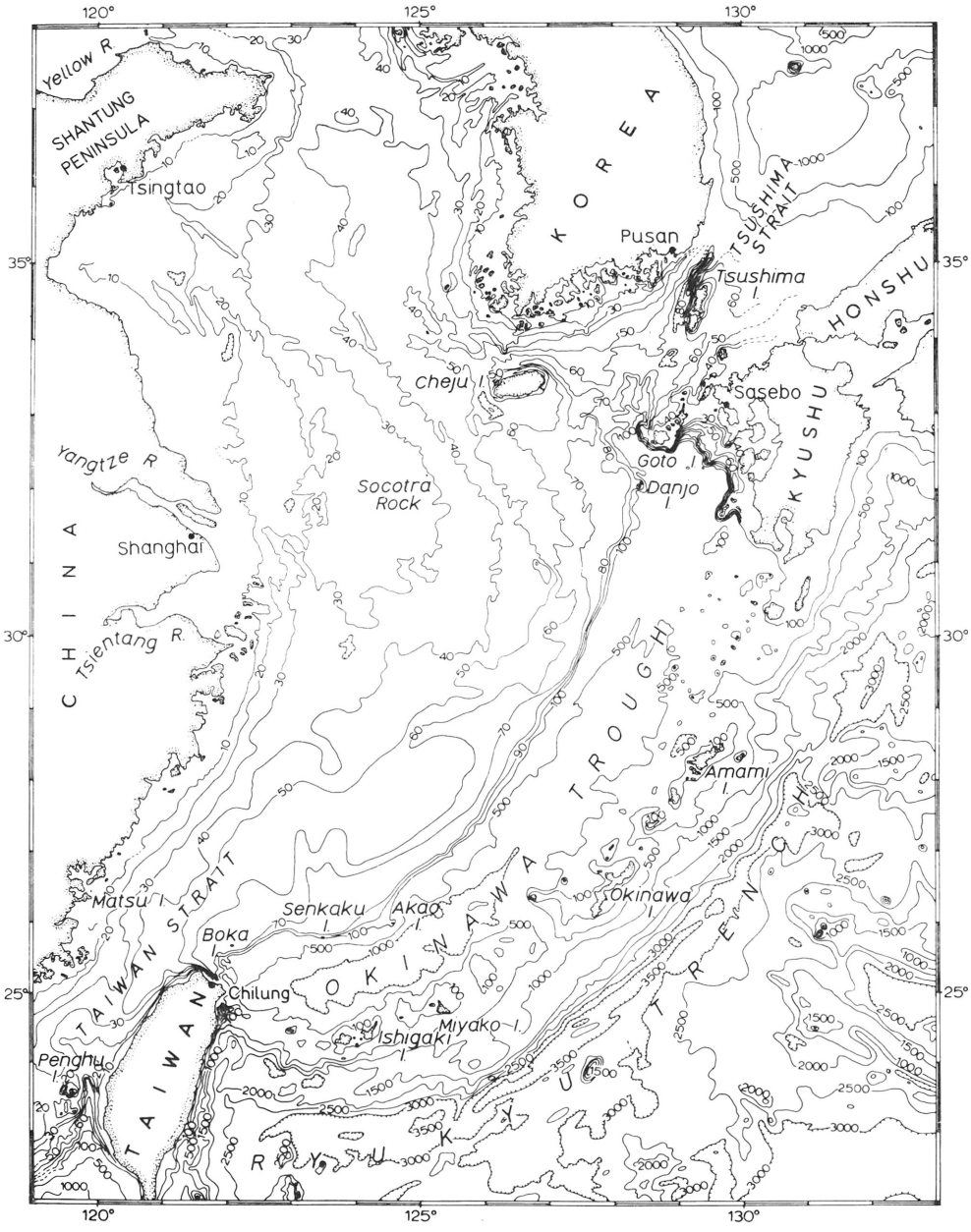

Figure 2. Topography of the region. The contours inshore of the Ryukyu Ridge are from a recent compilation by the U.S. Naval Oceanographic Office, and those seaward of the Ryukyu Ridge are from Scripps Institution of Oceanography. Note that the contours are in fathoms, whereas meters are used throughout the rest of this report.

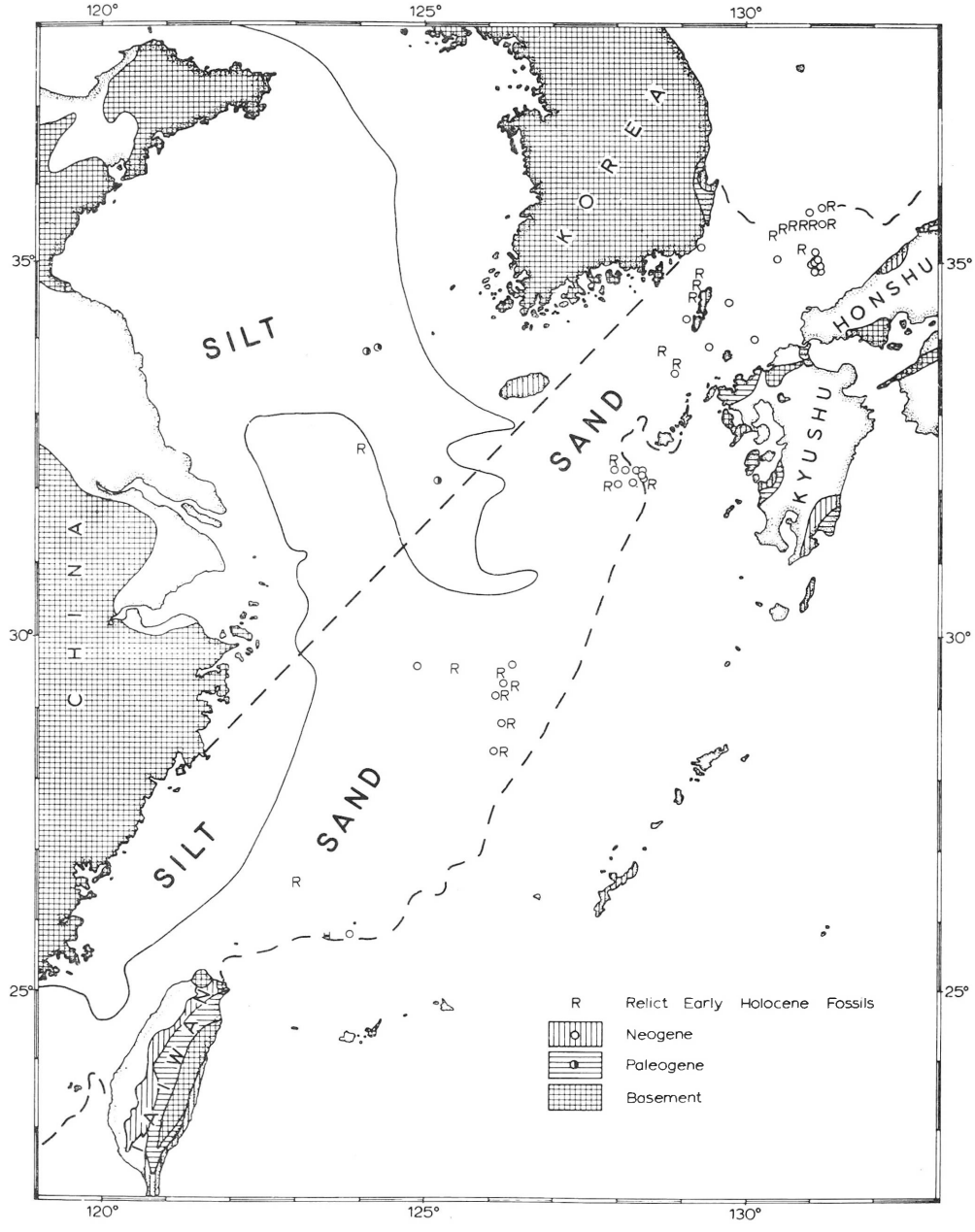

Figure 3. Generalized pattern of unconsolidated sediments (Niino and Emery, 1961; Wang, 1961), and positions of samples containing rock fragments identified by fossils or lithology as belonging to Paleogene or Neogene strata (Emery and Niino, 1967; Niino, 1968). Outcrops on land also are shown (Chinchang and Chang, 1953; Geol. Survey of Korea and Geol. Soc. of Korea, 1956; Geol. Soc. of Japan, 1964). Basement is shown in a rather generalized way to include areas having many small outcrops and presumbly only thinly overlain by Mesozoic and Cenozoic sediments.

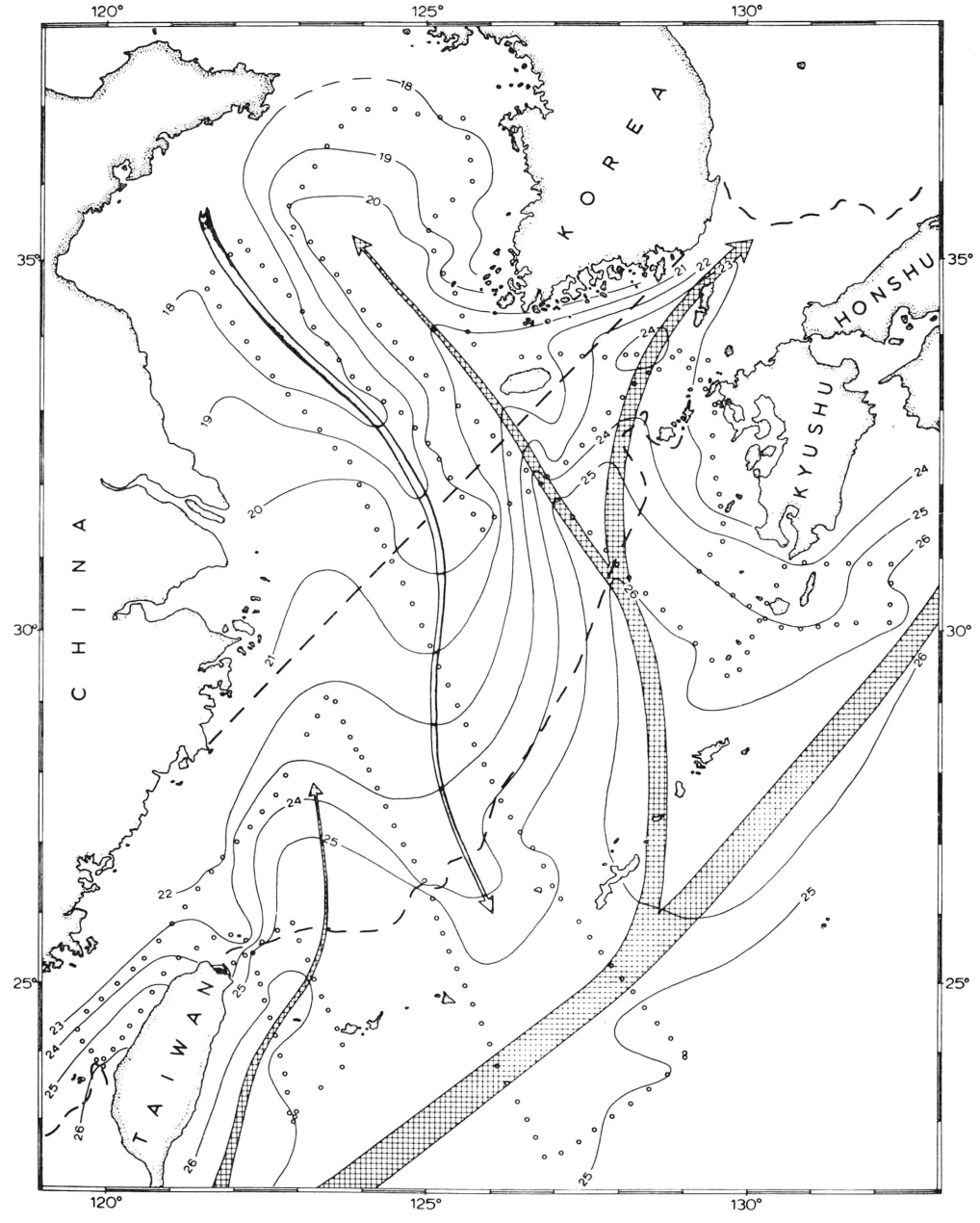

Figure 4. Temperature of surface water in the region, 12 October to 11 November 1968 in degrees Celsius. Temperatures between 16 and 29 November were about 2 degrees lower, but they exhibited the same areal pattern, in accordance with the trends described by Koizumi (1962). The cross-hatched arrows show the axes of flow of warm water brought into the area by the Kuroshio; the solid arrow shows the flow of cold water from the northern Yellow Sea.

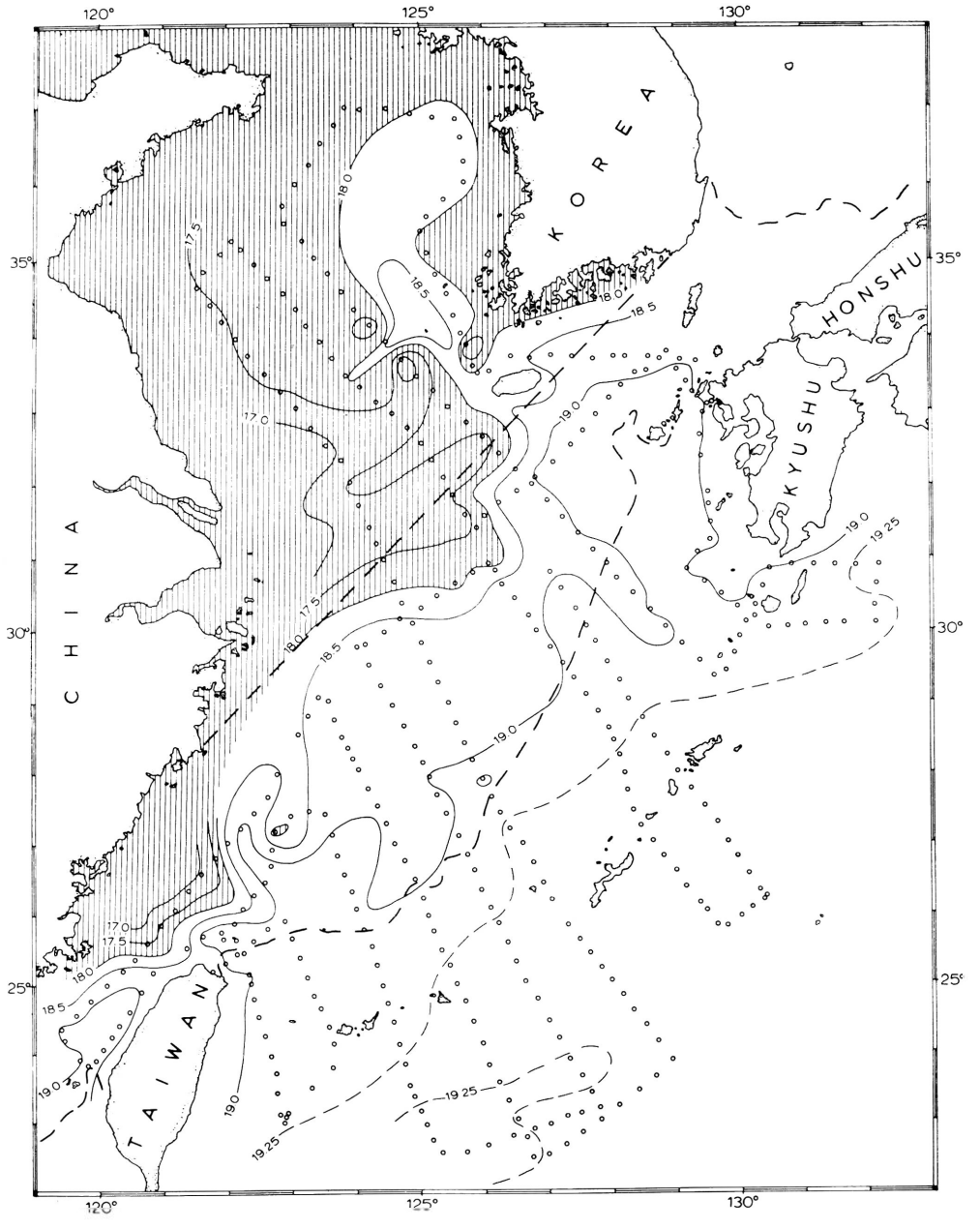

Figure 5. Chlorinity of surface water in the region, 12 October to 27 November 1968. Titrations were made by the Faculty of Fisheries, Nagasaki University, under the guidance of Haruhiko Irié.

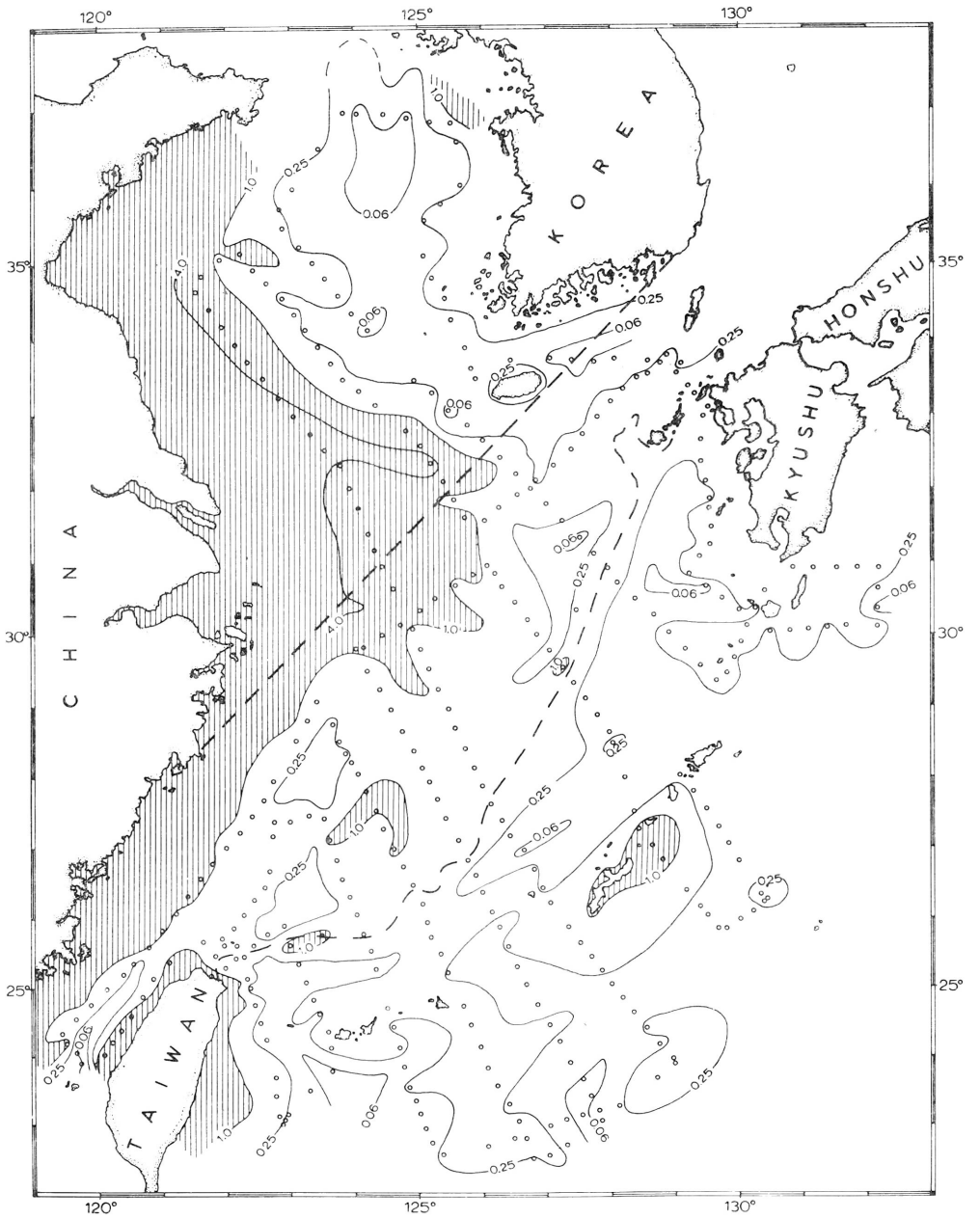

Figure 6. Color of surface water in the region in terms of percentage yellow by the Forel standard color vials, 12 October to 28 November 1968.

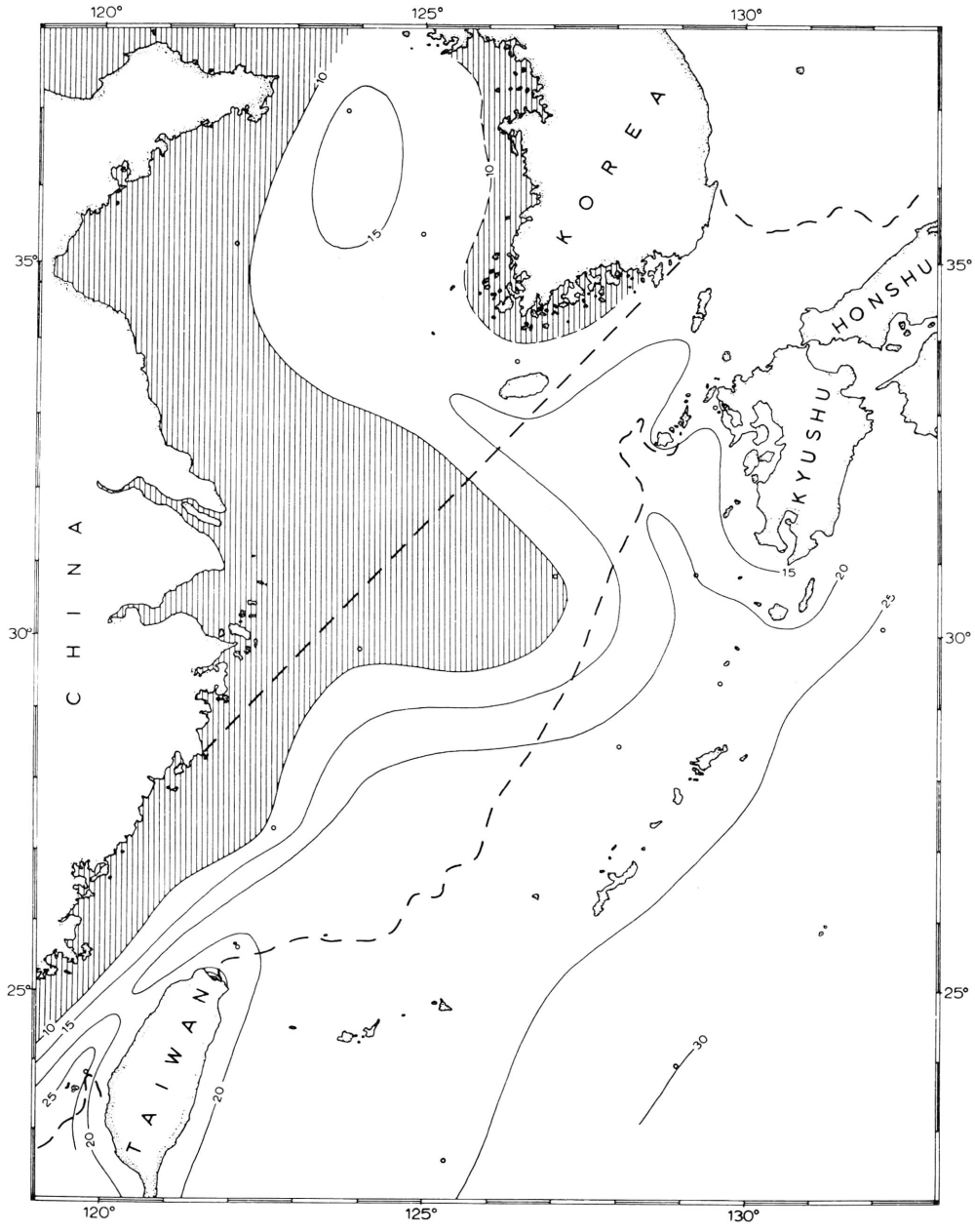

Figure 7. Transparency of the water in meters (depth at which a 30-cm Secchi disk is just visible), 12 October to 28 November 1968.

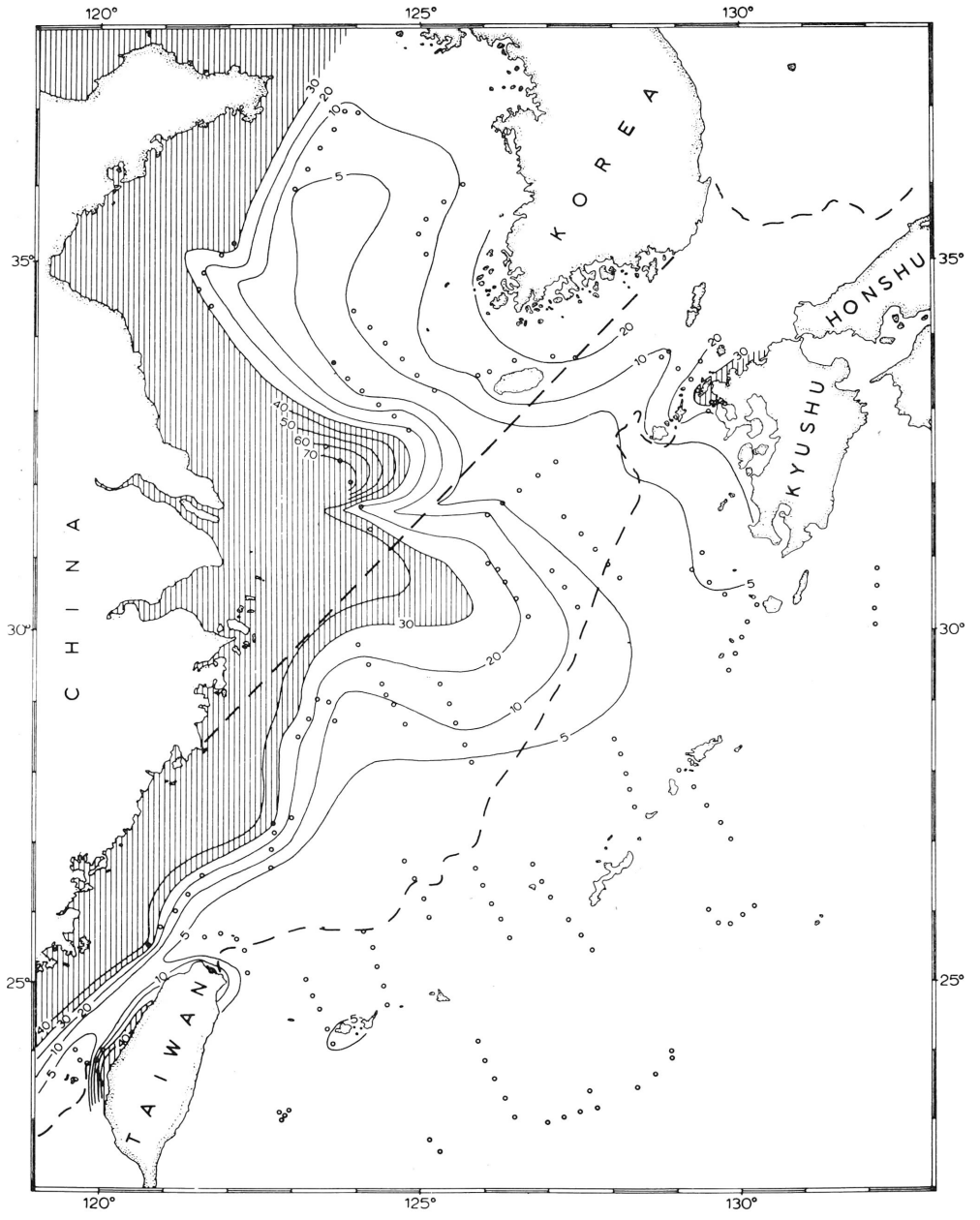

Figure 8. Concentrations of total suspended sediment (mg/*l*) in surface waters of the region, 12 October to 26 November 1968.

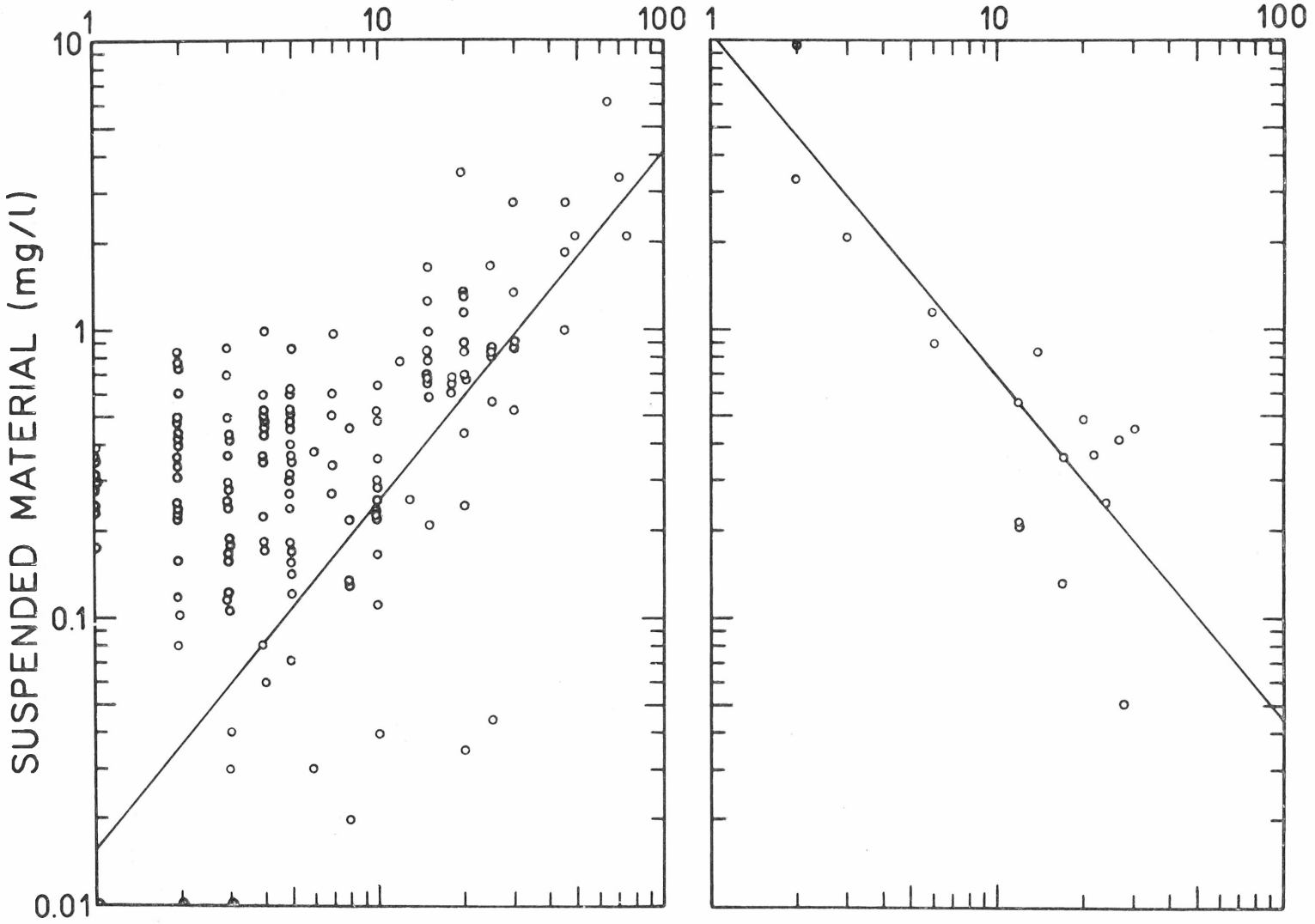

Figure 9. Relationships between concentration of suspended sediment and the color and transparency of the sea water. The diagonal lines in both graphs show correlations obtained for about 200 sets of similar measurements off the Atlantic coast of the United States (Manheim, Meade, and Bond, submitted for publication); the relationships are almost identical in the two areas.

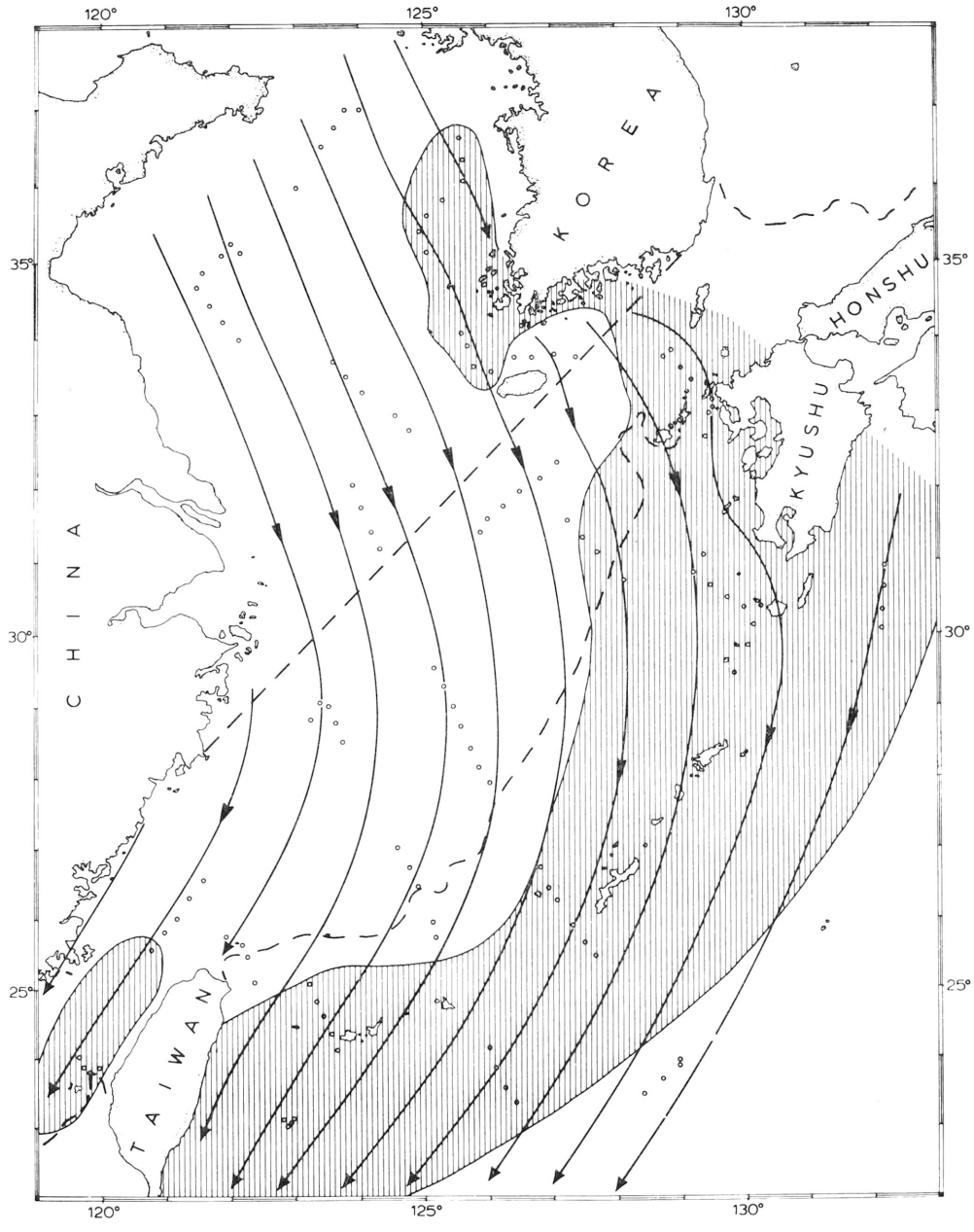

Figure 10. Wind streamlines and Beaufort wind forces observed 12 October to 11 November 1968. Effects of Typhoon Gloria are omitted. Winds between 15 and 29 November were more easterly. Areas of wind force more than 4 are cross-hatched.

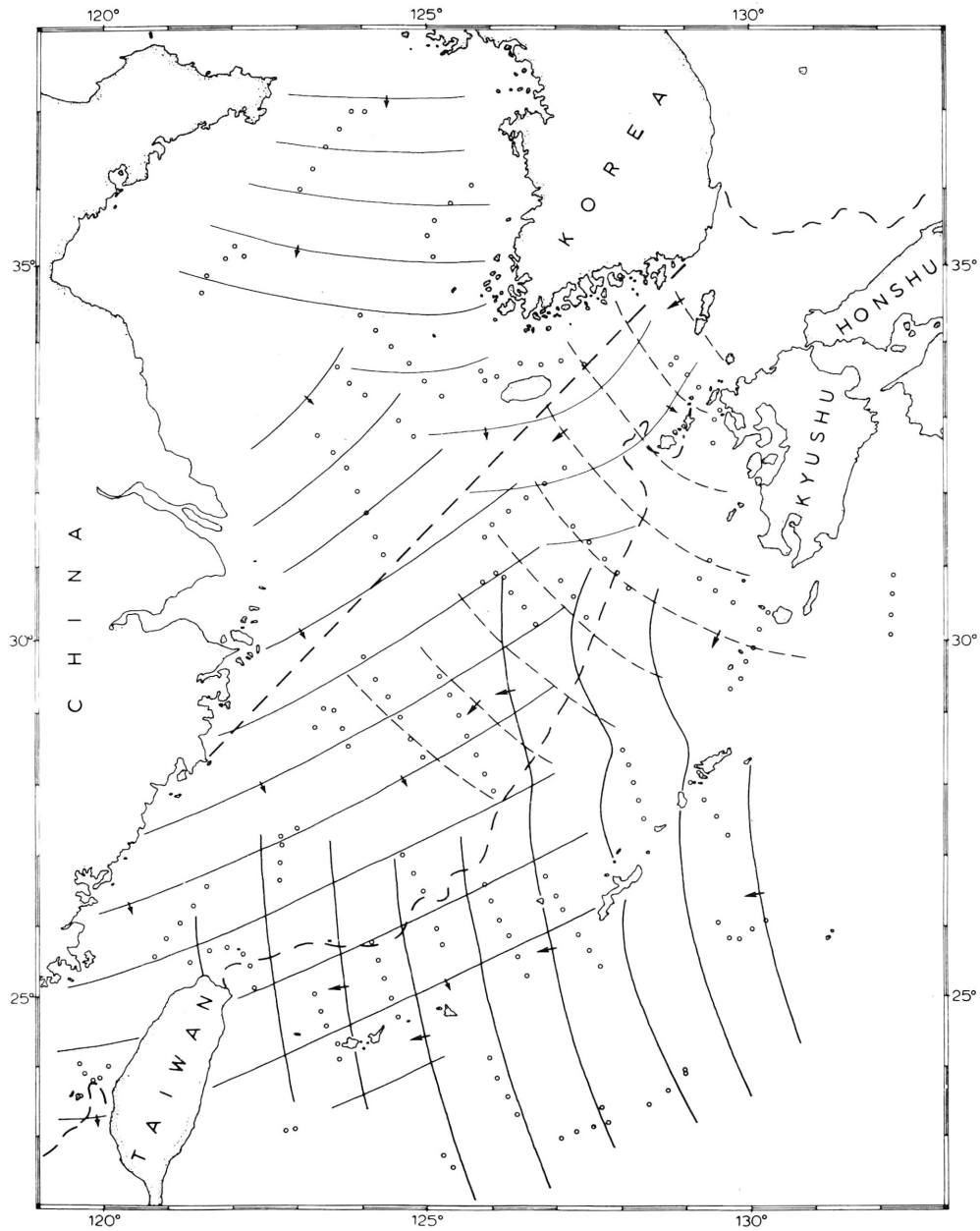

Figure 11. Generalized pattern of swells produced mainly in the northern Yellow Sea and Gulf of Pohai, in the Japan Sea, and in the open Pacific Ocean south of Japan, as observed between 12 October and 26 November 1968. Effects of Typhoon Gloria are omitted. Arrows show direction of movement of swells.

rivers, with more than 1 mg/*l* along the western half, and less than 0.1 mg/*l* for most of the eastern half (Figs. 8, 9). In comparison, the average concentration of suspended sediment in the Yangtze River is 0.8 gm/*l* and in the Yellow River, 45 gm/*l* (Holeman, 1968). Probably about 50 per cent of the suspended sediment in the Yellow Sea is detrital clay and silt; the rest is organic material derived from land areas or produced in the sea from nutrients contributed by the rivers. Such ratios are typical of waters off the Atlantic and Gulf coasts of the United States (Manheim and others, 1966; submitted for publication).

The general counterclockwise circulation of water in the Yellow Sea has long been known on the basis of the distribution of temperature and salinity, and it recently has been confirmed from the distribution of diatoms as well (Asaoka and Moriyasu, 1966). Winds over the Yellow Sea are of a general monsoon type, landward during the summer and seaward during the winter (McDonald, 1938; Tregear, 1965, pp. 15–17). The pattern during the cruise was typical of winter except during a few days (21 to 26 October) when the fringes of Typhoon Gloria intruded the area. Streamlines and Beaufort wind forces observed during daytimes of the rest of the cruise are shown by Figure 10. These winds produced waves and swells that moved throughout the sea (Fig. 11).

Rocks from outcrops that project through the sediments are not known from the central part of the Yellow Sea. Moreover, wells drilled to 960 meters depth in the Yellow River floodplain north of the Shantung Peninsula encountered only shallow-water deltaic sediments to their maximum depths (Niino and Emery, 1961; Tregear, 1965, p. 37). In contrast, notations of rocky bottom are shown on navigational charts in the nearshore regions of Korea, just south of Shantung Peninsula, and along the eastward projection of the peninsula. Rock outcrops also occur at the entrance of the Yellow Sea between Korea and the mouth of the Yangtze River. Several of the rocky areas rise above the ocean (Cheju Island) and others form shoals (Socotra Rock) of Tertiary volcanic rocks; other islands off the Yangtze River consist of Mesozoic volcanic rocks (Director Geol. Survey of India, 1959).

Continental Shelf

The second topographic unit of the region is the continental shelf. At the north the shelf takes the form of Tsushima Strait between Korea and Japan, a width of about 150 km (Fig. 2). The middle part of the shelf fronts the Yellow Sea, and the southern part borders the China mainland from the mouth of the Yangtze River to beyond the strait between Taiwan and the mainland. The outer edge of the shelf coincides approximately with the 120-meter contour. The maximum width of the shelf is off the Yangtze River where it reaches 450 km; farther soutwest the shelf narrows to about 125 km west of Taiwan. Within Figure 2 the area of the shelf is about 0.41 million sq. km.

Sediments of the continental shelf exhibit a simple pattern of silt and clay on the nearshore half and sand on the outer half (Fig. 3). The silt and clay forms a continuous belt that extends southwestward from the western part of the Yellow Sea; it clearly is a modern deposit carried from the Yangtze River and probably also the Yellow River by the inshore southwesterly-flowing current. Sands on the outer half of the shelf are calcareous (averaging about 30 per cent calcium carbonate) and they are iron stained, typical of relict sediments that have remained unburied on most continental shelves of the world since Pleistocene times of glacially lowered sea levels (Emery, 1968). Confirmation of the relict origin is provided by 27 bottom samples that contain the remains of land mammals, brackish-water mollusks, and shallow marine mollusks (Emery, Niino, and Marsters, in preparation). Radiocarbon dates for several samples range from 4,000 to 30,000 years.

Properties of the surface water are closely related to those of the two types of bottom sediment. The low temperature, low chlorinity, low transparency, and high percentage of yellow color and of suspended sediment (Figs. 4, 5, 6, 7, 8) denote the southwestward-flowing nearshore current. The northeastward-flowing warm saline clear water atop the outer part of the shelf marks the Kuroshio Current that continues out of the region and south of Japan, with a small branch extending through Tsushima Strait into the Japan Sea and another into the Yellow Sea. The high temperature, chlorinity, and transparency of the Kuroshio water favors the deposition of the calcareous shell and algal debris that is absent to rare below the nearshore current.

Rock projects above the sediments in the many islands near Japan and in a few others near the shelf edge farther southwest. Most of the islands consist of Tertiary and Pleistocene volcanic rocks that bury or are interbedded with mainly Neogene sedimentary strata. Dredgings from the continental shelf have recovered 34 samples consisting of Neogene sandstones and shales (Fig. 3). Fossils in most rocks from Tsushima Strait are shallow-water forms, whereas those from farther southwest indicate moderate depths of original accumulation. Additional geological data comes from coal mining operations at Nagasaki where seaward-dipping Paleogene coal beds have been mined to 5 km seaward of the shore (Yamamoto and others, 1967), and from deep oil borings at Taiwan that have penetrated more than 5,000 meters of Neogene strata (Schreiber, 1965; Meng, 1967, 1968). The pattern of stratigraphy and structure suggests that the seaward edge of the shelf may follow a belt of folded thick Neogene strata that extends from Japan to Taiwan, the Taiwan-Sinzi Folded Zone (Emery and Niino, 1967).

Trough, Ridge, and Trench Province

The third unit of the region includes the Okinawa Trough, the Ryukyu Ridge, and the Ryukyu Trench; these features also are known as the Nansei Shoto Trough, Ridge, and Trench. All of them extend in a seaward curving arc from Japan to Taiwan (Fig. 2), and their topography has been mapped and described by Hess (1948), Tayama (1952), Dietz (1954), Udintsev and others (1963), and Menard (1964). Their combined area within Figure 2 totals about 0.40 million sq. km.

The Okinawa Trough borders the continental shelf, and its western side is the continental slope. The deepest part, near Taiwan reaches 2270 meters, and its floor shoals northeastward toward Japan. Clearly, the trough is an area of deposition dammed by the Ryukyu Ridge in much the same manner that the Fukien-Reinan Massif dams the Yellow Sea basin, and the Taiwan-Sinzi Folded Zone may dam an elongate basin beneath the continental shelf.

The Ryukyu Ridge is an elongate island arc atop which rise many islands including Okinawa. Islands along the inner part of the arc mainly consist of volcanic rocks, but those on the outer part contain outcrops of Neogene, Paleogene, Mesozoic, and even Paleozoic sedimentary strata intruded by granitic or gabbroic masses (Konishi, 1964). Intense folding along the ridge identifies it as the Ryukyu Folded Zone that connects folds of southern Japan with the complicated alpine structure of Taiwan.

Seaward of the Ryukyu Ridge is one of the deepest parts of the ocean, the Ryukyu Trench. The axis of the trench between Japan and Taiwan is mostly deeper than 6,500 meters and near the midpoint is a sounding of 7,881 meters. The trench floor is flat over much of its length due to a thin undeformed sediment layer. The inshore slope is steep up to an extensive terrace at 2,000 to 3,000 meters (Yabe and Tayama, 1934), and it probably consists of both thick sediments and exposed igneous rock. The seaward slope has exposed

igneous rock (Murauchi and others, 1968). At its north end the Ryukyu Trench is terminated both topographically and structurally by the intersection with the continental slope of several subparallel ridges from the southeast. These are the Kyushu-Palau Ridge (the longest one) and the Daito and Oki-Daito ridges. A trench structure, the Nankai Trough (Hilde, Wageman, and Hammond, 1969) continues northeast of this intersection; however, it displays more gentle topography and a thick sediment layer that continues from the Philippine Basin into the trench. The difference in these trenches, the intersecting ridges, and the possible offsets in the Ryukyu Island Arc suggested by Konishi (1965) probably relate to differential movement of the oceanic crustal plate toward the continent (Le Pichon, 1968; Morgan, 1968; Isacks, Oliver, and Sykes, 1968). To the southwest the Ryukyu Trench terminates against the north-south folded structures of Taiwan.

Water above the Trough-Ridge-Trench Province is typical western oceanic water—deep blue (less than 5 per cent yellow) highly transparent (more than 25-meter depth of Secchi disk), very little suspended sediment (mostly less than 0.5 mg/*l*), warm (more than 25°C.) and saline (more than 19 parts per thousand chlorinity), as shown by Figures 4 to 8. Winds in the open ocean east of the Ryukyu Islands were northeasterly, and they merged into the northerly winds from the Yellow Sea (Fig. 10). Swells east of the Ryukyu Islands were from the open Pacific Ocean, in contrast with the more locally derived ones of the Yellow Sea and the continental shelf (Fig. 11). Essentially all of the area east of the Ryukyu Islands was occupied by the Kuroshio (Black Current) that moves northward past Taiwan to divide and flow on either side of Japan, predominantly on the southeastern side.

STRUCTURE

Compilation Procedure

Bathymetry was plotted from soundings at 5-minute intervals during the cruise on a horizontal scale of 1:1,000,000. A vertical exaggeration of 22.5 was selected as most convenient for the regional topography. The total-field magnetic profile was plotted at the same horizontal scale from readings of the magnetometer at 15-minute intervals plus intervening high and low points. Continuous seismic reflection profiles were studied at intervals of several days when the record rolls were removed from the recorder. Interpretations were drawn with grease pencil on sheets of transparent plastic laid atop the recordings. All reflecting horizons deemed significant were traced, including the profile of the sea floor. These grease-pencil lines were then transferred by hand to the bathymetric profile using half-hourly time marks as guides for the horizontal scale. An assumed sound velocity in the sediment of 2,000 m/sec provided the vertical scale.

Three general kinds of materials were considered as mappable facies in the region. The bottomoost and oldest facies is opaque to sound, and the recordings of it exhibit many hyperbolic reflections presumably produced by irregular surfaces. Overlying strata wedge out against the opaque facies or arch over it with the appearance of differential compaction. Where the opaque facies is shallow, the geomagnetic profiles are very irregular—indicating large variations in the magnetic susceptability of the material. In all respects the facies acts as an acoustic basement and it has an appearance on the record like that of intrusive igneous and metamorphic rocks that have been profiled by reflection seismic methods elsewhere in the world. However, in the absence of rock samples or of detailed seismic velocities, one cannot be certain that ancient sedimentary strata or thick lava flows are not also included in this facies.

Both the second and third facies are transparent to acoustic energy, but they differ in their structural attitudes. The second facies underlies the third one, and it generally exhibits evidence of structural deformation followed by erosion. Thus the second and third facies are commonly separated by an unconformity. In some parts of the region the second facies was identified only on the basis of an exceptionally good reflector that appeared to be continuous with a nearby unconformity, perhaps the result of orientation of the profile along the strike rather than at an angle to the strike of dipping beds. We term the age of the second facies as pre-deformation and that of the third one as post-deformation.

For convenience in presentation, the final plots of bathymetry, subbottom reflectors, and total field geomagnetics were grouped into the same three topographic units of the region that were discussed in the preceding section of this report.

YELLOW SEA

Four profiles were made in the Yellow Sea northwest of a line between southeastern Korea and the mainland of China south of the mouth of the Yangtze River (Fig. 12). The total length of these profiles is 2,500 km. The basement facies is present along most of the lengths of all profiles, especially profile 1, which is nearest the Korean coast. Its top may be exposed on the sea floor only for a small part of profile 1, and it deepens in the other profiles so that it mostly lies deeper than 1 km in profile 4. Examination shows that the magnetic profiles are highly irregular where the basement is near the surface, as in profile 1 and part of profile 2. Where the basement is deep, the magnetic profiles are only broadly undulating. The shoaling of the acoustic basement toward the Shantung Pensula, Korea, Cheju Island, and the China mainland south of the Yangtze River indicates that it consists mainly of the same Mesozoic and earlier igneous and metamorphic rocks that crop out in these land areas. More than 1,200 meters of Mesozoic continental sediments underlie western Korea, and the rise of acoustic basement toward this area indicates that these strata also act as acoustic basement, perhaps because of their included thick sandstone members. The ridge of acoustic basement across the entrance of the Yellow Sea probably is a continuation of the Fukien-Reinan Massif (Kobayashi, 1952) that crops out in southern Korea and south of the Yangtze River mouth (Fig. 3). Rocks of the same kind and age and with parallel structural trends occur in both areas. A second submerged ridge of igneous and metamorphic rock appears to prolong the Shantung Peninsula and limit the Yellow Sea basin at the northwest.

Strata of the second facies (pre-deformation sediments) are progressively more abundant to the southwest (Fig. 12). On profiles 1, 2, and 3 they lie below an unconformity that commonly also truncates adjacent areas of the basement. As shown by all profiles, the unconformity is broadly undulating, from less than 100 meters depth to about 1,600 meters. The wave length of the undulations is about 300 km. The fact that the unconformity commonly bevels basement as well as the pre-deformation sedimentary strata means that the unconformity is a major one. Considerations of general regional geology support the concept that the unconformity followed the widespread mid-Tertiary orogeny. Such an assumption means that the pre-deformation sedimentary strata are Paleogene or earlier, perhaps including some Late Cretaceous shales, but excluding igneous and metamorphic rock and sandstones that have acoustic properties similar to those of the basement complex. Support for this conclusion is provided by the three samples of Paleogene rocks that were dredged near the entrance of the Yellow Sea (Fig. 3) where overlying strata are thin enough to permit local projections of Paleogene strata above the sea floor.

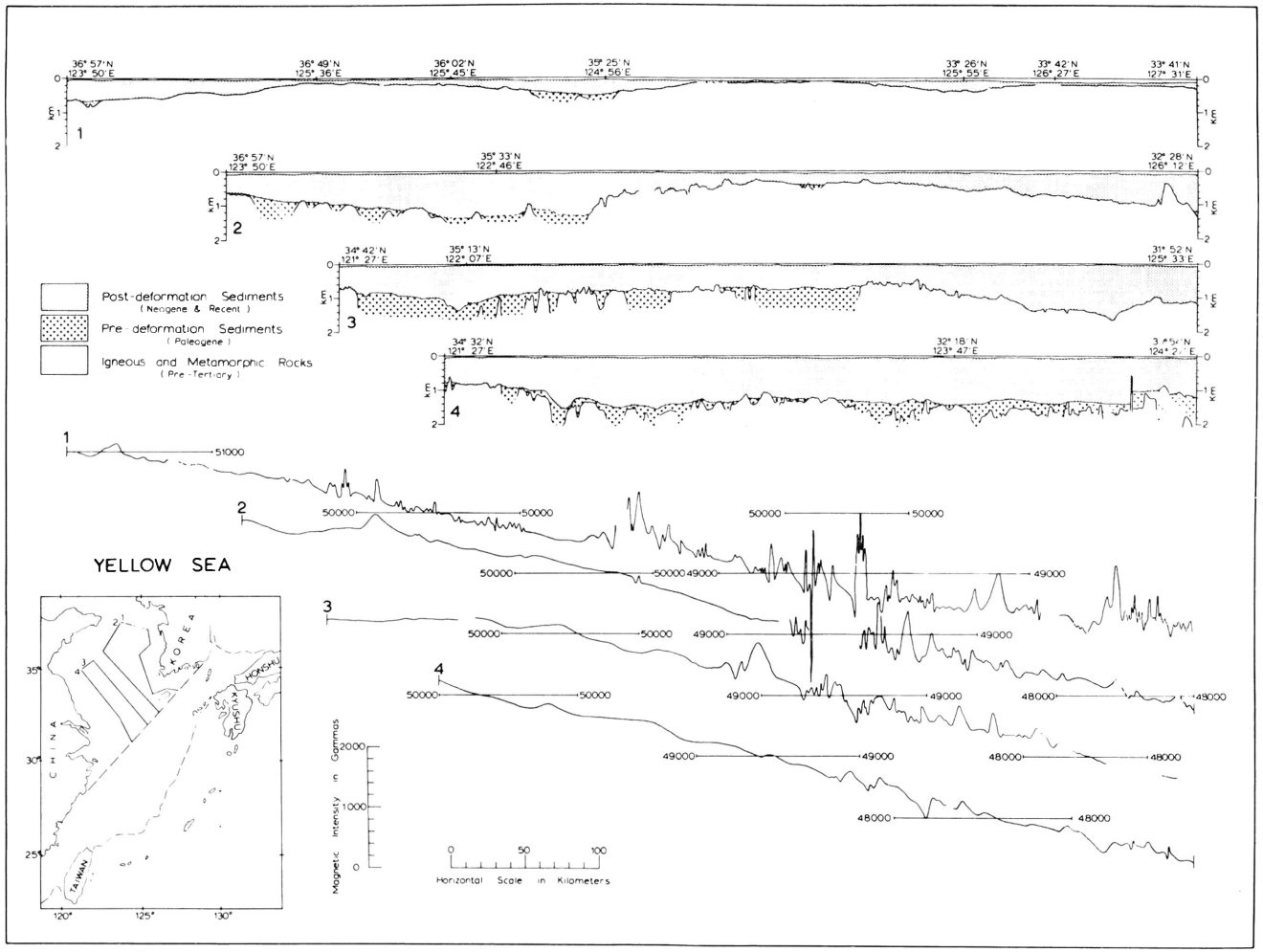

Figure 12. Continuous seismic reflection profiles and geomagnetic profiles of the Yellow Sea.

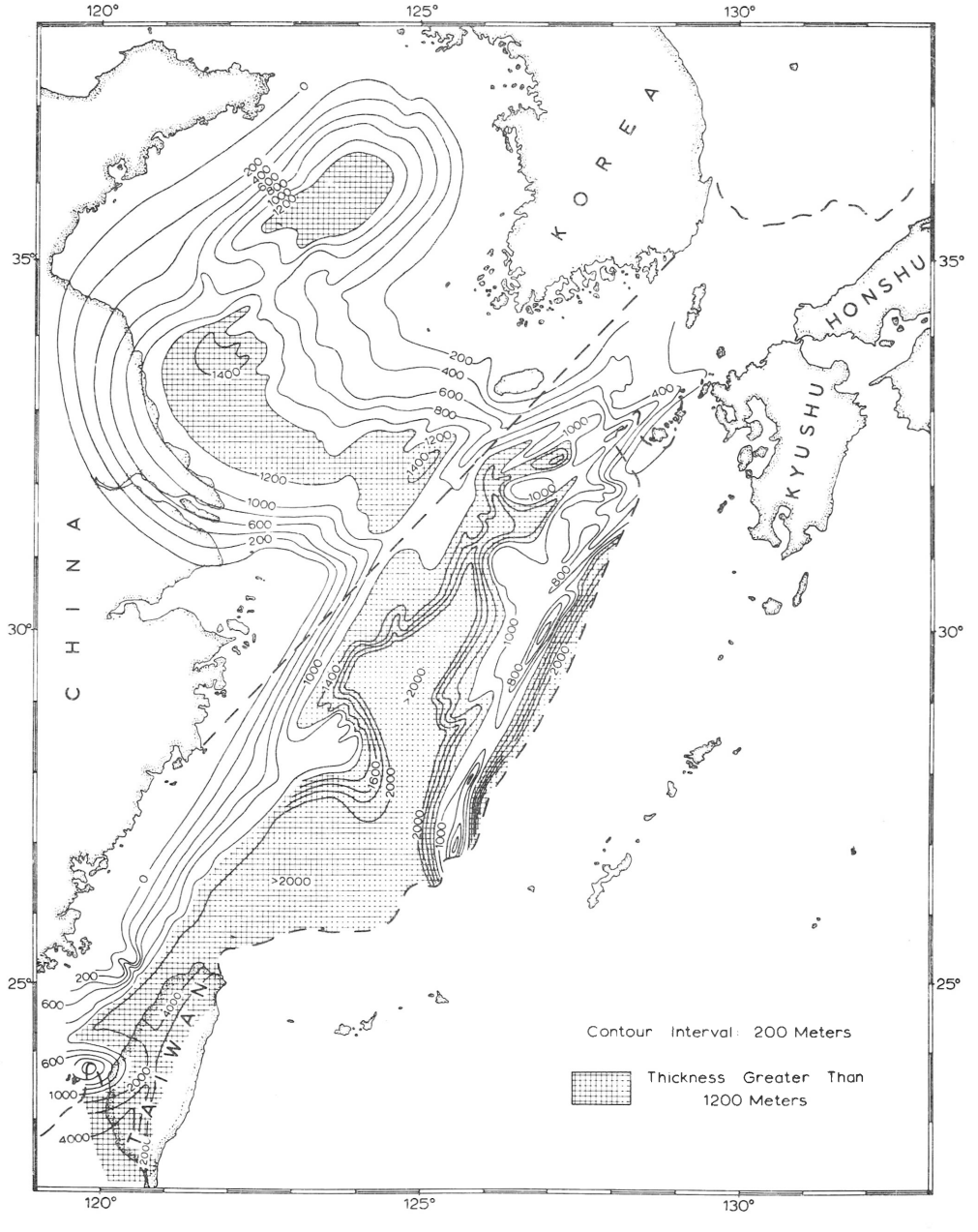

Figure 13. Isopach map of the third (post-deformational) facies in the Yellow Sea and the continental shelf. Contours are in meters. Because of the shallow water depths, this map also is essentially a structural contour map of the top of the second facies.

Atop the unconformity in the Yellow Sea is the most extensive facies, the post-deformation strata. Most reflecting horizons within it are so nearly horizontal as to not permit discrimination from the numerous multiple reflections of the flat sea floor. Only locally can subbottom reflections be identified in the third facies; mostly these are places where differential compaction atop basement hills has produced a dip, or where prominent discontinuities occur at such great depths as to be recorded after the bottom multiples have largely been attenuated. The third (post-deformational) facies was further investigated by plotting its thickness at half-hour intervals along the profiles to form an isopach map. This map (Fig. 13) clearly shows the presence of a large sedimentary basin which is dammed by a ridge between Korea and the Yangtze River mouth. The low point on the ridge appears to be about 1,100 meters below sea level. Within the Yellow Sea the basin contains three separate low areas. Two contain sediments that are 1,400 to 1,500 meters thick (or deep below sea level) and one has perhaps 100 meters less sediment. The shallowest one is just south of the tip of the Shantung Peninsula; the other two lie immediately off the Yangtze River delta. Outcrops of basement rocks on land in the Shantung Peninsula and near Shanghai (Director Geol. Survey of India, 1959; Roe, 1962) limit the westernmost margin of the basins to the vicinity of the delta front.

If the widespread unconformity in the Yellow Sea is mid-Tertiary in age, the post-deformation strata must be Neogene to Recent. A Neogene age is supported by the absence of known appreciable deformation in the land areas surrounding the Yellow Sea during this time interval. Also the thinning of the strata around the margins of the basin (Fig. 13) corresponds with the absence of Neogene strata on land except on Cheju Island, where their thickness is less than 100 meters. Pleistocene and Recent strata must also be included in the postdeformation facies, because at least 960 meters of Quaternary deltaic sediments have been encountered in water wells north of the Shantung Peninsula (Niino and Emery, 1961; Tregear, 1965, p. 31). Moreover, the volume of sediment annually discharged from the Yellow and Yangtze rivers is very great, 2,080 and 550 million tons each year, respectively, according to Holeman (1968). The rivers are the first and the fourth largest contributors of sediment to the ocean in the entire world. The total volume of the third facies in the Yellow Sea is about 200,000 cu. km. At a specific gravity of 2.0, this volume corresponds to 4×10^{14} tons. Thus, the third facies could have been deposited in only 150,000 years if the entire river load had been deposited in it. However, a large percentage of the sediment was deposited in the Gulf of Pohai (Zenkovich, 1967, pp. 75, 115, 644, 651, 659), and much more escaped seaward from the Yellow Sea, thereby increasing the time span by an unknown but probably very large amount.

Continental Shelf

Profiles across the continental shelf total about 4,500 km and consist of ten transverse lines and a composite one that follows the length of the shelf. The results show the bottom to be underlain by two main ridges of acoustic basement. The first ridge is the Fukien-Reinan Massif, most of which is within the Yellow Sea where it separates the Yellow Sea basin from the continental shelf. The part of the massif that is beneath the continental shelf is deeper (more than 1,000 meters below sea level) than the landward ends. Presumably the entire feature consists of Precambrian igneous and metamorphic rocks with some Mesozoic extrusives.

The second ridge lies near the edge of the continental shelf between Japan and Taiwan. Most of this one is buried beneath later sediments, and only near Japan does it rise above its

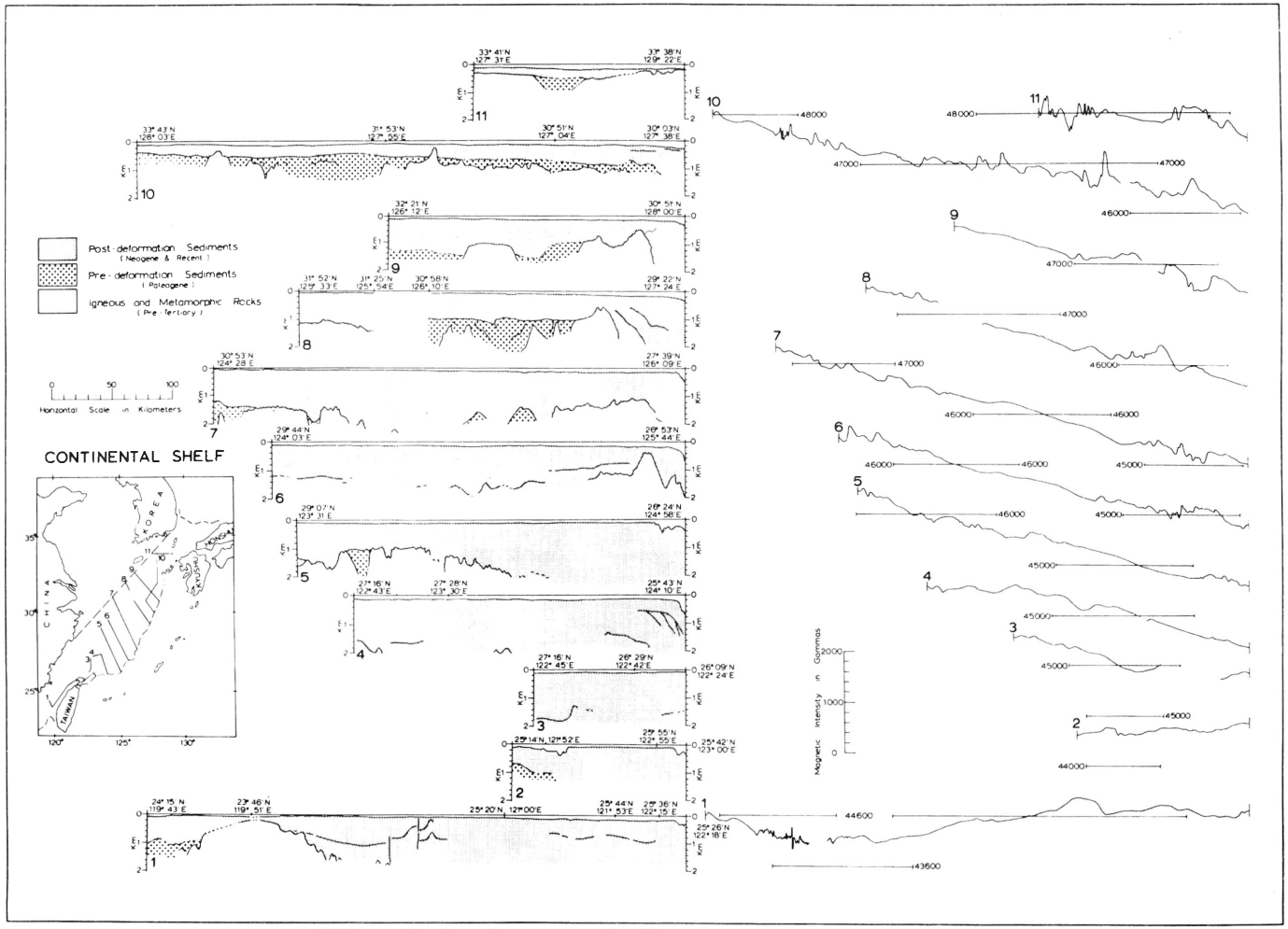

Figure 14. Continuous seismic reflection profiles and geomagnetic profiles of the continental shelf between Taiwan and Korea.

surroundings. Its greatest height occurs west of Kyushu in islands which contain folded sedimentary rocks and granodiorite, both of Tertiary age. Similar rocks occur farther northeast along the northwestern coast of Honshu, and thick folded Tertiary sediments are present in Taiwan as a southwestward extension of the ridge. Thus, the feature is termed the Taiwan-Sinzi Folded Zone, having its main deformation during Neogene times, but probably beginning during the Paleogene. The continuous seismic reflection profiles (Fig. 14) and the isopach map of Neogene sediments (essentially a structural contour map of the base of the Neogene sequence (Fig. 13) show that the ridge lies at the outer edge of the continental shelf between Japan and Latitude 26°30′. Between that latitude and Taiwan, about 400 km farther southwest, the ridge bows seaward and underlies the upper part of the continental slope. Two seismic refraction stations were made by Murauchi and others (1968) at the outer edge of the continental shelf and spanning our profiles 4, 5, and 6 (Fig. 14). They show that beneath 140 meters of water and 800 meters of sediments (seismic velocity of 2.0 km/sec) are 750 meters of material having a seismic velocity of about 3.4 km/sec. At greater depth is material of about 6.0 km/sec velocity. The intermediate seismic velocities of 3 to 5 km/sec support the concept that the Taiwan-Sinzi Folded Zone consists of sedimentary strata and acidic igneous rocks.

The magnetic profiles made during the cruise (Figs. 12, 14) reveal numerous anomalies where the profiles cross the Fukien-Reinan Massif and the Taiwan-Sinzi Folded Zone, attesting the presence of magnetic rocks, probably igneous intrusives and extrusives. Similarly, the isogams of the aeromagnetic survey by Project MAGNET (Fig. 15) exhibits a clear trend of positive anomalies that corresponds with the Taiwan-Sinzi Folded Zone, a less obvious one for the Fukien-Reinan Massif, and an intervening area of mostly negative anomalies that corresponds with the broad trough between the ridges. The anomalies rise to the south, even in the trough, so that almost the entire area just south of Taiwan has positive anomalies. At the north near Tsushima Strait the seismic and magnetic records of Figure 14 indicate that the trough shoals and divides into several secondary ridges that lie between and parallel to the two main ones.

Sediments above the acoustic basement are of two facies, as in the Yellow Sea: pre-deformation and post-deformation. The pre-deformation sediments are recognizable through their discordant dip beneath an unconformity that generally is 500 to 1,500 meters below sea level. On many profiles an unconformity is not evident, because it lies at great depth and is obscured by multiple reflections of the sea floor, or because the profiles are parallel to the strike of the dipping pre-deformation strata. Detailed laboratory comparison of all profiles from the continental shelf may permit mapping of the pre-deformation strata beyond the limits imposed by field examination of the records. For the present, the strata atop basement are best considered as a single unit, with the assumption that most of them are Neogene in age. The age of at least the upper strata is indicated by the presence of Neogene rocks, generally folded, on islands of the Goto Group near Kyushu, on Senkaku Island, and on Taiwan. In addition, 27 dredge samples of the continental shelf between Japan and Taiwan contain fossils or rock types of Neogene age. Evidently, Neogene strata forms a thick blanket beneath the continental shelf of the East China Sea.

The thickness of the Neogene (and of some Paleogene) strata is shown by the continuous seismic reflection profiles of Figure 14 and the isopach map of Figure 13. The strata are less than 200 meters thick in Tsushima Strait and they thicken southwestward to Taiwan, where the acoustic records show the presence of more than 2 km and where well borings have penetrated 5 km of Neogene beds. The linear trough fill is interrupted at only two places, at each of which shallow basement projects eastward into the trough. One place is beneath

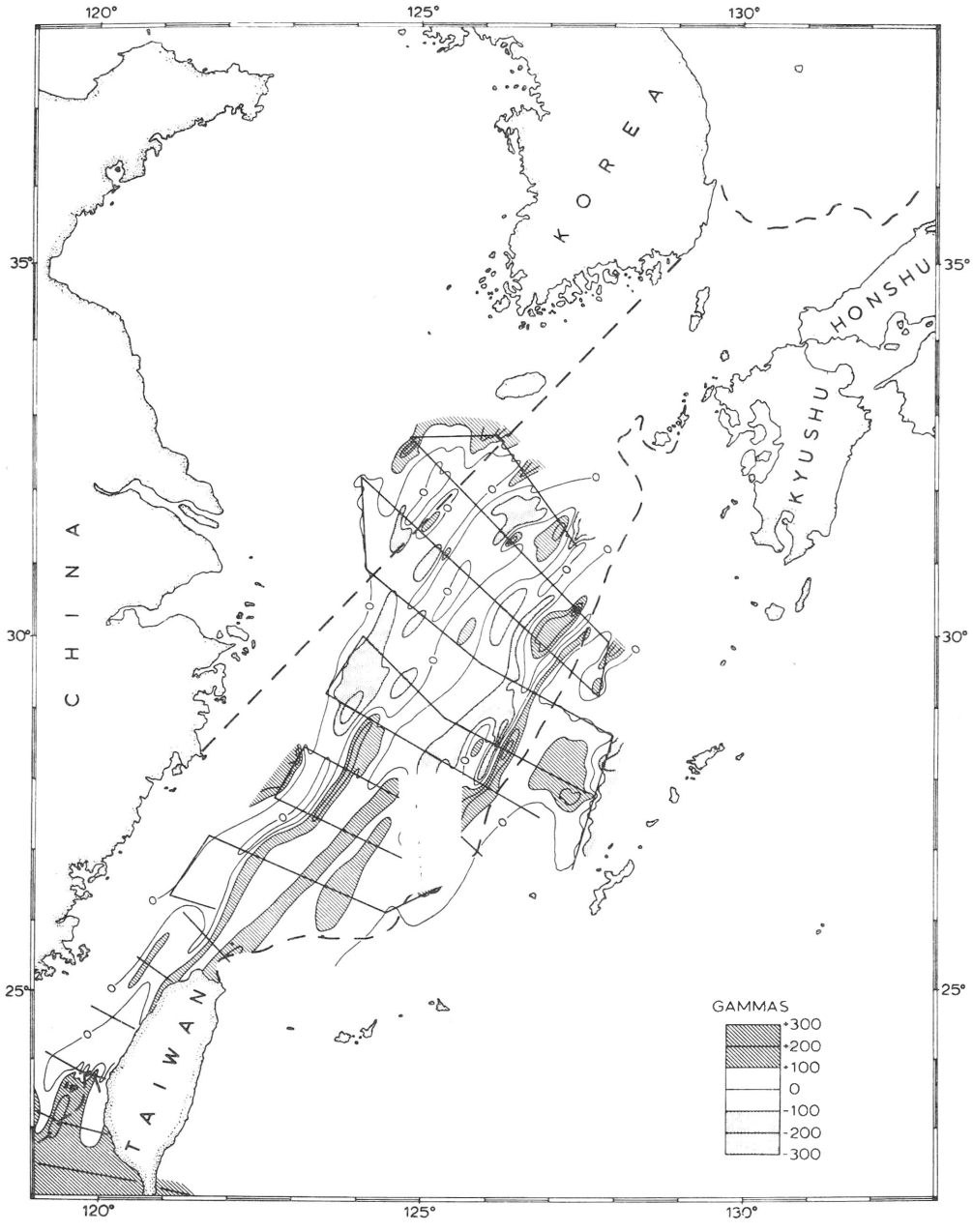

Figure 15. Geomagnetic anomalies of much of the continental shelf between Taiwan and Korea. Drawn from geomagnetic profiles of Project MAGNET supplied by Henry P. Stockard (Magnetics Division, U.S. Naval Oceanographic Office). Anomalies were obtained by subtracting from the total field measurements Cain's regional values plus 100 gammas.

the Penghu Islands and the other is at Latitude 28°. The first one is well known from exploration on land (Meng, 1968), and it must have existed during the filling of the trough because the fill south of it is much finer grained than the fill north of it (Stach, 1958).

The eastern side of the sediment-filled trough is the Taiwan-Sinzi Folded Zone that served as a dam from Japan to near Taiwan. Sediments have filled the trough and then surmounted the dam along most of its length. The main point of their escape is near Taiwan. In this area both the floor of the trough and the top of the dam are deeper than farther north. The total depth of fill in the trough from half way along the west side of Taiwan to a point about 200 km northeastward is too great to be measured with a 30,000-joule sparker and without electronic removal of the interfering multiple reflections of the sea floor. However, the seismic profiles reveal unconformities or tilted strata down to depths of 2,000 meters, so the thickness of sediments atop basement is at least that great. The area of sediments thicker than 2 km on the continental shelf is about 200,000 sq. km, indicating that the volume of sediments in this area alone is more than 400,000 cu. km and may approximate 700,000 cu. km. A reasonable estimate of the total volume of sediments atop basement throughout the entire continental shelf is 1 million cu. km. If deposited throughout the Cenozoic era, the average rate of deposition is about 4 cm 1,000 years. This is about five times the rate for the Atlantic continental shelf of the United States. Probably the greater rate off Asia is due to the huge drainage areas and sediment loads of the Yellow and Yangtze rivers.

Trough, Ridge, Trench Province

Ten transverse crossings of the sea floor beyond the continental shelf produced a total of 5,200 km of bathymetric, seismic, and magnetic records (Fig. 16). A system of alternating rocky ridges and sediment-filled trenches was defined. These features connect relatively well mapped zones in Japan and Taiwan that provide information about composition and age to supplement the geophysical measurements of this cruise and of previous cruises by other workers.

The first geological feature seaward of the continental shelf is the continental slope that has an average declivity of about 10 degrees for the steepest 200-meter section of each profile. The continental slope is also the western side slope of the adjacent Okinawa Trough. For the most part, both side slopes of the trough consist of sediments, with little exposed basement rock. The floor of the trough is generally flat in cross-section, but is incised by a narrow valley that probably owes its origin to turbidity currents that flowed along the axis of the trough. Sediment fill in the trough exceeds 1.2 km along all profiles, and it contains many subbottom reflectors that may be turbidite sand layers. The deepest part of the trough floor is opposite the gap in the Taiwan-Sinzi Folded Zone, as though tectonic activity had depressed both features. In this area the bottom depth is 2,200 meters. Nearer Taiwan the bottom shoals to less than 1,400 meters and the nature of its termination is not evident from existing soundings. At its northeastern end the trough shoals progressively until it reaches Japan, where it appears to be a direct continuation of the Amakusa Folded Zone. This folded zone underlies the Inland Sea of Japan still farther northeastward. Folding began during the Paleogene, earlier than in the Taiwan-Sinzi Folded Zone.

The next feature of the province is the Ryukyu Ridge above which rise many islands. This and the parallel Ryukyu Trench are the most prominent parts of the island arc. Both the continuous seismic reflection profiles and the geomagnetic profiles indicate the presence of volcanic rocks, which also are dominant on the islands. Also present on the islands of the arc, in southern Japan, and indicated by the profiler records are folded sediments. Where

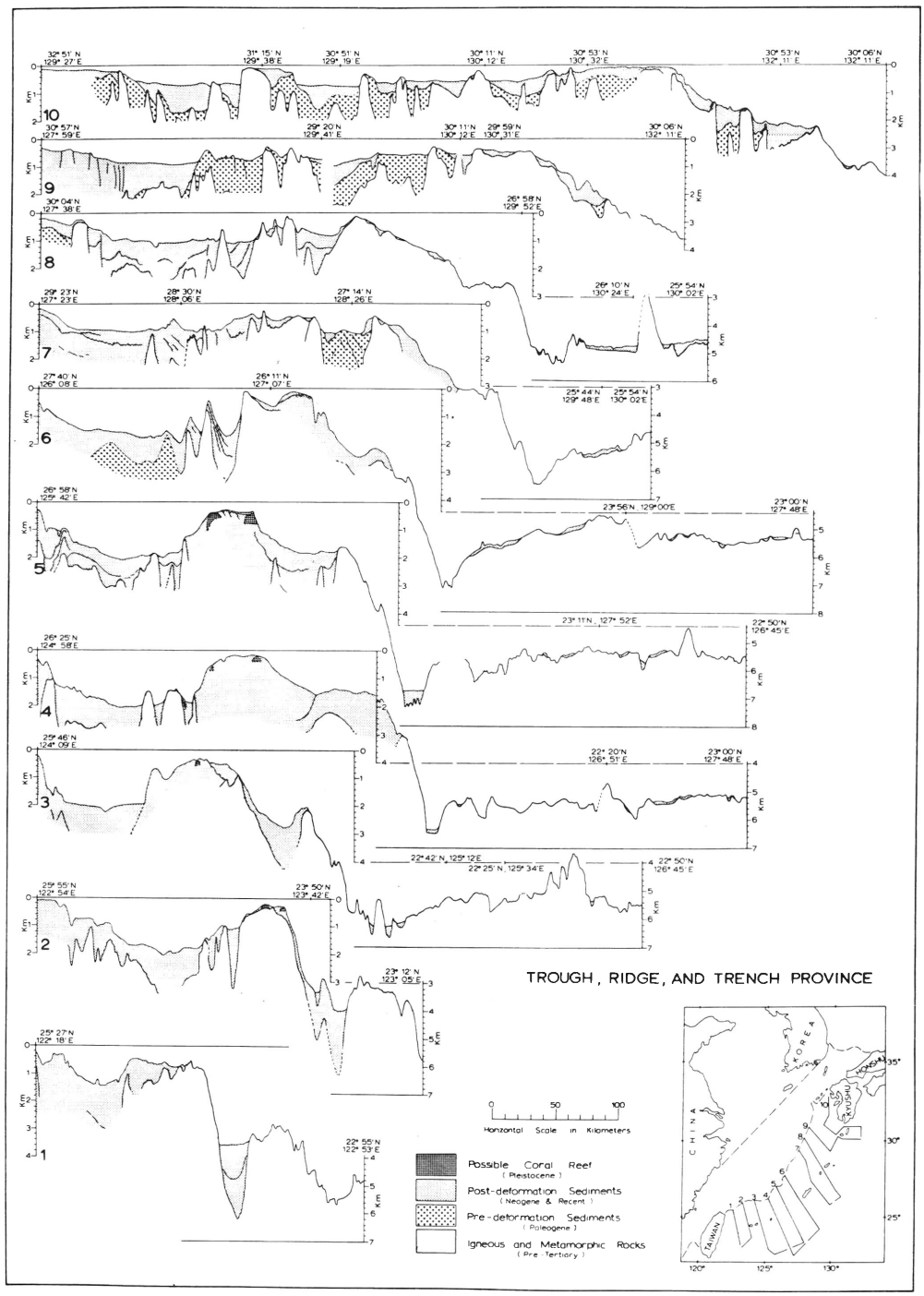

Figure 16. Trough, Ridge, and Trench Province:
a. Continuous seismic reflection profiles.

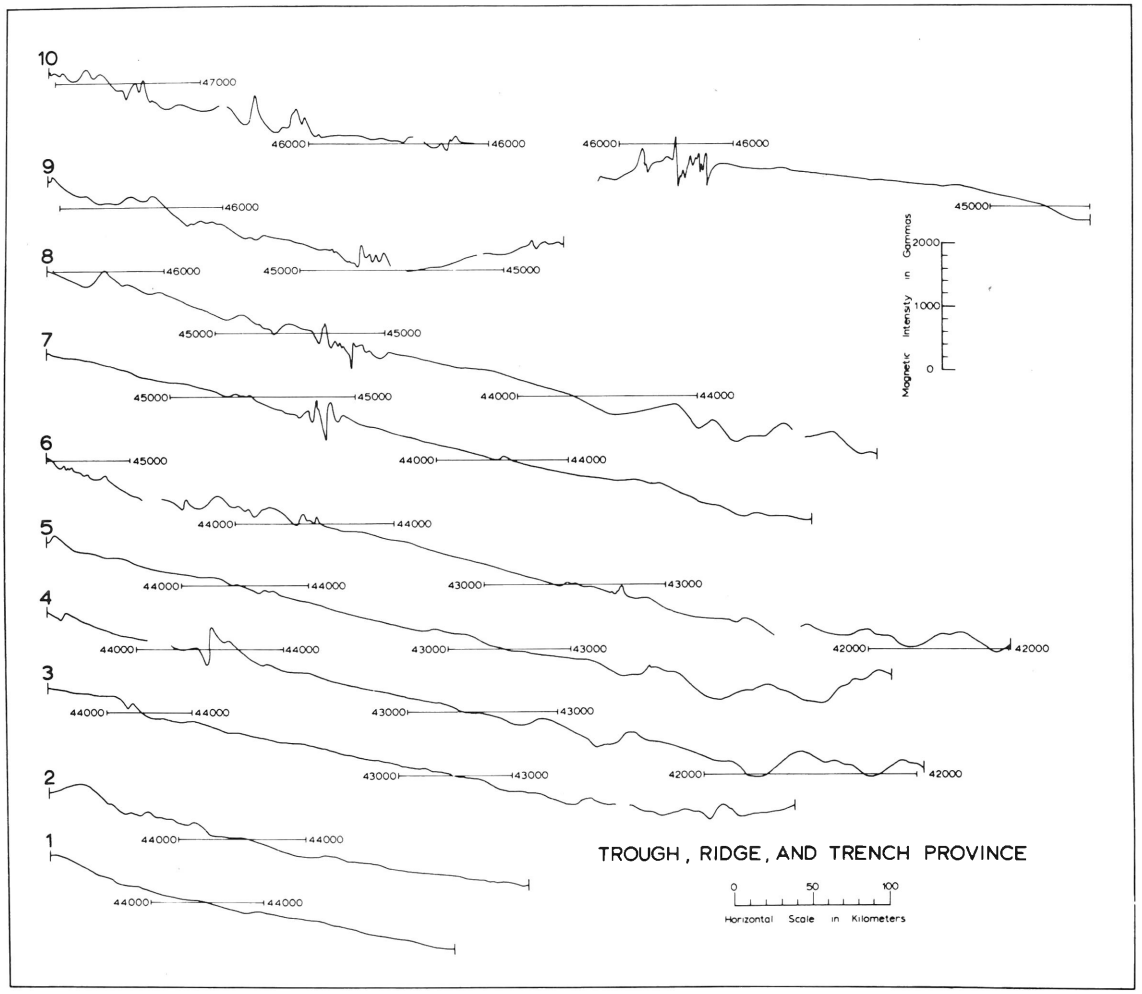

Figure 16. Trough, Ridge, and Trench Province:
b. geomagnetic profiles.

known on land, these are Neogene in age and they contain fossils that are characteristic of moderately deep water; thus the Ryukyu Folded Zone is at least largely Neogene in development. Several of the profiles reveal complex masses of low acoustic transparency near the edges of the flat top of the Ryukyu Ridge. The nature of the acoustic reflections and their depth (100 to 300 meters, about the same as the depth of the edge of the nearby continental shelf) are strongly suggestive of submerged coral reefs, probably Pleistocene in age. Living reefs fringe some of the southern islands of the arc; evidently reefs were somewhat more widespread during part of the Pleistocene Epoch than at present.

East of the Ryukyu Ridge the sea floor slopes downward at about 10 degrees to a terrace that was formed by ponding of sediments behind a dam presumably of fault origin and consisting of volcanic or consolidated sedimentary rock. The terrace fill and its confining dam can be traced nearly continuously from Taiwan to southern Japan, where part of it has been named and described as the Tosa Terrace (Tayama, 1952; Hilde, Wageman, and Hammond, 1969). The depth of the broadly concave surface of the terrace on the several crossings is somewhat irregular, in accordance with an irregular depth of the crest of the confining fault-block dam. Depths range from 1,800 to 4,000 meters, and thicknesses of sediment from "more than 600" to 2,700 meters.

Slopes continue beyond the terrace down to the floor of the Ryukyu Trench. These slopes and the ones on the seaward side of the trench are the steepest of the region, averaging about 13 degrees for the steepest 200-meter section of each sounding profile. Because the soundings were obtained with wide-angle equipment, the true slopes are steeper than the apparent ones. Seismic profiles show only little sediment mantling rock on either side of the trench, unlike the findings in the asymmetrical Japan Trench by Ludwig and others (1966). Due to lack of penetration beneath the western slope of the trench, we have indicated igneous rock there (Fig. 16a); however, the low (2.8 to 3.0 km/sec) seismic velocities obtained by Murauchi and others (1968) are indicative of sedimentary rock. Their seismic refraction stations reveal that material having seismic velocities less than 5 km/sec below the western slope of the trench continue westward beneath the terrace, the Ryukyu Ridge, the Okinawa Trough, and the continental shelf. Under this layer is another one having seismic velocities of about 6 km/sec; this layer continues eastward beneath the Ryukyu Trench to form the surface rock east of the trench. The floor of the trench deepens northeasterly from 5,600 meters near Taiwan to at least 6,800 meters near Okinawa. It shoals and disappears at the northeast, and just south of Japan it reappears as the Nankai Trough at 4,800 meters. Our seismic reflection profiles show the floor of the trench to be underlain by zero to 600 meters of sediment having several subbottom reflectors presumably of turbidite origin.

The deep-sea floor beyond the Ryukyu Trench is very irregular and mostly is impervious to acoustic energy at the level used in reflection profiling. It shoals irregularly eastward, where several ridges extending from a general southeasterly direction add to the roughness of the bottom. The bottom is underlain by material having a seismic velocity of 6 km/sec, presumably volcanic rock of layer 2 (Murauchi and others, 1968). Patches of sediment less than 200 meters thick are present in some of the depressions and on some of the flatter areas.

CONCLUSIONS

The six weeks of ship-board survey with R/V F. V. HUNT provided information to supplement and extend seaward the geological knowledge of the adjacent land areas. Forming the structural framework of the region is a succession of northeast-southwest-trending

ridges that separate sediment-filled depressions (Fig. 17). Farthest landward of these ridges (250 km northwest of the Gulf of Pohai, and thus beyond the limits of Figure 2) is the Taihung—Great Kingan Range that was uplifted in Caledonian (Early Paleozoic) times. An older (Precambrian) uplift formed the Tai Shan—Laoyehling Range that is the backbone of the Shantung Peninsula at the head of the Yellow Sea.

Next of the ridges is the Fukien—Reinan Massif that was uplifted during the Middle to Late Mesozoic Era across the mouth of the Yellow Sea. So far as can be learned from the geology of China and Korea, this massif barred the ocean from the continent until the end of the Cretaceous Period. The only strata of Cretaceous age northwest of the massif are non-marine, but these reach a thickness of several thousand meters. Evidently, the barrier was breached in Paleogene Times because Paleogene and especially Neogene sediments are widespread and thick in the Yellow Sea, if our seismic profiles have been interpreted correctly. Deposition of these sediments was aided by the uplift of the Taiwan—Sinzi Folded Zone that was raised probably throughout Neogene and probably part of Paleogene time damming sediments from land to build the present continental shelf and to cover the floor of the Yellow Sea.

Beyond the continental shelf two additional ridges formed between Paleogene and Recent time. These are the Ryukyu Ridge and a parallel unnamed ridge that lies about half way down the east side slope of the Ryukyu Trench. A third ridge still farther seaward beyond the Ryukyu Trench has an irregular, deep, and discontinuous crest. Most of the ridges have recognizable continuations on land in Japan, but the manner of their junction with Taiwan is uncertain, owing to a lack of geological and geophysical data from the sea floor near Taiwan. The general appearance of the trends (Fig. 17) suggests a concentration or knotting of the structures near Taiwan, much like the constriction of the Himalaya Mountains northeast of India. The drag-like bend of the ridges, the great width of the shelf northeast of Taiwan, and the broad submarine canyon that separates the southwesternmost section of the deep-sea terrace from Taiwan, the probable main source of its sediments (Fig. 2) may all be results of an inferred right-lateral strikeslip fault that is shown in Figure 17. The sequence of generally younger ridges toward the southeast is typical of other parts of the Pacific margin (Umbgrove, 1947, pl. 5; Yanshin, 1966). Here, it has produced a step-like growth of the Asian continent. Between the ridges that lie seaward of the continental shelf are linear depressions that contain partial fills of sediment. In general, the fill is thickest, widest, and most continuous in the Okinawa Trough, and it is least important in the Ryukyu Trench that is farthest from the continental shelf and from the two large rivers that contribute sediment from nearly one third of the total area of China.

Most important for the oil and gas potential in the region is the sediment fill beneath the continental shelf and the Yellow Sea. In these areas sediments were deposited rapidly owing to the large area of China that is drained by the Yellow and Yangtze rivers. High contents of nutrients in the river effluents also lead to high organic productivity in the seas of the region. Surface samples from the sea floor contain as much as 1.5 per cent organic matter, but higher contents are to be expected at greater depths of burial that were not affected by glacially lowered sea levels.

The most favorable part of the region for oil and gas is the 200,000 sq. km area mostly northeast of Taiwan. Sediment thicknesses exceed 2 km, and on Taiwan they reach 9 km, including 5 km of Neogene sediment. Most of the sediment fill beneath the continental shelf is believed to be Neogene in age, on the basis of general low dips shown by the seismic profiles, outcrops on islands and on the sea floor, and thickness in well borings of Taiwan. Nearly all of the oil and gas that is produced on land in Japan, Korea, and Taiwan comes from

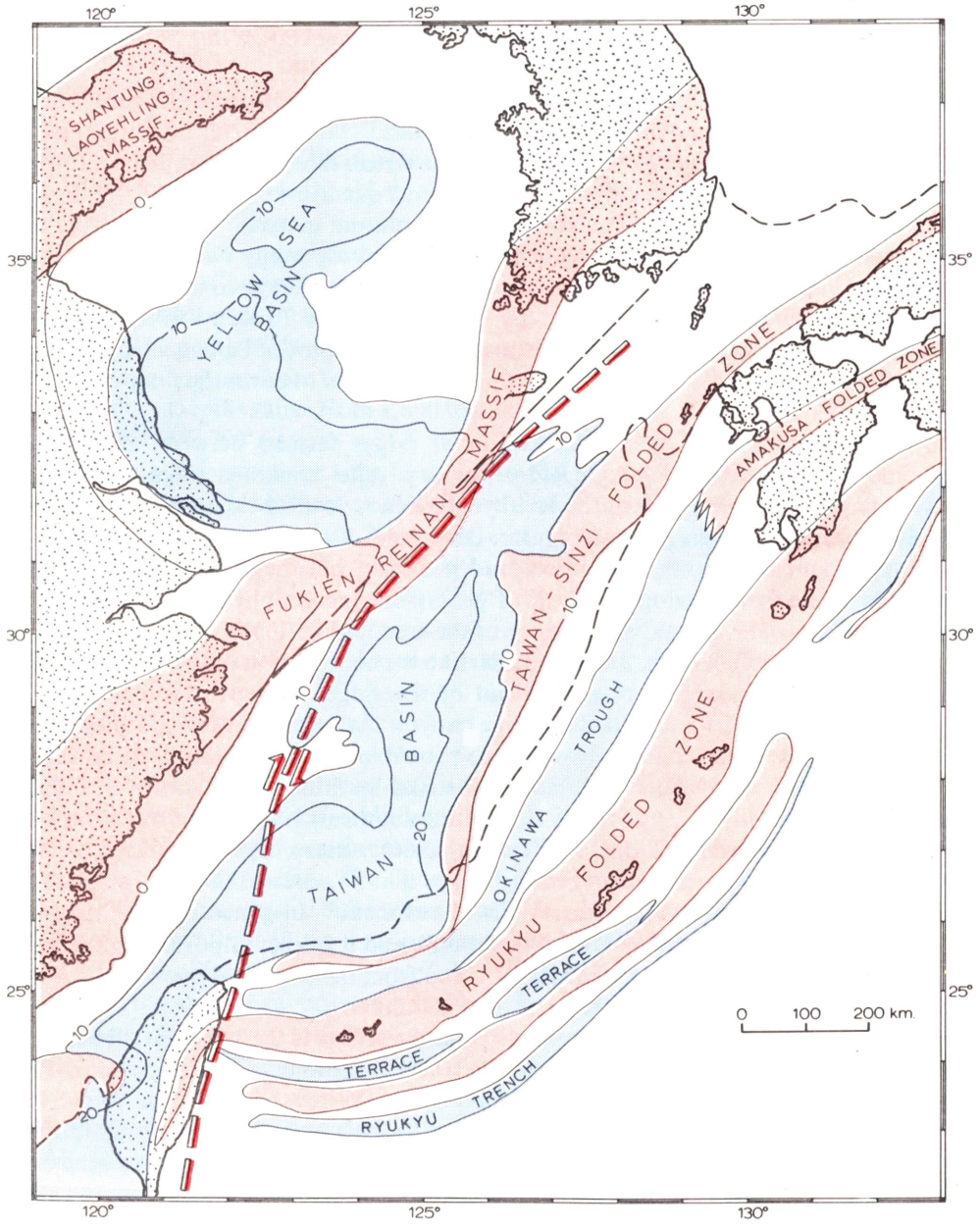

Figure 17. Generalized pattern of ridges and of troughs, basins, and trenches in the East China Sea and vicinity based upon the results of the cruise of R/V F. V. HUNT and previous information. Contours indicate sediment thickness (hundreds of meters) beneath the Yellow Sea and the continental shelf.

Neogene strata. A high probability exists that the continental shelf between Taiwan and Japan may be one of the most prolific oil reservoirs in the world. It also is one of the few large continental shelves of the world that has remained untested by the drill, owing to military and political factors, as well as to a lack of even reconnaissance geological information such as provided by this short survey.

A second favorable area for oil and gas is beneath the Yellow Sea where three broad basins are present. These basins are interconnected, but the center of one is near Korea and the centers of the other two are near the mainland of China. The basins contain a thickness of nearly 1.5 km of sediment, according to this survey, and the sediments probably have a higher content of organic matter than do the sediments beneath the open continental shelf. The good reflecting horizons within the bottom probably are sandy layers that can serve as reservoir beds between organic-rich source beds.

The present reconnaissance study depicted unconformities, anticlines, and faults below both the continental shelf and the Yellow Sea. Such features may serve as the local structures that trap quantities of oil and gas. Further detailed seismic studies are required within the general sedimentary basins in order to adequately portray the shapes and extents of these small structures. After completion of these detailed surveys, many of the structures may warrant the final test—by the drill.

REFERENCES

Asaoka, Osamu, and Shigeo Moriyasu, (1966) On the circulation in the East China Sea and the Yellow Sea in winter: Oceanographical Magazine, vol. 18, nos. 1–2, pp. 73–81.

Chingchang, Biq, and Li-Sho Chang, (1953) Geologic Map of Taiwan, scale 1:300,000, two sheets: Geol. Survey of Taiwan.

Dietz, R. S., (1954) Marine geology of northwestern Pacific: Description of Japanese bathymetric chart 6901: Bull. Geol. Soc. America, vol. 65, pp. 1199–1224.

Director of the Geological Survey of India, (1959), Geological Map of Asia and the Far East, scale 1:5,000,000, six sheets: Secretariat of the United Nations Economic Commission for Asia and the Far East, Bangkok, Thailand.

Emery, K. O., (1968) Relict sediments on continental shelves of the world: Bull. Amer. Assoc. Petroleum Geologists, vol. 52, pp. 445–464.

Emery, K. O., and Hiroshi Niino, (1967) Stratigraphy and petroleum prospects of Korea Strait and the East China Sea: Geol. Survey of Korea, Rept. of Geophys. Explor., vol. 1, pp. 249–263; also in (1968) Economic Commission for Asia and the Far East, Committee for Co-ordination of Joint Prospecting for Mineral Resources in Asian Offshore Areas, Tech. Bull., vol. 1, pp. 13–27.

Emery, K. O., Hiroshi Niino, and Beverly Marsters, (in preparation) Post-Pleistocene sea levels of the East China Sea: Science.

Geol. Soc. of Japan, (1964) Geological Map of Japan, scale 1:2,000,000, one sheet.

Geol. Survey of Korea and Geol. Society of Korea, (1956) Geologic Map of Korea, scale 1:1,000,000, two sheets.

Hess, H. H., (1948) Major structural features of the western North Pacific, An interpretation of H.O. 5485, bathymetric chart, Korea to New Guinea: Bull. Geol. Soc. America, vol 59, pp. 417–446.

Hilde, T. W. C., J. M. Wageman, and W. T. Hammond, (1968) The structure of the Tosa Terrace and Nankai Trough off southwestern Japan: Deep-Sea Research, vol. 15, pp. 415–422.

Holeman, J. N., (1968) The sediment yield of major rivers of the world: Water Resources Research, vol. 4, no. 4, pp. 737–747.

Ichiye, T., (1960) On the hydrography near Mississippi Delta: Oceanographical Magazine, vol. 11, no. 2, pp. 65–78.

Isacks, B., J. Oliver, and L. R. Sykes, (1968) Seismology and the new global tectonics: Jour. Geophys. Research, vol. 73, no. 18, pp. 5855–5899.

Kobayashi, T., (1952) On the southwestern wing of the Akiyoshi orogenic zone in Indochina and South China and its tectonic relationship with the other wing in Japan: Japanese Jour. of Geology and Geophysics, vol. 22, pp. 27–37.

Koizumi, Masami, (1962) Seasonal variation of surface temperature of the East China Sea: Jour. Oceanographic Soc. Japan, 20th Anniv. vol. pp. 321–329.

Konishi, Kenji, (1964) Geologic notes on Tonaki-Jima and width of Motobu Belt, Ryukyu Islands: Sci. Repts. of Kanazawa Univ., vol. 9, pp. 169–188.

Konishi, Kenji, (1965) Geotectonic framework of the Ryukyu Islands (Nansei Shoto): Geol. Magazine of Japan, vol. 71, pp. 437–457 (in Japanese).

Le Pichon, X. (1968) Sea-floor spreading and continental drift: Jour. Geophys. Research, vol. 73, no. 12, pp. 3661–3697.

Ludwig, W. J., J. I. Ewing, M. Ewing, S. Murauchi, N. Den, S. Asano, H. Hotta, M. Hayakawa, T. Asanuma, K. Ichikawa, and I. Noguchi, (1966), Sediments and structure of the Japan Trench: Jour. Geophys. Research, vol. 71, no. 8, pp. 2121–2137.

Manheim, F. T., R. H. Meade, and G. C. Bond, submitted for publication, Suspended matter in surface waters of the Atlantic continental margin from Cape Cod to the Florida keys: Science.

Manheim, F. T., R. H. Meade, J. V. A. Trumbull, and G. C. Bond, (1966) Suspended matter in Atlantic coastal waters between Cape Cod, Massachusetts, and the Florida Keys (Abs): Amer. Assoc. Adv. Science, Ann. Mtg., 133rd, Washington, 1966, Program, Sec. E, p. 23.

McDonald, W. F. (supervisor), (1938) Atlas of Climatic Charts of the Oceans: U.S. Dept. Agriculture, Weather Bureau Publ. 1247, Govt. Printing Office, Washington, D. C., 129 charts (folio).

Menard, H. W., (1964) Marine Geology of the Pacific: McGraw-Hill, New York, 271 pp.

Meng, C. Y., (1967) Structural development of the southern half of western Taiwan: Proc. Geol. Soc. China, no. 10, pp. 77–82.

Meng, C. Y., (1968) Geologic concepts relating to the petroleum prospects of Taiwan Strait: Economic Commission for Asia and the Far East, Committee for Co-ordination of Joint Prospecting for Mineral Resources in Asian Offshore Areas, Tech. Bull., vol. 1, pp. 143–153.

Morgan, W. J., (1968) Rises, trenches, great faults and crustal blocks: Jour. Geophys. Research, vol. 73, no. 6, pp. 1959–1982.

Murauchi, Sadanori, Toshio Asanuma, and Hiroshi Hotta, (1968) Studies of the continental slope off the Sanriu Coast by seismic profiler survey: Natl. Sci. Museum, Mem. no. 1, pp. 37–40 (in Japanese).

Murauchi, S., N. Den, S. Asano, H. Hotta, T. Yoshii, T. Asanuma, K. Hagiwara, K. Ichikawa, T. Sato, W. J. Ludwig, J. I. Ewing, N. T. Edgar, and R. E. Houtz, (1968) Crustal structure of the Philippine Sea: Jour. Geophys. Research, vol. 73, pp. 3143–3171.

Niino, Hiroshi, (1968) A study of the marine geology around Danjo Islands in the East China Sea and Mishima Island in the east part of the Korea Strait: Economic Commission for Asia and the Far East, Committee for Co-ordination of Joint Prospecting for Mineral Resources in Asian Offshore Areas, Tech. Bull., vol. 1, pp. 87–92.

Niino, Hiroshi, and K. O. Emery, (1961) Sediments of shallow portions of East China Sea: Bull. Geol. Soc. America, vol. 72, pp. 731–762.

Nishizawa, Satoshi, and Naoichi Inoue, (1958) Turbidity distribution and its relation to some oceanographical factors in the Eastern China Sea in the late summer of 1956: Rec. Oceanog. Works in Japan, Spec. no. 2, pp. 101–115.

Roe, F. W. (coordinator), (1962) Oil and Natural Gas Map of Asia and the Far East, scale 1:5,000,000, four sheets: United Nations Economic Commission for Asia and the Far East, Bangkok, Thailand.

Schreiber, Alfred, (1965) On the geology of the Cenozoic goosyncline in middle and northern Taiwan (China) and its petroleum possibilities: Petroleum Geol. of Taiwan, no. 4, pp. 25–87.

Stach, L. W., (1958) Subsurface exploration and geology of the coastal plain region of western Taiwan: Proc. Geol. Soc. China, no. 1, pp. 55–96.

Tayama, R., (1952) On depth curve chart of the adjacent seas of Japan (chart 9601): Hydrog. Bull. Japan, vol. 32, pp. 160–167 (in Japanese).

Treagear, T. R., (1965) A Geography of China: Aldine Publ. Co., Chicago, 342 pp.

Udintsev, G. B., G. V. Agapova, A. F. Bereznev, L. Ya. Boudanova, L. K. Zatonskiy, N. L. Zenkevich, A. G. Ivanov, V. F. Kanaiev, I. P. Koutcherov, N. I. Larina, N. A. Marova, V. Mineiev, and E. I. Rantskiy, (1963) The new bathymetric map of the Pacific: Okeanolog. Issled., Rez. Issled., Progr. Mezhd. Geofiz. Goda, Mezhd. Geofiz. Kom., Prezidiume, Akad. Nauk, SSSR, no. 9, pp. 60–101.

Umbgrove, J. H. F., (1947) The Pulse of the Earth: Martinus Nijhoff, The Hague, 358 pp.

Wang, C. S., (1961) Sand-fraction study of the shelf sediments off the China coast: Proc. Geol. Soc. China, no. 4, pp. 33–49.

Yabe, H., and R. Tayama, (1934) Bottom relief of the seas bordering the Japanese islands and Korea: Earthquake

Res. Inst., Tokyo Imperial Univ., Bull. vol. 12, pp. 539–565 (in Japanese).

Yamamoto, Eichi, Shiro Hinokuma, Sadao Iesaka, Norio Arimatsu, and Tetsuo Nishi, (1967) Geological exploration of Mitsuse and Hashima offshore area in the Takashima coal field: Mining Geology, vol. 17, no. 84, pp. 200–213 (in Japanese).

Yanshin, A. L. (chief editor), (1966) Tectonic Map of Eurasia, scale 1:5,000,000, twelve sheets, Akademia Nauk SSSR, Ministerstvo Geologii.

Zenkovich, V. P., (1967) Processes of Coastal Development: Oliver & Boyd, London, 738 pp.

Blank page

Page blanche

REPORTS ON THE SEISMIC REFRACTION SURVEY ON LAND IN THE WESTERN PART OF TAIWAN, REPUBLIC OF CHINA

By

K. Sato[1], C. Y. Meng[3], J. Suyama[1], S. Kurihara[2]
S. Kamata[1], H. Obayashi[2], E. Inoue[1], and P. T. Hsiao[3]

ABSTRACT

During the period 20 June 1968 to 6 August 1968, seismic refraction survey on land was conducted. The study was the first China—Japan joint work for the off-shore geological prospecting. The purpose of this investigation was to obtain the basic data for further exploration in the Taiwan strait and in the nearby area. The four traverse lines were selected within the west coast of Taiwan individually and the total length was approximately 160 km.

The subsurface deep structures up to 5 km and the following interesting results were revealed.

(1) The Miocene formation in the west coast of Taiwan indicates a higher velocity than the Tertiary formation in Japan and in other territory.
(2) The depths of the basement are unexpectedly deep and the minimum possible depth of the basement would be estimated more than 7 km.
(3) The lateral change of seismic velocity was recognized near the hinge belt.
(4) The thickness of the Miocene formation would gradually increase basin ward.
(5) The composite interpretation suggests that another shelf may extend in the south-west part of Taiwan strait.

INTRODUCTION

The scope of the project

The project of the seismic refraction survey on land was discussed at the fourth session of the Committee for Co-ordination of Joint Prospecting of Mineral Resources in Asia Off-shore Area. The purpose of the survey was to study the subsurface deeper structural feature including the basement structure, in the west coast of Taiwan. Four traverse lines were selected within the region and the total length of the traverse line was approximately 160 km.

After the diplomatic agreement between the Japanese government and the government of Republic of China, nine member and two sets of seismic instruments, including accessories and wireless communication systems, were provided by the Japanese government. The government of Republic of China also offered thirty-three member, preparatory work, material including dynamites and other facilities. The Japanese mission was responsible for the technical execution of the project including field operation, analysis and interpretation of field data and the preparation of the report of the survey. The Government of Republic

1) Geological Survey of Japan.
2) Ube Industries Ltd.
3) Chinese Petroleum Corporation.

of China also sent the one geologist for the joint geologic interpretation of the surveyed result undertaken in Japan.

Field work was performed during the period 20 June 1968 to 6 August 1968 with the intimate joint effort between the chinese organization concerned and the Japanese mission.

Selection of traverse line

Four separated traverse line were selected by Dr. C. Y. Meng, chief geologist of Chinese Petroleum Corporation (see Fig. 1)

Traverse line 1, whose length is 42.7 km, runs from Hsinchu[1] to Yuanli[2] along the coast and is parallel to the major structural trend. It passes through Tiehchenshan[3] gas field. The results of this line will be the most important reference data to the future marine seismic survey.

Traverse line 2 is approximately trending north-south perpendicular to the major structures, such as Pingchen[4] and Hukou[5], and runs from Kuanyin[6] to Kuanhsi[7]. The length of this line is 33.7 km.

Traverse line 3, whose length is 45.1 km, is approximately NE–SW in direction, and runs from Wufeng[8] south west ward across the Pakuashan[9] anticline and the Hsilo-chi[10] River to Lungpei[11]. To the east of the Pakuashan anticline is the center of the Taichung[12] basin, where the gravity low is shown, and to the south west of this line is the Peikang[13] Massif.

Traverse line 4 is nearly in NW–SE direction and its length is 32.2 km. It runs from Entungli[14], north of Tainan[15] city, across the northern plunge of the Tainan anticline and the Chungchou[16] anticline.

GEOLOGY

Outline of Geology of Western Taiwan (see Fig. 1)

The western Taiwan is the west of the Central Ranges Province which is the site of the Tertiary geoanticline and the nucleus of the Taiwan tectonic frame work. The sedimentation and the tectonics of the western Taiwan have been affected by the tectonic movement from the Central Ranges. During Neogene time, the eastern part of the region was a great asymmetrical geosynclinal trough and the western part was a stable shelf area.

The basement rocks and the Peikang and the Kuanyin shelves

The sediments occurring in the region are the Neogene and the Quaternary. The underlying older rocks, the basement rocks, are not exposed on the region. The basement rocks have been revealed at the depth of less than 1500 meters in the subsurface of Peikang near the Chiayi[17] city of the middle of the region by several stratigraphic test well of C.P.C. The rock at Peikang are composed mostly of sandstones and shales containing fragments of lower Cretaceous ammonites. Except the Peikang area, the basement has not been discovered throughout the region up to day.

The thickness of the Miocene series in the Peikang area is remarkably thinner than in other areas. It is considered that the Peikang area, in Miocene time, was ridge-like shelf composed of Mesozoic massif trending E–W from the Pescadores Channels to Peikang and

1) 新竹 2) 苑裡 3) 鉄砧山 4) 平鎮 5) 湖口 6) 観音 7) 関西
8) 霧峯 9) 八卦山 10) 西螺渓 11) 崙背 12) 台巾 13) 北港 14) 渕東里
15) 台南 16) 中州 17) 嘉義

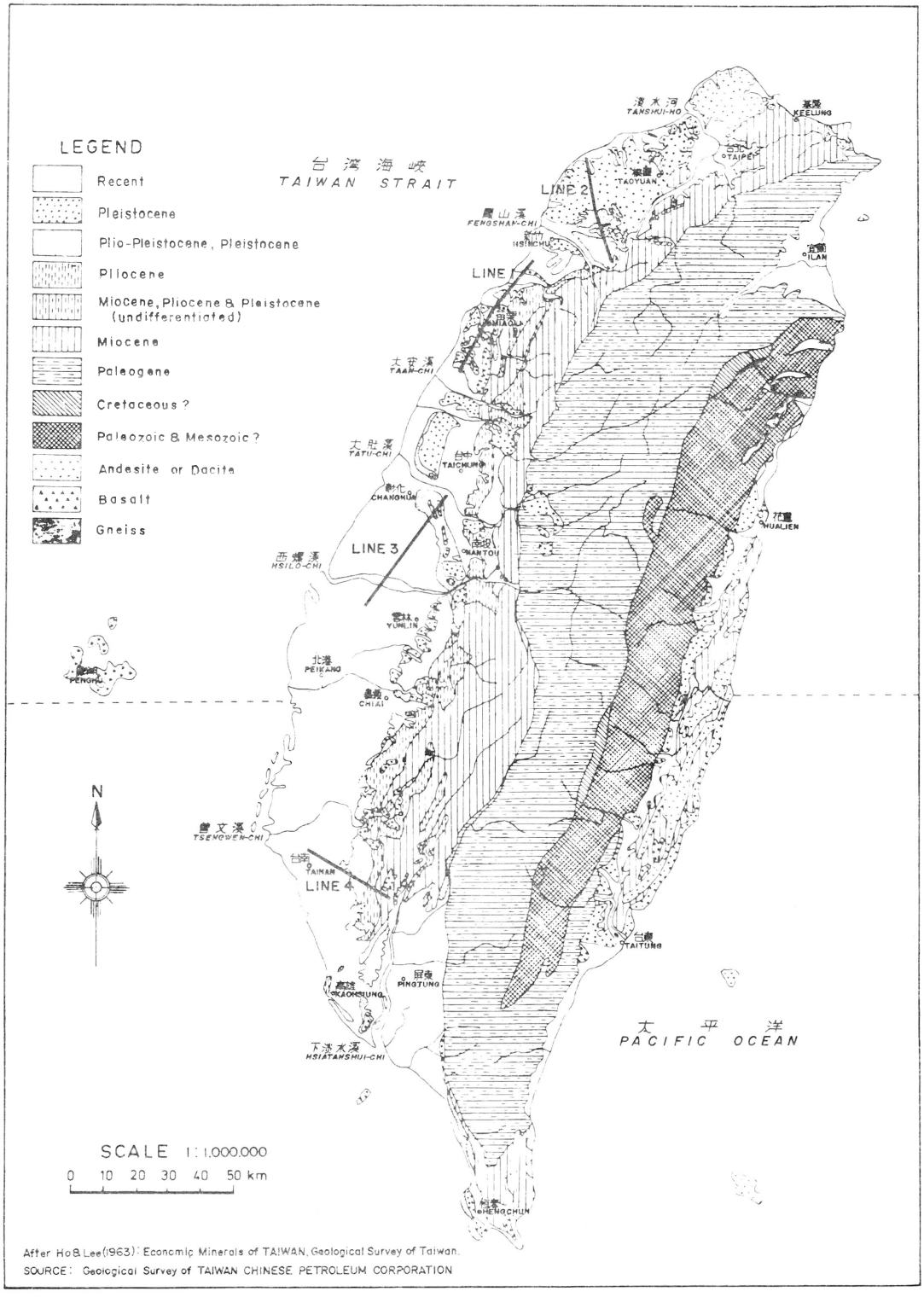

After Ho & Lee (1963): Economic Minerals of TAIWAN, Geological Survey of Taiwan.
SOURCE: Geological Survey of TAIWAN CHINESE PETROLEUM CORPORATION

Figure. 1 Map showing outline of geology and location of seismic refraction traverses.

Table 1. Tentative Correlation Chart of Western Taiwan Neogene Strata.

時代 Age		北部台湾 Northern TAIWAN		北—中部台湾 North-Central TAIWAN		中—南部台湾 South-Central TAIWAN	南部台湾 Suthern TAIWAN
鮮新～更新世 Plio-Pleistocene		頭嵙山層 TOUKOSHAN F.	火炎山相 HUOYENSHAN Facies	頭嵙山層 TOUKOSHAN F.	火炎山相 HUOYENSHAN Facies		
			香山相 HSIANGSHAN Facies		香山相 HSIANGSHAN Facies	六双層 LIUSHUANG Formation	B層 B Formation
						二重溪層 ERHCHUNGCHI 〃	A層 A Formation
鮮新世 Pliocene		卓蘭層 CHOLAN Formation		卓蘭層 CHOLAN Formation		坎下寮層 KANHSIALIAO 〃	上部古亭坑層 Upper GUTINGKENG F.
						六重溪層 LIUCHUNGCHI 〃	下部古亭坑層 Lower GUTINGKENG Formation
						雲水溪層 YUNSHUICHI 〃	
						烏嘴層 NIAOTSUI 〃	
		錦水頁岩層 CHINSHUI Shale		錦水頁岩層 CHINSHUI Shale		中崙層 CHONLUN 〃	
中新世 Miocene	上部 Upper	桂竹林層 KUEICHULIN Formation		桂竹林層 KUEICHULIN F.	大窩細砂岩 TAWO Siltstone	竹頭崎層 CHUTOUCHI 〃	坑内層 KENGNEI Form. (木柵層 MUCHA F.)
						茅埔頁岩 MAUPU Shale	
						隘寮腳層 AILIAOCHIAO F.	
					十六份頁岩 SHIHLIUFEN Sh.	塩水坑頁岩 YENSHUIKENG Sh.	
					關刀山砂岩 KUANTAOSHAN S.S.	糖恩山砂岩 TANGENSHAN S.S.	
		南庄層 NANCHUANG Formation		上福基砂岩 SHANGFUCHI S.S.		長枝坑層 CHANGCHIHKENG F.	
				河排層 HOPAI F.	東坑層 TUNGKENG F.	紅花子層 HUNGHUATZU F.	
	中部 Middle	南港層 NANKANG Formation	南港砂岩 NANKANG S.S.		觀音山砂岩 KUANYINSHAN S.S.	水裡坑層 SHUILIKENG F. (和社層 HOSHE F.)	三民層 SHANMIN Formation
			蒸合層 TSOOHP F.		打鹿頁岩 TALU Shale		
				北寮層 PEILIAO F.	北寮砂岩 PEILIAO S.S.		
		石底層 SHIHTI Formation		石底層 SHIHTI F.	出磺坑層 CHUHUANG-KENG F.	大坑層 TAKENG Formation	
	下部 Lower	大寮層 TALIAO Formation		大寮層 TALIAO F.	碧雲頁岩 PILING Sh.	粗坑層 TSUKENG Formation	
		木山層 MUSHAN Formation		木山層 MUSHAN Formation			
		五指山層 WUCHIHSHAN F.		五指山層 WUCHISHAN F.			
古第三紀 Paleogene		烏来層群 WULAI Group					

separated the northern and the southern depositional basin from each other. The shelf is called the Peikang shelf. Although the basement lies at too great depth for discovery in other areas, it is estimated that another shelf exists in the north western margin of the region according to geologic informations obtained by C. P. C. The shelf estimated is called the Kuanyin shelf, in which the basement is presumed to underlie the Miocene series at the comparatively shallow depth and the Miocene series is thinner. The shelves mentioned above would extend to the Taiwan strait from the western coastal part of the region.

There is relationship between the thickness of the Miocene and the buried depth of the basement in the region.

Miocene Series

The Miocene series contains petroleum and gas reservoir rocks and atlains the composite thickness of over 4,000 meters. It consists of marine flysch-type sediments deposited in the geosyncline and of non-marine and brackish sediments formed near and in the shelves; the latter sediments are developed in the northern areas and the former are predominant in the southern areas. Generally the series becomes thinner from east to west and is the thinnest in the Peikang and the Kuanyin shelves.

There are distinct differences in the Miocene sedimentation between the north and the south sides of the Peikang shelf area. The differences are summarized as follows.

1) The Miocene series is divided into three stratigraphic parts by sedimentary cycle, but it cannot be divided into such the parts on the south side. It seems that the lower part of the series is lack in the south side.
2) The middle and the upper parts of the series in the south side are much thicker and more predominant in mudstones than those in the north side.
3) The non-marine sediments are distributed in the north side, but they thin out in the south side.

As the lithofacies and the thickness of the series vary from place to place, the different stratigraphic divisions and the local formations of the series have been established by various authors. Table 1 shows a tentative correlation of them of the Miocene series.

Pliocene and Quaternary Strata

The Pliocene series overlying the Miocene conformably is developed west of the area where the Miocene series is distributed. The Pliocene series consists of marine flysch-type sediments of the thickness of about 2,000 to 3,000 meters. The series becomes thicker and of finer grade southwards; that is, the series is composed mostly of thick and massive mudstones in the southern areas. The petroleum and gas reservoir rocks are not found whithin the series up to day.

The Plio-Pleistocene series overlying the Pliocene conformably or slight disconformably is composed mainly of thick molasse-type sediments deposited during the early period of the post-Pliocene orogenic movement. The thick and massive conglomerates of fluvial and deltaic deposits occupying the upper part of the series are extremely developed in the northwestern area near the coast. The total thickness of the series is over 2,000 meters.

During or after the deposition of the Plio-Pleistocene series, the Neogene strata were strongly deformed by tectonic compressions from east to west or from the Central Ranges to the western stable shelf area.

The Quaternary strata are composed of the lateritic deposits forming tableland planes of the northwestern Taiwan, the terrace deposits and the alluvium covering the coastal plains.

STRUCTURES

The trend of the main tectonic lines is N.–S. or N.E.–S.W. in the middle and the southern areas and is E. N. E.–W. S. W. or E.–W. in the northern area of the region. This trend represents also the major pattern of the axial trends of petroleum and gas producing structures in the western Taiwan. As the tectonic forces come from east to west throughout the post-Pliocene orogenic movement, the tightness of the folds decreases westwards and the structures become gentler to west. The folds in the eastern part of the region are tight, are overturned to west in places and are disturbed by thrust faults along their axes, on the other hand, the folds in the western part are broad and gentle, and the faulting is less effective as compared with the eastern part. These gentler folds in the western part are more favorable structures for petroleum and gas accumulation than the tight folds in the eastern part. In the western margin of the region, specially in the Peikang and the Kuanyin shelf areas, there are not folded structures, but gently tilted structures to east or to south at lower angle than 20°.

Most of the faults run parallel to the directions of the fold axes and shift the fault blocks westwards with a large amount of their down-throws. These thrust faults have high angle planes usually, but a few of them are over-thrusts with low angle planes.

There are normal faults trending E–W in the south part of the Peikang shelf area.

Geological Notes on the Areas along the Traverse Lines and Purposes of the Refraction Seismic Survey.

1) Traverse line–2

The area where the traverse line–2 runs N–S is the northwestern part of the region and comprises two geological provinces; the northern province is the Kuanyin shelf and the southern province is a site of the Miocene geosynclinal trough.

The Miocene strata become thinner and dip southward gently in the Kuanyin shelf area, on the other hand the strata become thicker and are structurally deformed in the southern province. The basement is presumed to rise up to north or to the shelf from south by the petroleum explorations of C. P. C. Throughout the area there are three anticlinal structures which appear to be favorable to produce petroleum and gas; namely, the Pingchen[1], the Hukou[2] and the Tungkeng[3] anticlines from north to south. They have anticlinal axes trending E–W and are disturbed by great faults running along the axes.

The main purposes of the present seismic survey in the area are to get the geologic information with regard to the gradient of the basement downslope southwards and to know the subsurface structures of these anticlines expected as the petroleum and gas production structures.

2) Traverse line–1

The traverse line–1 runs parallel to the coast line near the northwestern margin of the region. Geologically the area containing the traverse and the Tiehchenshan[4] gas field consists of the Miocene, the Pliocene and the Plio-Pleistocene strata which are folded rather gently. The traverse line runs along the Tiehchenshan-Tunghsiao[5] anticlinal axis. The abundant geological data have been obtained by the geological and geophysical explorations of C. P. C. in this field. The subsurface structures in the area are then known well, but the

1) 平鎮　2) 湖口　3) 東坑　4) 鉄砧山　5) 通宵

depth of the basement has been still unknown. The seismic survey along the traverse line has been carried out in order to know the depth of the basement and to add the useful and basic data for further explorations in the Taiwan strait and in the nearby areas.

3) Traverse line–3

The area where the traverse line runs N.E.–S.W. across the Pakuashan[1] hills is located in the middle part of the region and extends from the north part of the Peikang shelf area to the south part of the Taichung basin. There are important changes in the thickness, the stratigraphy and the lithofacies of the Miocene series between the northern and the southern parts of the area. Namely, the changes are due to the differences in depositional environments between the Peikang shelf and the Taichung depositional basin. The basement slopes down to the Taichung basin from the shelf, and the Miocene series becomes thicker to north from south. The lack of the lower part of the Miocene series is recognized in the Peikang shelf. According to the geological and geophysical explorations of C.P.C., it is presumed that the location of the radical changes in the gradient of the basement down-slope and in the Miocene stratigraphy may be situated near the west of the Pakuashan anticline.

The main purposes of the seismic survey are to know the gradient change of the basement down-slope northward and to know the subsurface structure of the Pakuashan anticline which is considered to be a favoured structure for petroleum and gas production.

4) Traverse line–4

The traverse line runs between the north of the Tainan[2] city and the west of Chishan[3]. The eastern half of the area is occupied with the foothills composed of the thick Pliocene and the Miocene mudstones, and the western half of the area is a coastal plain covered by alluvium.

The structures of the Neogene strata are complicated in the eastern half, but they are gentler folds in the subsurface of the western half; namely, there are the Tainan and the Chungcho[4] anticlines composed of very thick Pliocene mudstones. The seismic survey has been made to know the shape of the base of the anticlines and the depth of the basement.

SEISMIC REFRACTION SURVEY

Field Operation

Prior to the seismic operation, drilling of the shot-hole, positioning of shot-point and spread, and other preparatory work had been completed by members of C. P. C. The acquisition of seismic data, which was done by the joint operation, was commenced on 22 June 1968 and terminated on 3 August.

Due to the reconnaissance character of the survey, each four traverse line consisted of three shot point and nine or twelve spreads. One of the shot point was located in the center of traverse line and the other two shot point were located at the both ends of traverse line. The spreads were intermittently arranged and each spread consisted of twenty-four geophone stations. Normally, the separation of the geophone station was selected 100 meters but, in the case of the mountainous terrain and of the spread obliquely crossing with traverse line, the separation of the geophone station was taken as 75 meters. Near the shot-point,

1) 八卦山　2) 台 南　3) 旗 山　4) 中 州

three geophone stations were located at 30 meters, 50 meters and 100 meters aparts from the shot point. The length of traverse line, the number of the shot point and the spread are tabulated in Table 2.

The magnetic recording system and the high sensitivity geophone having low frequency response were used to detect the seismic wave from the distant shot point at the good signal noise ratio.

The magnetic recording system also has a particular advantage for detecting the later phase arrival of seismic waves, but some minor modifications of device and operation were needed to adjust the recording time.

Office Work

Immediately after the termination of the field operation, all of the personnel return to Miaoli and equipment was crated for shipment. The necessary data were also sent back to Japan for undertaking the interpretation. The geologic interpretation of the result of the seimic refraction survey was also undertaken as joint work in Japan.

The processing of the seismic data was conducted in following manner.

(1) The measured travel time of first and later arrival were corrected for the variation in the surface elevation of shot point and geophone station, for the change in the thickness of the weathered layer from up hole time and for the off set arrangement of spread.

(2) The plotted travel time curve were regulated with regard to the basic law which controlled the transmission of the refracted seismic wave; that is, reciprocity of travel time, equality of each intercept time for the corresponding travel time curve measured by a shot point, parallelism of the corresponding segments of travel time curve measured by several shot points, etc.

(3) The seismic refraction profiles were determined from the regulated travel time curves. The refraction interface could be obtained by the envelop of circular arc, whose radius is given by the normal depth to the refraction interface, drawn from the each geophone station. The normal depth from the geophone station to the refraction interface could be easily calculated by the use of the electronic computer from the mathematical relations between the zero travel time and the normal depth to the refraction interface. The zero travel time curve defined at any geophone stations is the imaginary travel time which is obtained as the difference between the sum of travel time from the two shot points to the geophone station and the travel time between two shot points. Practically, if the distance from a shot point to each geophone stations, zero travel times at each geophone stations and apparent seismic velocities are obtained from the regulated travel time curves, the normal depth to the refraction interface at each station and velocity and dip angle of velocity layer are calculated from the ordinary mathematical equations of the refracted seismic wave for the dipping multilayered structure. The seismic refraction profiles were deduced from the refraction interfaces obtained by the envelops of circular arc and then were reexamined by the ordinary graphical interpretation method.

RESULT AND ITS INTERPRETATION

Figs. 2 to 5 show the regulated travel time curves and the corresponding interpretated seismic sections. Each seismic section consists of five to seven velocity layers, which might be summarized as shown in Table 2. The first column of Table 2 indicates the geologic interpretation for the distribution of velocity layers, which would be deduced from the known

Table 2. Summarized results of distribution of velocity layers in western parts of Taiwan.

	Velocity Layer	Seismic Wave Velocity		
		Northern Portion (Traverses 1, 2)	Central Portion (Traverse 2)	Southern Portion (Traverse 4)
Plio-Pleistocene	1st Layer	1,700～1,900 m/s	1,500 m/s 1,950～2,000 2,200～2,550	1,810～1,850 m/s 2,050～2,080 m/s
Pliocene	2nd Layer 3rd Layer	2,100～2,300 2,400～3,200	2,850～3,540	2,420～2,560 2,900～3,080 3,630～3,850 4,000 (Blind Layer)
Miocene	4th Layer 5th Layer 6th Layer	3,000～3,840 3,690～4,430 4,340～5,190	3,800～4,330	4,000 (Blind Layer) 4,310～4,730
Cretaceous (?)	7th Layer 8th Layer		5,230～5,460 5,620～5,860	

Table 3. Summary of seismic wave velocities of Cenozoic formation and its basements rocks on coal fields in Japan. after K. IIDA et al.

Area		Seismic Wave Velocity		
		Tertiary	Basement	Rock and Formation
Hokkaido	Kushiro Ishikari	1,700～3,100 m/s 2,000～3,800	3,800～3,900 m/s	Cretacieous, Sediment
Eastern Honshu	Jōban	2,000～3,800	4,400～5,500 m/s	Cenozoic, Paleozoic Sediment Schist
Western Honshu	Ube	2,200～2,700	4,200 m/s–	Schist, Cenozoic Granite, Metamorphic
Northern Kyushu	Kokura	2,100～3,700	4,500 m/s–	Granite, Volcano
	Chikuho	3,500～3,500	4,500 m/s–	Granite, Paleozic
	Kasuya	2,100～3,500	4,500 m/s–	Granite, Metamorphic
	Fukuoka	2,000～3,500	4,600 m/s–	Granite
	Miike	3,000～3,500	4,500 m/s–	Granite, Schist

geologic data, the well shooting data and the velocity data of rock samples.

From this, it is considered that the Miocene formation already known in the northern portion of the western coast part of Taiwan could be divided into three velocity layers but, in the central and southern portions, the known Miocene formations would correspond to a single velocity layer. But unfortunately the relationship between the distribution of these velocity layers and the stratigraphic parts divided by sedimentary cycle and the geologic interpretation of this phonomena are not yet clarified. These Miocene formations also have higher seismic wave velocity than that of the Tertiary formations in Japan (see Table 3) and in other territory.

Therefore, the selection of longer traverse line, exactly speaking, longer distance between shot point and geophone station, would be necessary to detect the subsurface deeper structure underlying the upper part of the Miocene formation.

Scale 1 : 200000

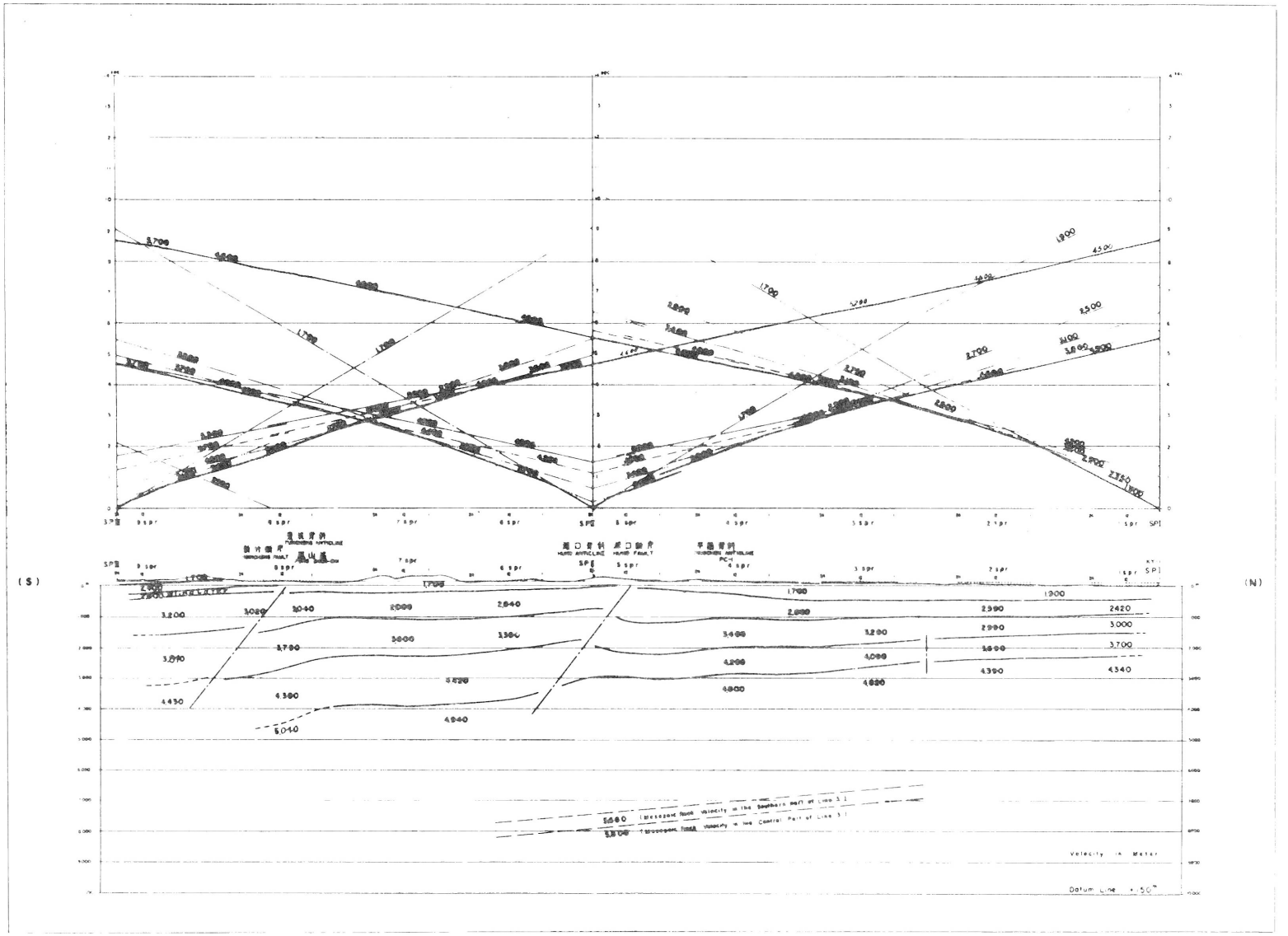

Figure 2. Travel-time curves and seismic refraction profile of traverse line 2.

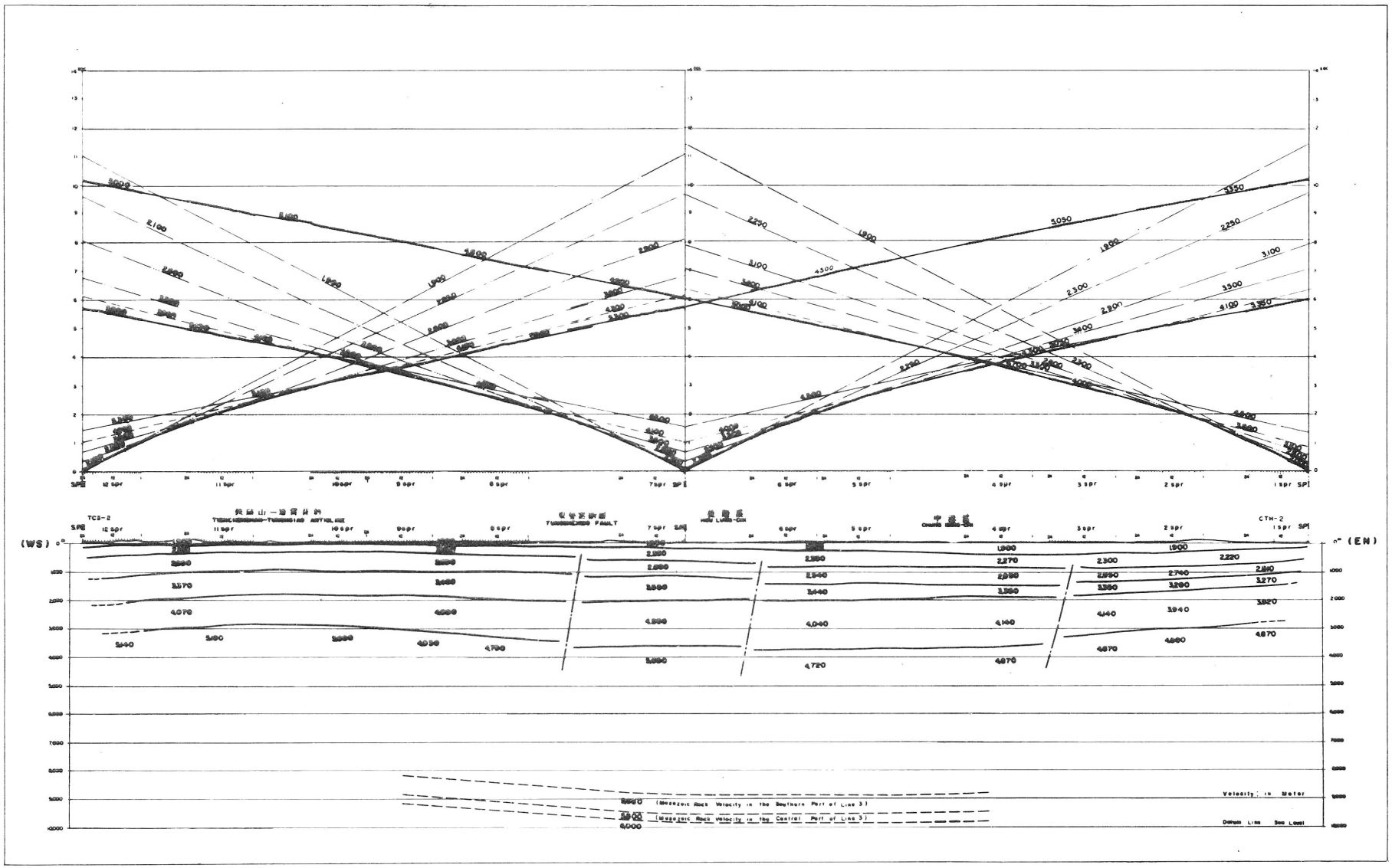

Figure 3. Travel-time curves and seismic refraction profile of traverse line 1.

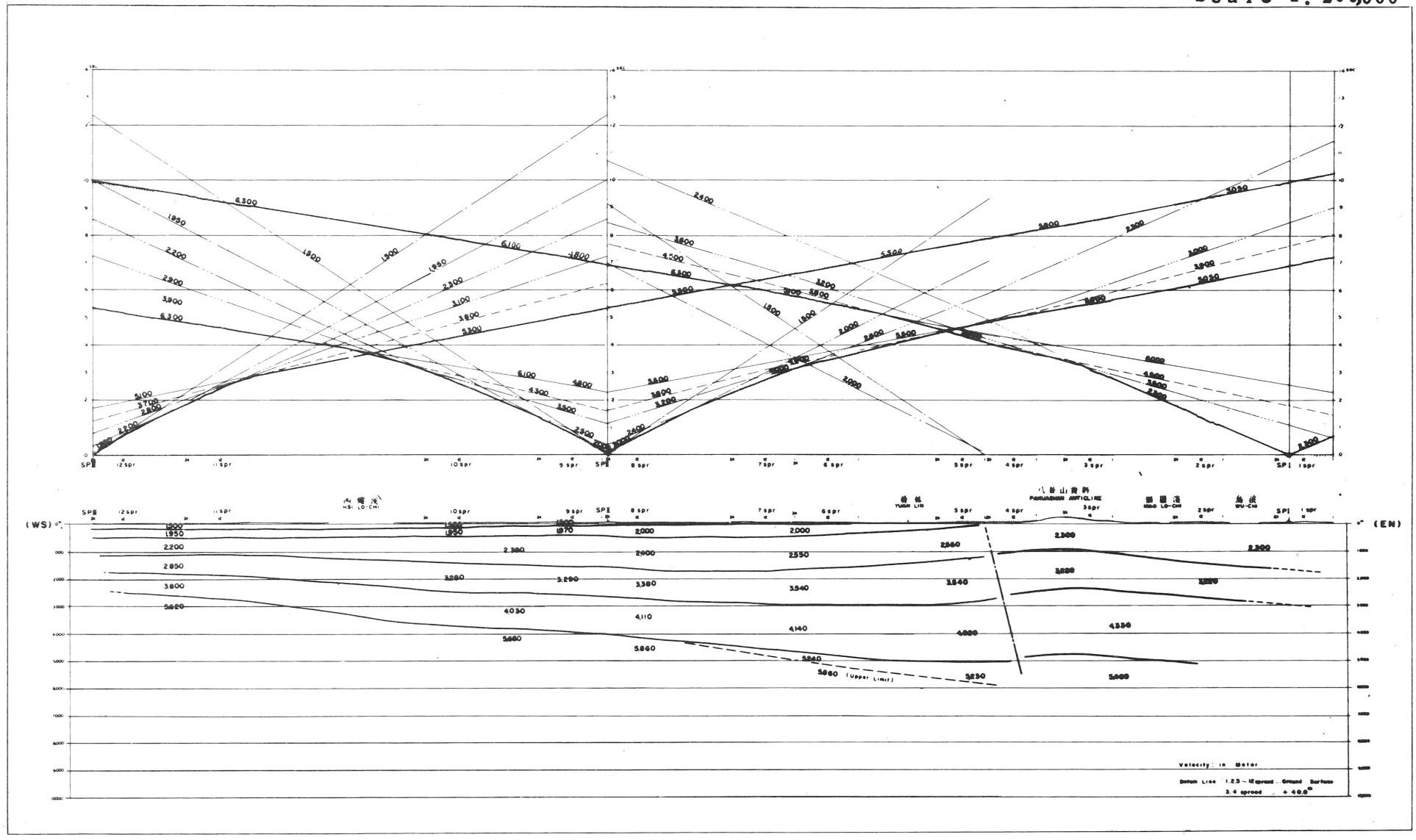

Figure 4. Travel-time curves and seismic refraction profile of traverse line 3.

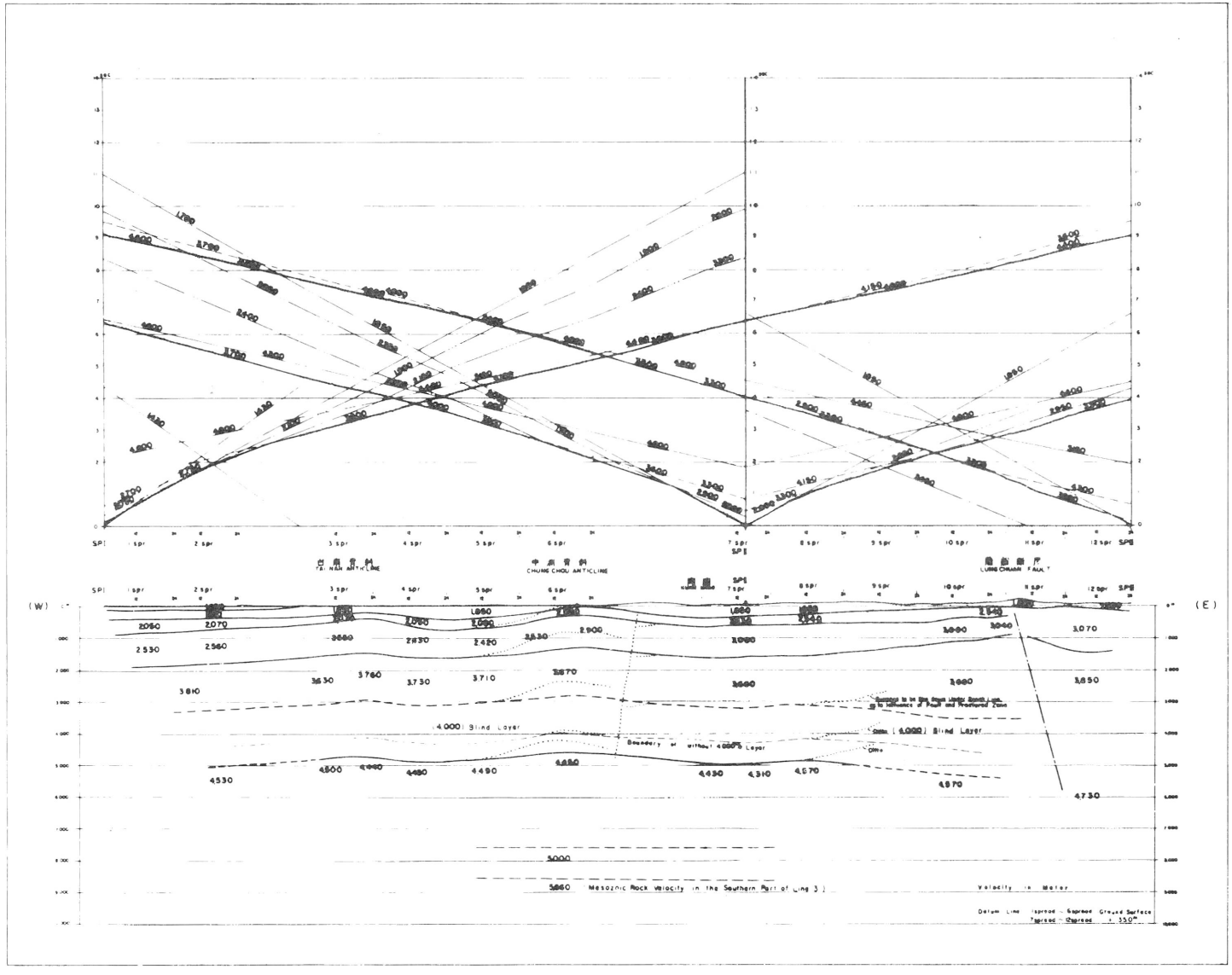

Figure 5. Travel-time curves and seismic refraction profile of travers line 4.

The seismic refraction profiles of traverse line 1, 2, and 3 show that the lateral changes of seismic wave velocities would possibly occur near the hinge belt of the basin deduced from the known geologic data, and the velocities inside of the hinge belt are lower than the velocities outside of it. Since the same formation at a greater depth will usually have a higher velocity and the depth of burial may increase outside of the hinge belt, the lateral change of seismic wave velocity might be affected by the change of the buried depth of the formation. However, the lateral change of seismic wave velocity mentioned above would not be controlled by the change of the depth of burial and it rather should be seen as a characteristic feature of the hinge belt which might be closely related to the depositional and tectonic history of this region. In other words, this lateral change of seismic wave velocity suggests the possibility of a sharp change in lithofacies and thickness of the sediments which would be anticipated to occur in the hinge belt of the basin.

With regards to the lateral change of seismic wave velocity of the lowest layer in traverse line 3, only the western portion of the upper interface of this layer, whose velocity is 5,660 m/s, could be traced as a good reflector obtained by the seismic reflection survey of C. P. C., and the velocity of the eastern portion shows the similar velocity of the lowest layer of traverse line 1. From this, the western portion of the lowest layer would be possibly corresponds to the basement and the other would be probably correlated with the middle or lower Miocene series. Because of the higher velocity of Neogene formation, the depth of the basement could not be detected directly from the observed travel time curve, except the western half of traverse line 3. However, the minimum possible depth of the basement, whose velocity would be assumed as 5660 m/s, was estimated from the seismic refraction profile, which showed the velocity distribution of the upper part of the subsurface structure, and the observed travel time curve. The seismic refraction profiles and the estimated minimum possible depth of the basement (shown by broken-line in seismic refraction profile) presumably suggest that the thicker Miocene sediments would develop in the area, at which the pre-Tertiary basement deeply lied.

From the composite interpretation of the surveyed result, it can be seen that the geologic situation on the area along traverse line 2, 3 and 4 are similar in each other. The tentative correlation of the geologic structure on these area suggest that the synclinal structure observed in the western end of traverse line 4 would possibly correspond to the synclinal structure located at the north-west side of the Pingchen anticline and to the synclinal structure developed at the west side of the Pakuashan anticline. Since the latter two synclinal structures are situated near the hinge belt of Kuanyin or Peikang shelf, it is possible to consider that the hinge belt of another shelf would exist near the western end of traverse line 4. Therefore, the tentative interpretation possibly indicates that another shelf may extend in the south-east part of Taiwan strait.

CONCLUSION

The joint seismic refraction survey of both Japan and Republic of China was efficiently and fruitfully performed. The results of this investigation also would be believed to contribute the further exploration in Taiwan strait and in the nearby area.

The interesting conclusions derived from the interpretation of the seismic data are presented as follows.

(1) Because of the unexpectedly deeply lying basement and the higher velocity of the Miocene formation, the buried depth of the basement could not be detected directly from the

travel time curve, except the western half of traverse line 3. However, the estimated minimum possible depth of the basement would be more than 7,000 meters.

(2) In the Miocene formation, the lateral change of seismic wave velocity was recognized near the hinge belt of the basin. The velocity outside of the hinge belt is higher than inside of it.

(3) In the area, at which the depth of the basement is greater, the thickness of the Miocene formation would increase.

The conclusions of (2) and (3) would be closely related with the depositional and tectonic history of the development of the Tertiary deposits in the western coast part of Taiwan.

(4) From the similarity of the geologic situation, the tentative correlation among the profile along traverse line 2, 3 and 4 suggests the possibility of the extension of another shelf in the south-east part of Taiwan strait.

ACKNOWLEDGEMENT

The authors wish to express their sincere thanks to the staff of Chinese Petroleum Corporation for their kind assistance.

They are indebted to the Government of Republic China which have authorized the use of data contained in the report.

REFERENCES

Biq, C.C., (1959): The structural patern of Taiwan compared with the eta type of shear form, Geol. Soc. China Proc. no. 2.

——, (1965): The east Taiwan rift, Ptr. Geol. Taiw. no. 4.

Chang, S.S.L. (1963): Regional straitigraphic study of Pleistocene and upper Pliocene Formations in Chiayi, Petr. Geol. Taiw. no. 2.

——, (1964): Regional straitigraphic study of the lower Pliocene and upper Miocene formations in the Chiayi and Hsinying area, Taiwan, Petr. Geol. Taiw. no. 3.

Chiu, H.T. (1967): Straitigraphic correlation of subsurface formations in northwestern Taiwan, Petr. Geol. Taiw. no. 5.

Fujinaga, Y. & Kumano, T. (1968): Some Examples of Computer Application to Analysis and Computation in Geophysical Prospecting, Geophysical Exploration, Vol. 21, no. 2.

Heh, K. & Hsiao, P.T., (1957): Geology of the Tunghsiao anticline, Miaoli district, Symposium, Petr. Geol. Taiw.

Ho, C.S., Tsan, S.F. & Tan, L.P. (1956): Investigation report on the Chichitashan coal field Taiwan, China, coal exploration.

Ho, C.S. & Lee, C.N. (1963): Economic minerals of Taiwan, Geological Survey of Taiwan, China.

Hsiao, P.T. (1957): Subsurface data from ST-1 on the Shantzechiao structure, Taoyuan district, Taiwan, Symposium, Petr. Geol. Taiw.

Hsu, C.S., (1957): Stratigraphic column on west flank of the Lungchuan fault, Kuanmiao section, C.P.C. file.

Huang, T. & Lee, P.J., (1962): Straitigraphy of the Kuanyin well, Taoyuan, and its relation to that of the Peikang well, Yunlin, Taiwan, Petr. Geol. Taiw. no. 1.

Huang, T. (1963): Planktonic foraminifera from the Peikang PK-3 well in the Peikang shelf area, Yunlin, Taiwan, Petr. Geol. Taiw. no. 2.

Iida, K., Fuchida, T., Hayakawa, M., Hattori, Y., Kaneko, T., & Omote, S., (1951): Compilation of Coal Seismic Exploration Data in Japan, Geophysical Exploration, Vol. 4, no. 2.

Lee, P.J., (1962): Mesozoic and Cenozoic rocks of the Paochung well, Yunlin, Taiwan, Petr. Geol. Taiw. no. 1.

Kurihara, S., (1960): On the Regulation of Travel-Time Curve of Refraction and the Analysis of Zero-Travel-Time, Journal of Mining Institute of Kyushu, Vol. 28, no. 4.

——, (1964): The Studies on the Charge Amounts Used in Seismic Method and the Density of Rays of the Refracted Wave Produced by Explosion, Journal of Mining Institute of Kyushu, Vol. 32, no. 10., no. 11.

Makiyama, J., (1934): Explanatory text of the geological map of Taiwan, Tyureki sheet, Bereaw of Productive Industries, Government Central of Taiwan Pub. no. 692.

Matsumoto, T., Hayami, I. & Hashimoto, W. (1965): Some molluscan fossils from the buried Cretaceous of western Taiwan, Petr. Geol. Taiw. no. 4.

Meng, C.Y., (1965): Lateral movement in the northern half of western Taiwan, Petr. Geol. Taiw. no. 4.

——, (1968): Geologic concepts relating to the petroleum prospects of Taiwan Strait, Bull. Vol. 1., Committee Coordination Joint Prospecting, ECAFE

Pan, Y.S., (1960): Report on seismic survey conduced on Taiwan prospect, Taiwan, C.P.C. file.

——, (1963): Seismic Velocity Distribution in the Cenozoic Sequence in the Plain Areas of Taiwan, no. 2.

——, (1965): Interpretation and seismic coordination of the Bouguer gravity anomalies obtained in northwestern Taiwan, Petr. Geol. Taiw. no. 4.

——, (1965): Interpretation and Seismic Coordination of the Bouguer Gravity Anomalies Obtained in Northwestern Taiwan, no. 4.

——, (1967): Interpretation and seismic coordination of the Bouguer gravity anomalies over west central Taiwan, Petr. Geol. Taiw. no. 5.

Schreiber, A. (1965): On the geology of the Cenozoic geosyncline in middle and northern Taiwan (China) and its petroleum potentialities, Petr. Geol. Taiw. no. 4.

Shih, T.T. (1967): A survey of the active mud volcanoes in Taiwan and a study of their types and the character of the mud, Petr. Geol. Taiw. no. 5.

Stach, L.W., (1956): Petroleum potentialities and exploration for oil in Taiwan, Symposium on Petroleum Geol. Taiw.

——, (1958): Subsurface exploration and geology of the coastal plain region of western Taiwan, Geol. Soc. China Proc., no. 1.

Sun, S.C. (1964): Photogeologic study of Tainan Kaoshung coastal plain area, Taiwan, Petr. Geol. Taiw. no. 3.

——, (1965): Geology and petroleum potentialities of the Chinshui-Yuanlin area, Taiwan, Petr. Geol. Taiw. no. 4.

Tang, C.H., (1963): Geology and oil potentialities of the Hukou anticline, Hsinchu, Petr. Geol. Taiw. no. 2.

——, (1964): Subsurface geology and oil potentialities of the Taoyuan district, Petr. Geol. Taiw. no. 3.

Wang, Y.L. & Chang, S., (1957): Coordination of data from the Chungchou wildcat and seismic survey in the Tainan district, Symp. Geol. Taiw.

Wang, C.M., (1964): Reflection seismic survey conduced on Hukou-Yangmei structure, Taiwan, Petr. Geol. Taiw. no. 3.

NEW DEVELOPMENTS CONCERNING THE HIGH SENSITIVITY CSF MAGNETOMETER

By
G. Royer, Compagnie Générale de Géophysique, Paris, France
(with figures 1–13)
(Submitted to the fifth session of CCOP as document I&NR/R.84)

SUMMARY

New developments concerning the use and application of the high sensitivity CSF[1)] magnetometer include the following: (a) extensive experiments on sedimentary basins in many parts of the world; (b) standardization of measurements; (c) improvements on new equipment and especially in radio-navigation recordings; (d) development of processing, compilation and interpretation; and (e) use of digitalization for aeromagnetic mineral surveys.

WORLD-WIDE UTILIZATION OF THE CSF MAGNETOMETER

According to statistics published in the journal "Geophysics" it is evident that airborne surveys made with the CSF magnetometer represent a large percentage of the airborne magnetic surveys conducted in recent years, excluding gradiometer surveys for which two Varian Cesium magnetometers were used. In general, therefore, the overall statistics for aeromagnetic surveys are to a large extent representative of the surveys conducted with the CSF magnetometer.

Between April 1964 and April 1968 aeromagnetic surveys were flown over parts of the territories of the following countries: France, Spain, Australia, New Caledonia, Tunisia, Sicily, Kenya, Saudi Arabia, South Africa, Iran, Indonesia, Malagassy, New Guinea, Ivory Coast, Mauritania, Malaysia, Libya; and on the American continent, over Labrador, Canada and Texas. In this period, a total of 650,000 line-km were flown over offshore areas; for the latter, the Toran system of radio-location was mostly used. In addition, about 60,000 line-km were flown in connexion with surveys for metallic minerals.

Most of the possible geologic conditions were encountered in the areas covered by these surveys, ranging over shallow and deep sedimentary basins, some being affected by volcanism, diapirism or other structural features. The high degree of sensitivity of the magnetometer, and the various types of digital processing applied, enabled isobath contour maps of the basement surface to be constructed and these were particularly effective in delineating fault patterns. Some types of geologic data could be obtained which could not be obtained by other geophysical methods, including seismic reflection, and useful data could be interpreted in areas where the anomalies were even less than 5 gammas.

STANDARDIZATION OF MEASUREMENTS

Although mentioned in articles published elsewhere it is necessary to stress the importance

1) A French Electronics Manufacturing Company.

of standardization of procedures and measurements, as the success of high sensitivity magnetometer surveys depends on this.

Navigation

It is necessary to adhere as closely as possible to the planned positions of the flight traverses and to obtain sufficient data from which the aircraft's actual flight paths can be plotted accurately. The altitude of the towed magnetometer must be measured as accurately as possible, in relation to the altitude of the aircraft; when the air is calm, the flight path of the magnetometer would normally be parallel to that of the aircraft.

Adherence to the planned traverse grid

The advantages of the 3 × 5 km grid for production of an optimum quality isogam map are explained later. From the viewpoint of navigation, however, it is necessary that the actual flight paths should conform as closely as possible to the planned grid network to ensure good correlation between the profiles and to facilitate more accurate construction of isogam maps.

Data required for plotting flight paths

For navigation over land areas either photomosaics or accurate topographic maps are used and the flight paths are recorded either continuously by movie camera or by successive photos taken with a still camera installed in the aircraft. The movie film facilitates the location of intersections of the traverses and the still photos enable the flight paths to be plotted readily. The quality and accuracy of the location map showing the flight paths directly influences the accuracy of the isogam map and the definition of the magnetic anomalies in the vertical plane and these, in turn, affect the degree of reliability of the interpretation of the results.

The anomalies can be considered in two groups, namely, strong anomalies of more than 10 gammas and weak anomalies of less than 10 gammas. The intersections of the traverses forming the grid of flight paths provide a check on the accuracy of the plotting of the flight paths and the difference between values at the intersections of the traverses and cross-lines of the grid is distinguished as "delta" or "d."

In the case of strong anomalies, the maximum error would be obtained from the formula: $dF=\frac{2Fdx}{h}$, where F is the value of the anomaly, dx the error of location, and h the depth of the body below the aircraft, on the assumption that the body is a thin sheet. In the case of navigation over land the accuracy of location for an intersection in the grid of traverses should not exceed ± 50 metres, taking into account also the effect of the camera's position inside the aircraft. In the case where F is 30 gammas, h is 3,000 metres and dF is $\pm$ one gamma, the possible error would be ± 0.7 gammas.

For weak anomalies, two cases have to be considered. The effect of a thin sheet where F is 10 gammas, h is 2,000 metres and dF is ± 0.1 gamma would give a possible error of about the same value. The effect of the regional gradient of the anomaly is less than 2 gammas. When the regional gradient is subtracted an error in the location of the intersection of traverses can produce a distortion of the isogam contours and consequently the correlation between very weak anomalies could be difficult. If the gradient were 5 gammas per kilometre, the possible error would be ± 0.25 gammas. In the case of both strong and weak anomalies the distortion due to an error of ± 50 metres at the location of an intersection would not affect the interpretation to any significant extent.

Flight altitude

In calm weather, and with an accurate altimeter installed in the aircraft, it is possible to maintain the correct flight altitude to a limit of ±30 metres. The type of aircraft is important and larger models such as the B–17 or DC–3 should be used.

With regard to isogam maps, the effect of altitude is considered as follows: assuming the body to be a thin sheet, the formula is $dF = \frac{2Fdh}{h}$ where dh is the variation in altitude. Applying this to the same strong anomaly as above (i.e. F is 30 gammas and h is 3,000 metres) dF would equal ± 0.6 gammas and the possible error would be dF_p = ± 0.4 gammas. In the case of weak anomalies the effect would be insignificant.

Both the weak and strong anomalies are not significantly affected by the variations in altitude unless these exceed ± 100 metres over strong superficial anomalies; these strong superficial anomalies, however, are of little significance for petroleum surveys, but they are of great importance for mineral surveys.

Utilization of ground station data (figure 1)

Two main effects have to taken into account – diurnal magnetic variation and sporadic instantaneous variations.

Diurnal variation follows roughly the same pattern over large areas but its amplitude varies from day to day at different locations. From our experience with the surveys in France and over the Mediterranean Sea, conducted for the Centre National de la Recherche Scientifique (CNRS) the diurnal variation in this region seems flat enough to be considered as a "surface correction" defined by a square with sides of 200 km. Where possible, it is necessary to subtract the effects of diurnal variation; however, if the flight traverses are too long, the application of a general correction could be open to criticism, as there are examples of two stations about 500 km apart along a meridian at which the patterns of the diurnal variations are completely different.

Instantaneous variations, especially in the case of small anomalies, can have the same period and amplitude as those recorded during normal aeromagnetic surveying. It is therefore essential to have ground stations as close as possible to the area being surveyed, recording instantaneous variations which can be subtracted second by second from the records obtained from the aircraft.

Digital recorders

Their characteristics have been fixed so as to avoid the introduction of appreciable inaccuracy which would add to other causes of error, related to altitude, variations of the magnetic field, and other factors.

It can be seen, therefore, that the quality of measurements required to obtain the complete range of anomalies in oil exploration depends on (a) the digitalisation of data; (b) the accuracy of navigation, which could give rise to possible errors in the data of up to ± 0.7 gammas in the case of strong anomalies and ± 0.1 gammas in the case of weak anomalies; (c) proper recording of flight altitude, in which the possible error could be ± 0.4 gammas in the case of strong anomalies; and (d) the choice of location of the ground stations, on which the interpretation of small anomalies depends.

However, in order to obtain the optimum result for the final compilation and interpretation there are two other important factors which must be taken into account, namely, the grid spacing intervals, and the altitude of the magnetometer.

Arrangement of the flight lines (Grid)

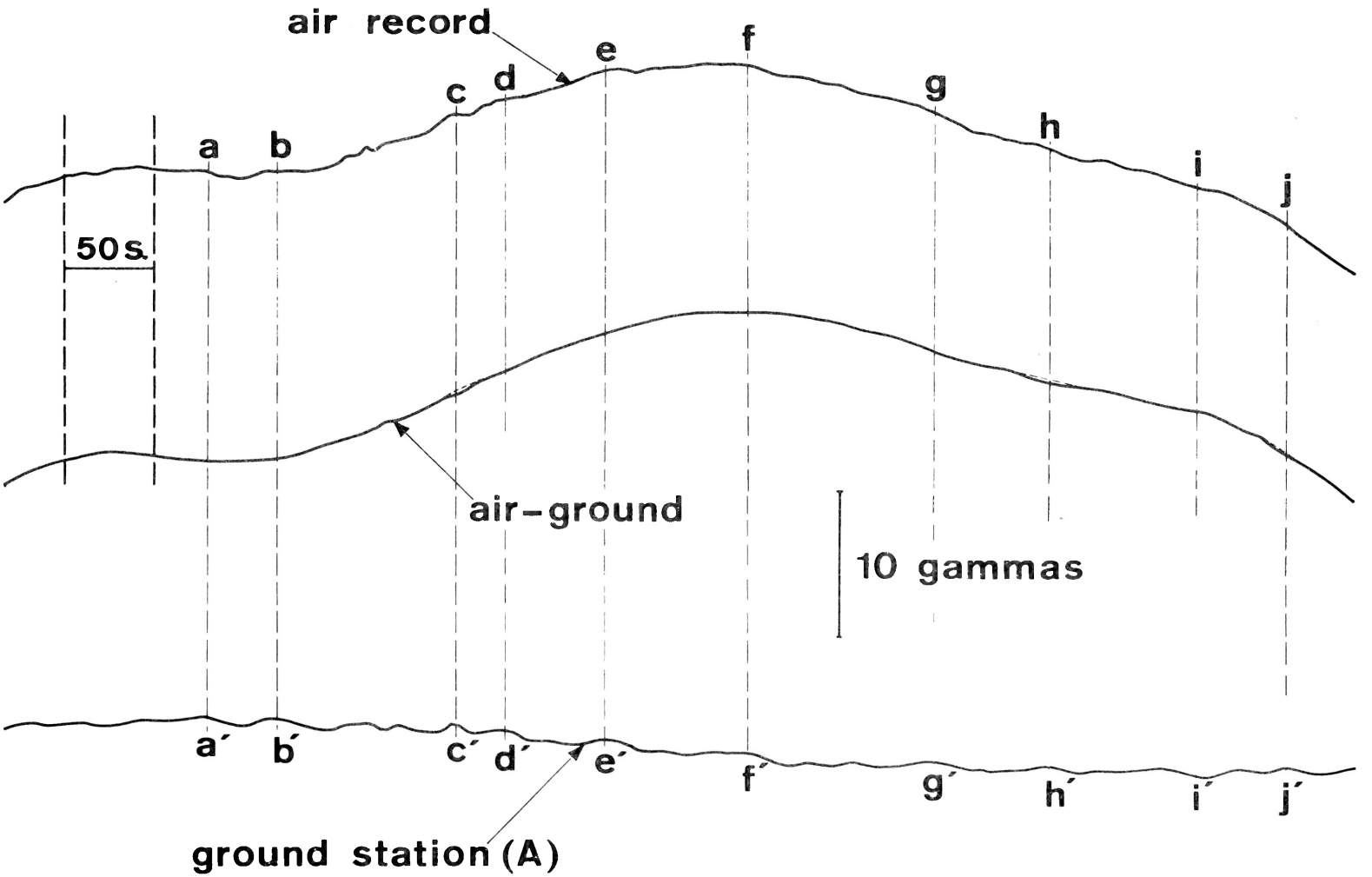

Figure 1. Validity of the process of subtracting ground from air magnetometric values.

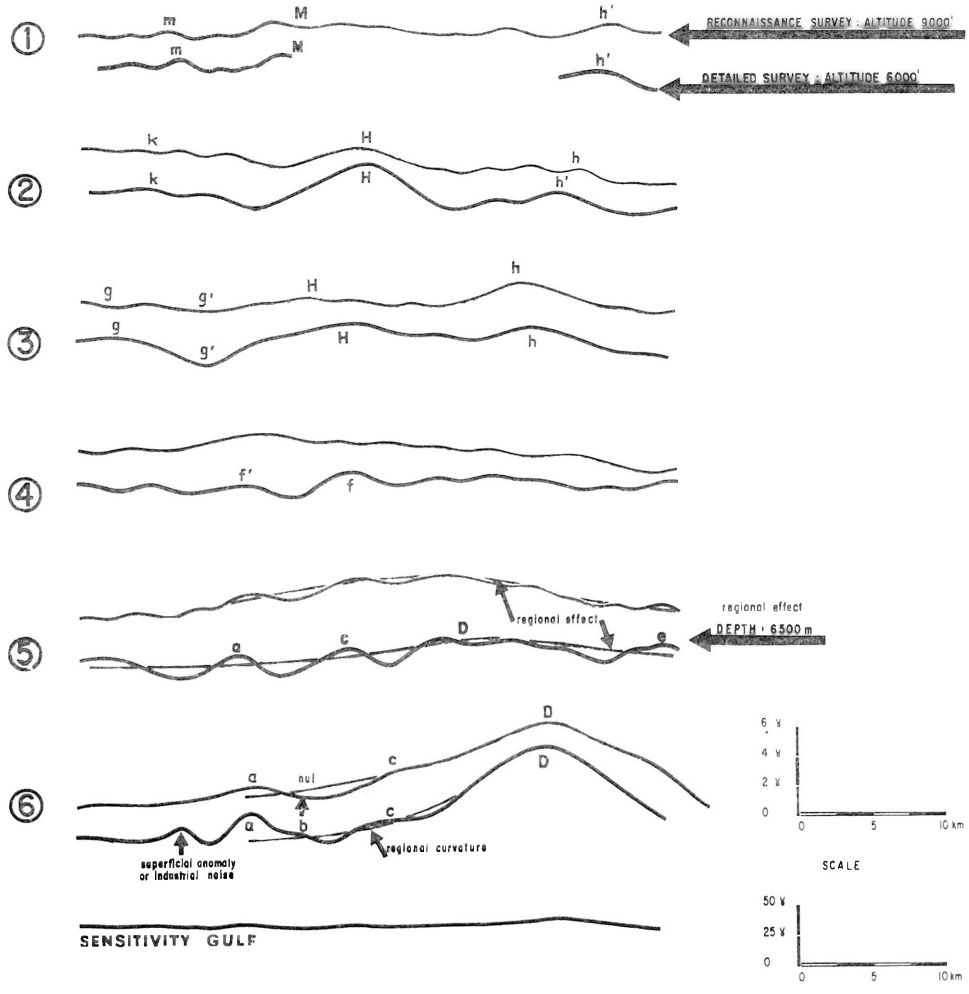

Figure 2. Comparison between reconnaissance and detailed survey lines flown at different altitudes.

From our experience it is our firm opinion that, wherever possible, an aeromagnetic survey should be planned to be flown along a grid of traverses with spacing of 3×5 km. This would amount to about the same total length of traverse as for a grid of 2×10 km, which was commonly used previously. Experience shows that the trends of the anomalies are usually very variable and that circular anomalies are rare, and often have no direct connection with the basement picture. The 3×5 km grid provides a better chance of obtaining more intersections across the axis of a cylindrical anomaly (with length about five times the width) and the possibility of obtaining better correlations and a truer picture of the closures.

In conclusion, it is useful to recall the paper by W.B. Agocs (Geophysics Vol. XX, No. 4, 1955); although it concerns only mineral surveys, we agree entirely with the conclusions. To be sure of having an economical arrangement of the flight lines in accordance with the geophysical problem, it is necessary to take into account the area of the anomaly as well

as its depth. Without strictly applying the law of probabilities, the formula given by Agocs shows interest in having a narrow interval; this is more important in cases where the anomalies are superficial and narrow.

Altitude of the magnetometer

After many experiments, we conclude that the altitude of the magnetometer should not generally exceed 1,000 m above the ground. However, when lava flows or intrusions in sedimentary strata are present more care should be given to the correctness of the flight altitude so that a good filtering process could be applied to separate the different levels. In places where the influence of industrial noise, caused by electrical installations, is great, the sensitivity of the magnetometer allows it to be flown at a greater altitude to eliminate this noise and obtain better data. In fact, with the high sensitivity magnetometer the altitude factor is less important than with the flux gate magnetometer, as is shown in figure 2; in this figure it is seen that all the main anomalies have remained. Obviously the definition is poorer at 9000′ but sufficient when we have to avoid industrial noise which, perhaps, at 6000′ would affect the anomalies or make it difficult to distinguish them from the true anomalies.

IMPROVEMENTS ON EQUIPMENT

For digital processing to be applied to analysis of aeromagnetic data, it is essential to have a well fitted magnetic recorder for the recording of various measurements. Figure 3 is a photograph of the type of incremental recorder used; this recorder allows the digitalization of all radio-navigation systems commonly used (Doppler, Toran), the altitude of the plane, field magnetic frequency converted up to 0.01 gamma, measurements, and the time in seconds.

The equipment installed in the aircraft (Fig. 4) comprises all necessary control instruments (including oscilloscope) and one printing machine on which the Toran measurements and field magnetic frequency are recorded, together with the time.

DEVELOPMENTS IN PROCESSING

Compilation

Figure 5 shows the different steps in compilation which are now involved in processing through a computer, in this case an IBM model 360–40. The final result is the automatic isogam map of which an example is given in figure 6. The automatic contouring eliminates all possibility of personal bias and displays inflections, curves and trends which would escape even the best draftsman. The interpreter can then make use of this map for the drawing of tectonic events such as the fault patterns shown in figure 6.

Interpretation

Great improvements have been made in this field. The most important of the interpretations made from aeromagnetic data is profile analysis because this provides information in a most accurate and practical form. The main result from this analysis is the depth determined for each anomaly.

The ideal method for analysing an observed anomaly on a profile is the comparison of this anomaly, as a whole effect, with theoretical anomalies. The bilogarithmic charts are very practical for such a comparison but their utilization requires too much time when a few

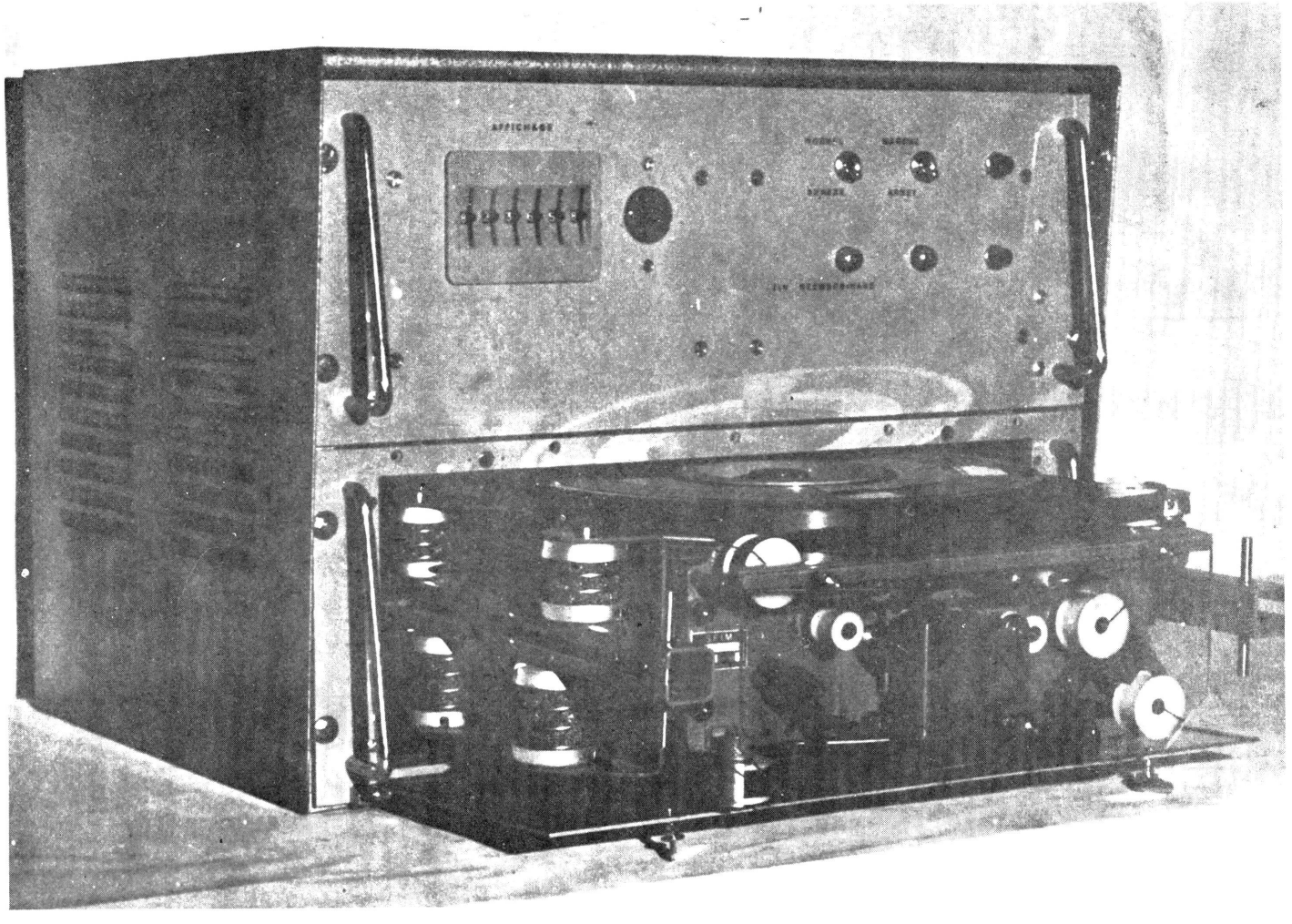

Figure 3. Digital recording unit.

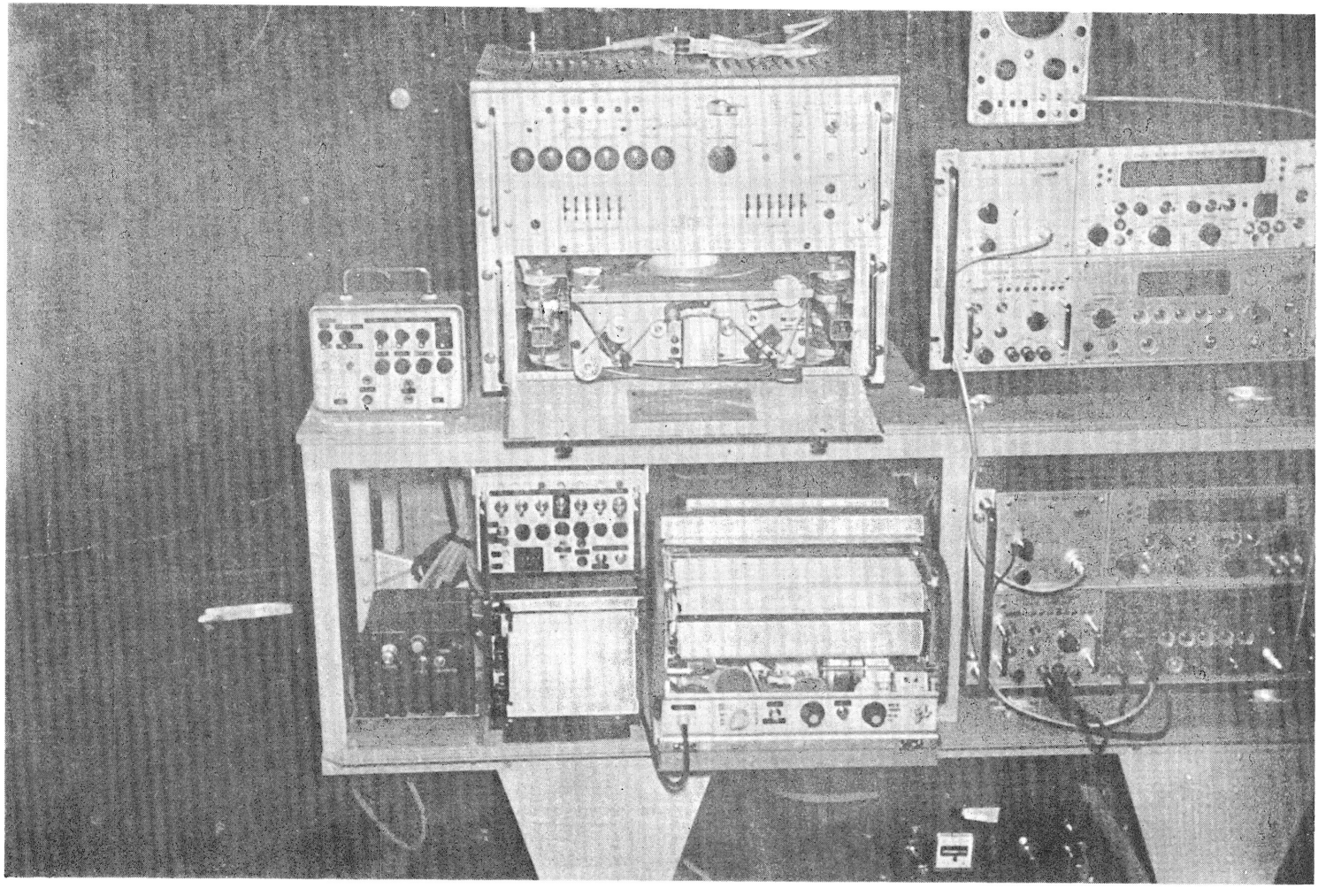

Figure 4. Aeromagnetic survey equipment installed in aircraft.

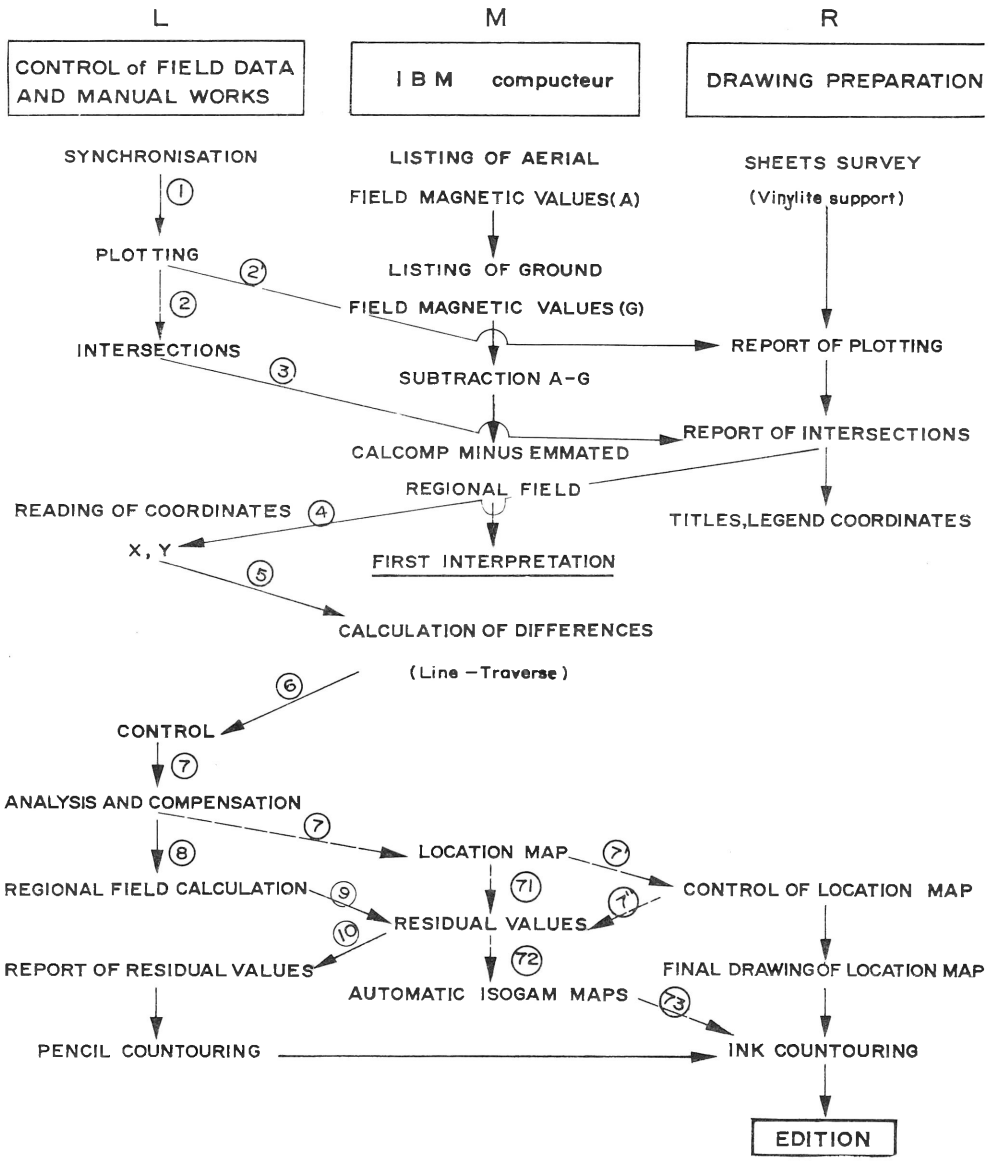

Figure 5. Compilation procedures for preparation of automatic isogam maps.

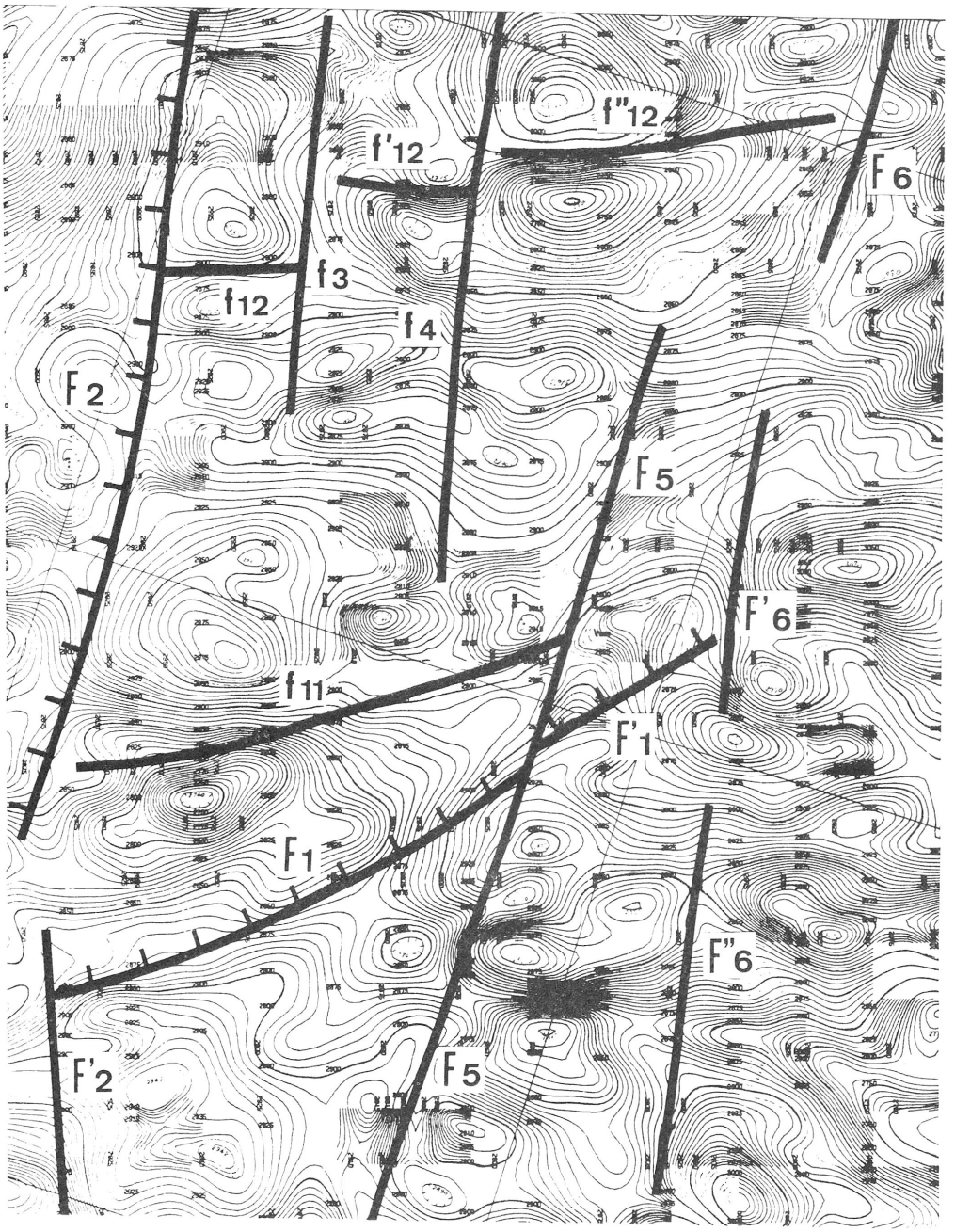

Figure 6. Example of automatic isogam map.

tens of thousands of line-km of traverses have to be interpreted, and faster methods must therefore be used. Figure 7 shows two well known methods. The first consists of drawing the main inflexion tangent of the anomaly locating the two points where the tangent is not mixed with the curve, and then measuring the horizontal distance U1. The second uses the two tangents of which the slope is half of the inflexion tangent slope itself. The horizontal distance U2 is measured between the contact points of the two tangents. In both cases, the depth is determined by multiplying U1 or U2 by an appropriate coefficient.

When high sensitivity measurements are being interpreted it is necessary to spend much time on profile analysis. Figure 8 shows three theoretical anomalies of the total field which correspond to the same structure and to three different values of the magnetic field inclination (90°, 63° and 45°). Drawn on each anomaly were the asymptote, the inflexion tangent and the tangent which is parallel to the asymptote. These straight lines allow definition of the B C D parameters, involving the asymptote and the inflexion tangents, and the E F parameters which originate in the inflexion tangents and the tangents which are parallel to the asymptote. G is the horizontal distance between the inflexion points.

Figure 9 shows the same anomalies as above, but now the vertical parameters are measured: J is the intensity of the anomaly, and k, l and m are measured between the curve and the intersection points already used on the horizontal parameters. In difficult cases it is necessary to combine horizontal and vertical parameter charts. The chart catalogue is now completed. It comprises:

Cylindrical structure type

Downward infinite compartments (all widths)
Downward limited compartments ($H/h = 2$, all widths)
Thin slides (all widths)
Faults (all thicknesses)
Two downward infinite and narrow compartments (various spacings). This last chart is very useful for resolving the difficult problem of interferences.

Square horizontal cross section structures

Downward infinite compartments (all widths)
Thin slides (all widths)

Vertical gradient

The same charts exist for the vertical gradient either from gradiometer data or from total-magnetic field transformed into vertical gradient.

Considering the broad sensitivity of the magnetometer, it becomes necessary to separate various magnetic sources in respect of their level or nature. This can be achieved by "filtering."

Linear filtering is a simple operation: it is a convolution, but as each anomaly has a rather wide spectrum, the constant of convolution cannot be exactly defined, to produce the optimum result; anomalies to be evened out are not completely erased, and anomalies to be preserved are slightly modified in shape (for instance, the top may be flattened on a bell-shaped anomaly). For this reason, it is necessary to use more complex automatic methods of filtering.

Non-linear filtering utilizes as a basic parameter the width of the anomalies and it is assumed that the depth of the magnetic source and the width of the corresponding anomaly are in close relationship. Firstly, the profile is tested with a small sampling interval in order to try and eliminate those anomalies in which the elongation is of a similar length.

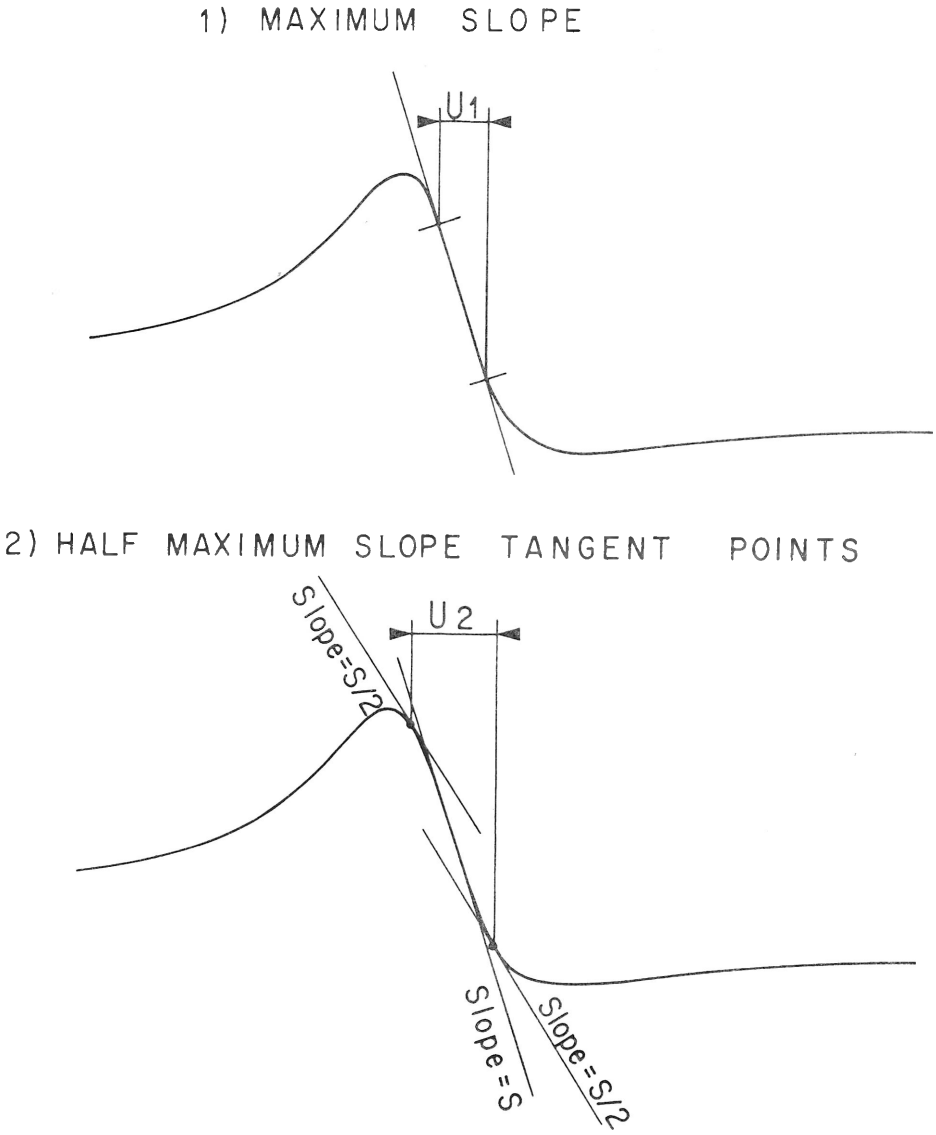

Figure 7. Two methods usually used for profile interpretation.

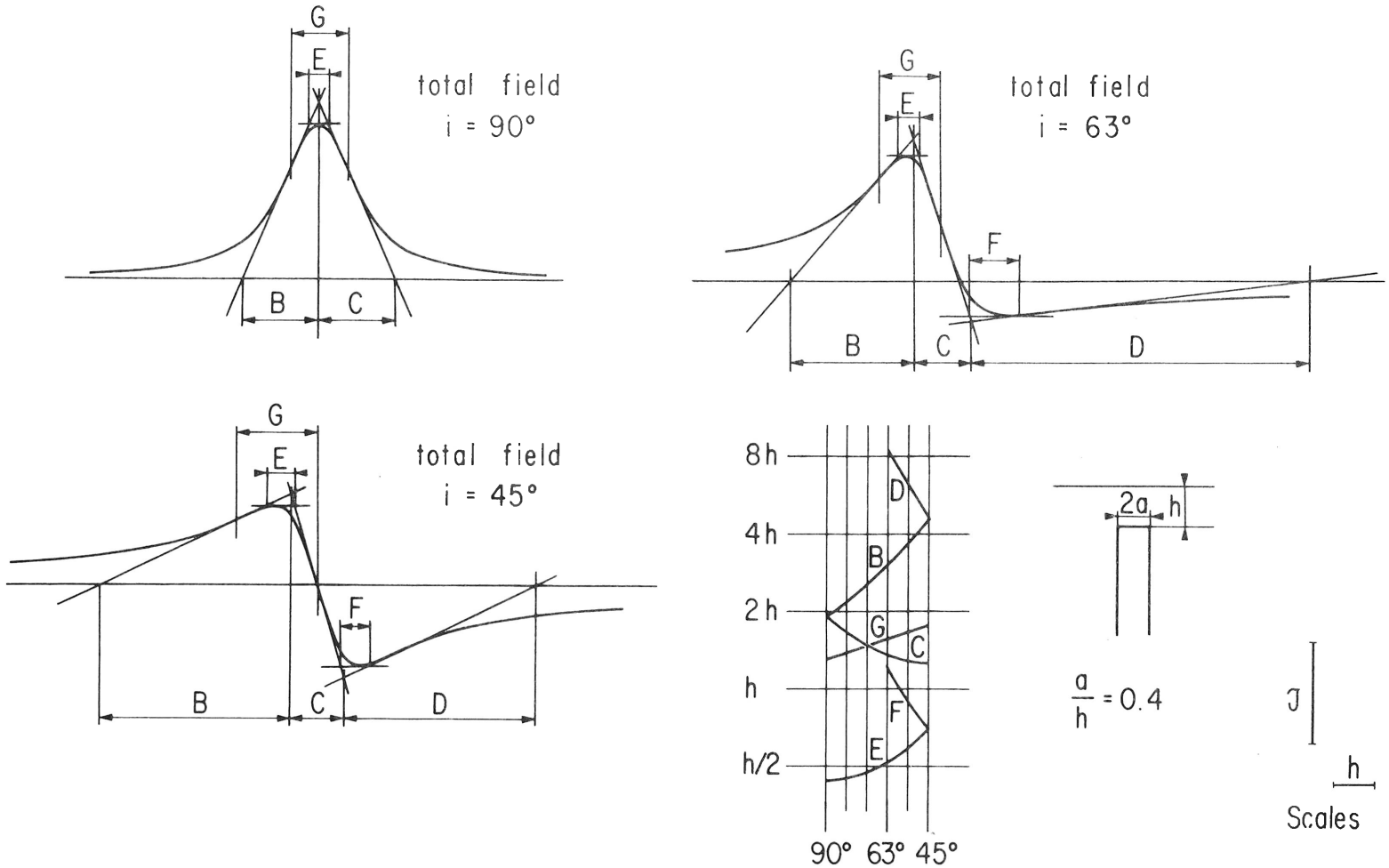

Figure 8. Horizontal parameters for profile analysis.

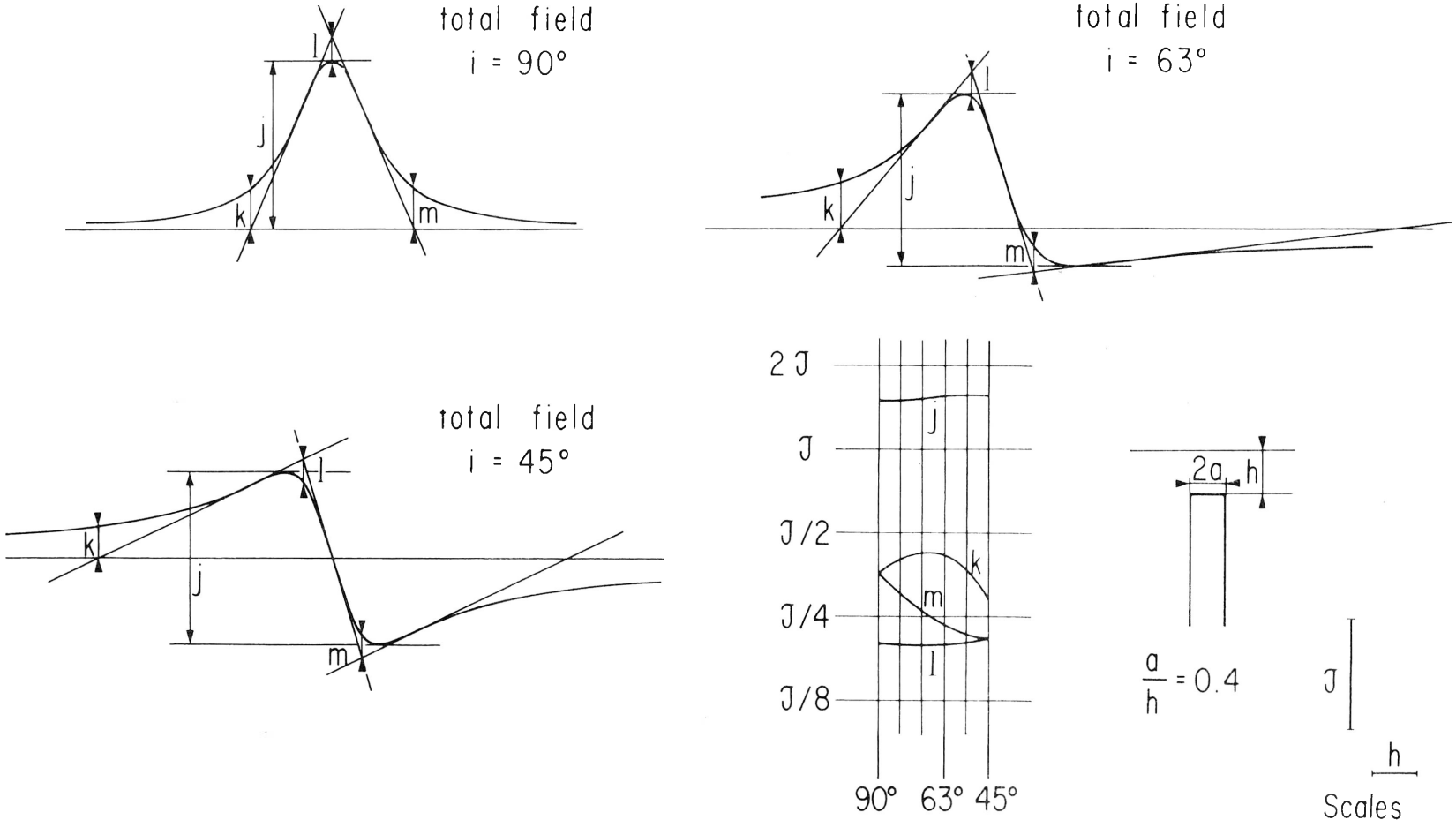

Figure 9. Vertical parameters for profile analysis.

In this respect second half differences are calculated, and the parts of the profile on which alternation of sign is shown are taken into consideration. Actually, these parts of the profiles are processed while the rest is not altered at all. The interesting parts of the profile are tested in several ways in order to confirm whether or not anomalies of width under investigation exist. If such anomalies are found, it is necessary to make a distinction between single bell shaped and several arch anomalies as they must be processed in a different manner. After all the operations concerning the initial sampling interval have been carried out, the processing is carried out as before, but changing the sampling interval for every operation. It is therefore possible to double the sampling interval several times until all interesting anomalies have been separated by filtering. Some examples of filtering are shown in figures 10, 11 and 12.

UTILIZATION OF DIGITALIZED MEASUREMENTS IN AEROMAGNETIC MINERAL SURVEYS

Some of the reasons why it is necessary to maintain a constant altitude to obtain optimum quality in isogam maps for aeromagnetic mineral surveys have been explained earlier, and this has been supported by experiment. From our experience, it is necessary to divide the area to be flown into a few panels, each with its own altitude defined by hm = ht + 100 m (ht being the highest point of these panels). In this case the utilization of digitalized information permits accurate analysis of the closure within the grid and good anomaly pictures resulting from Calcomp processing. Analog recording is completely upset by sharp variations in anomalies. Furthermore, if the sensitivity of the flux gate magnetometer is adjusted to define large anomalies it cannot at the same time define small anomalies. An accurate isogam map can be obtained only by using a computer. A good example of structural belts is shown in figure 13; without automatic contouring it would have been impossible to obtain such a good picture. Digitalized data also permits processing by filtering and vertical gradient.

CONCLUSION

The high sensitivity magnetometer is becoming increasing by recognized as the only type of magnetometer presently available that can provide the degree of accuracy needed as far as measurement of the total magnetic field is required for petroleum exploration purposes. It is evident that the optimum results cannot be obtained from the high sensitivity magnetometer without digitalization to process the data and produce automatic isogam maps from which an elaborated interpretation can be made. The reliability of these results, however, is dependent on the accuracy with which all the parameters involved in the field operations are measured.

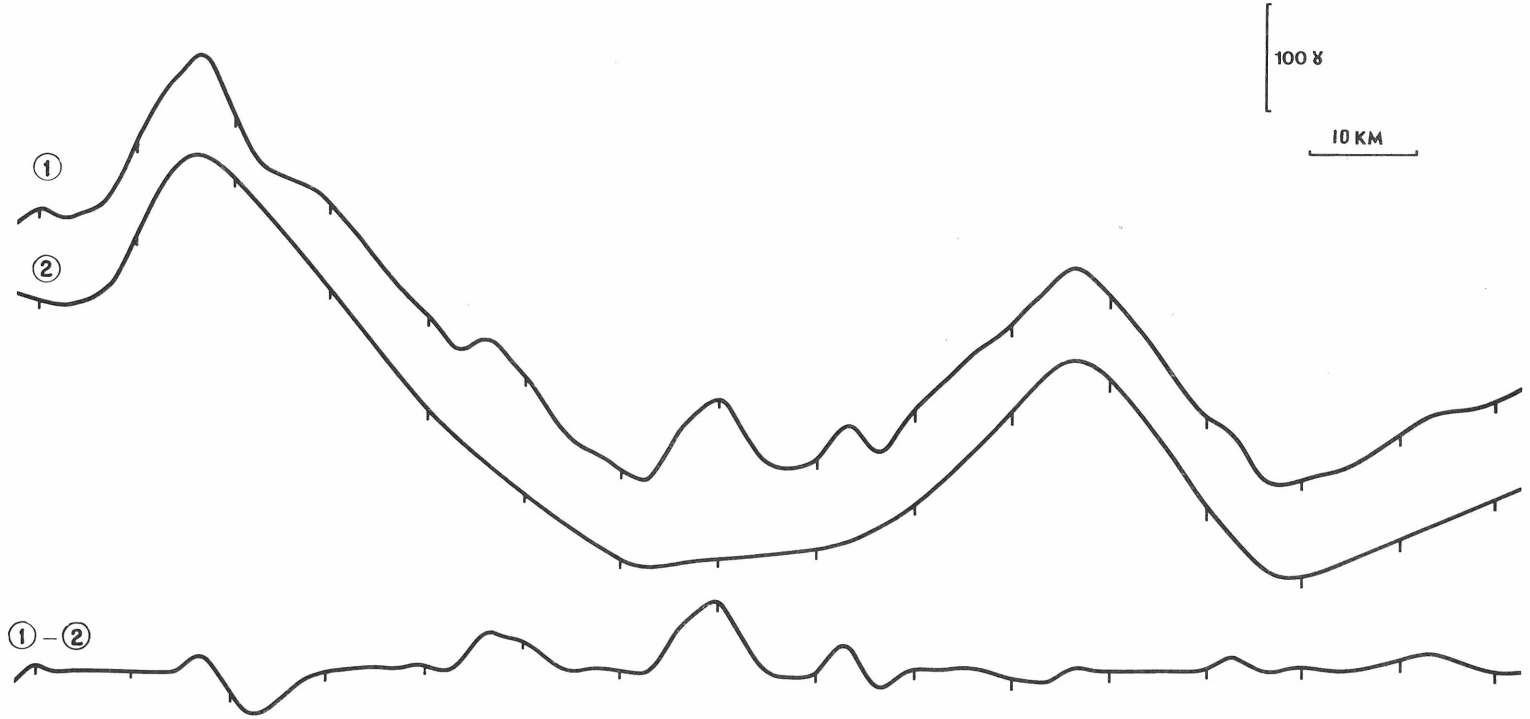

Figure 10. Example of filtering.

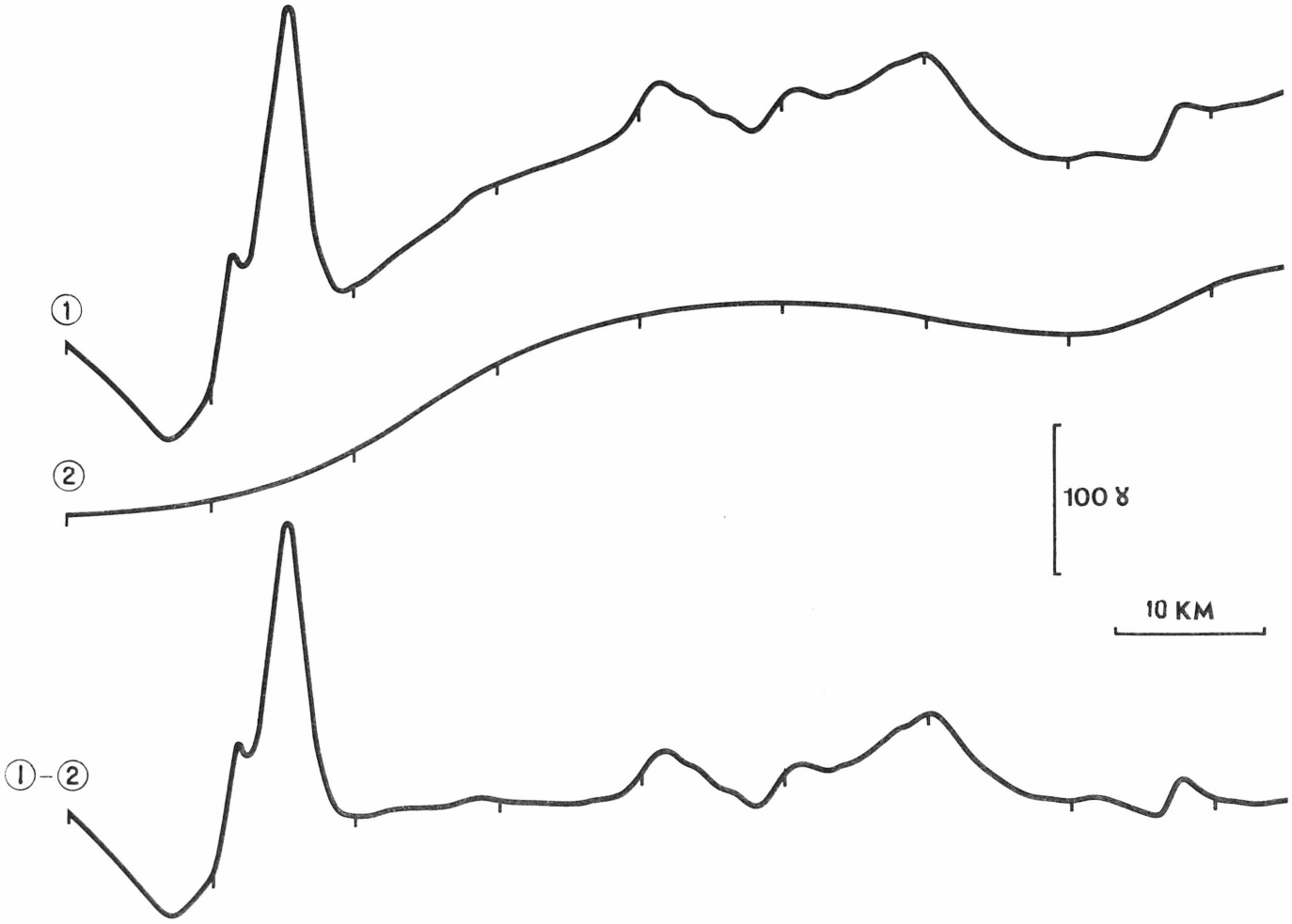

Figure 11. Example of filtering.

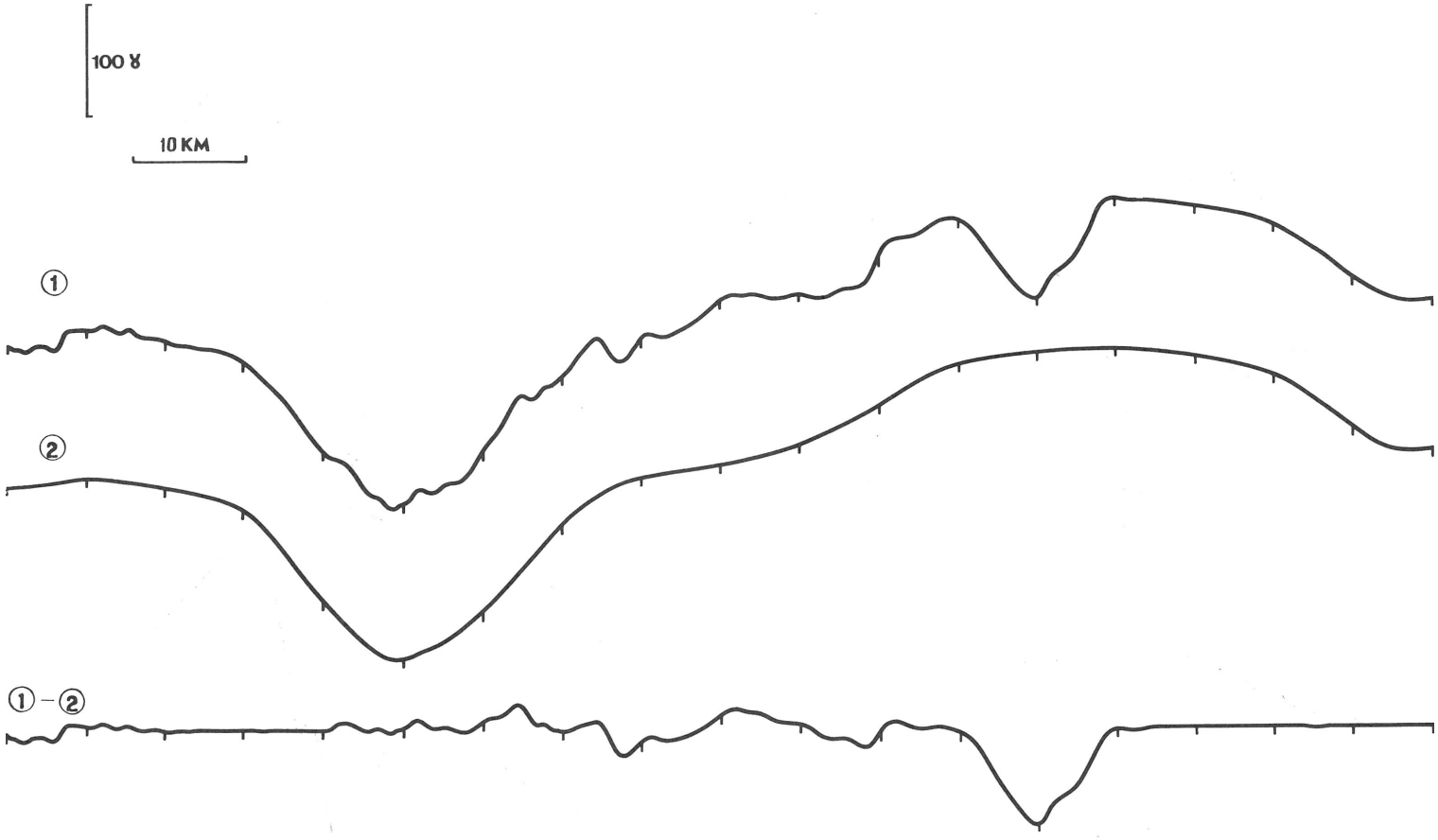

Figure 12. Example of filtering.

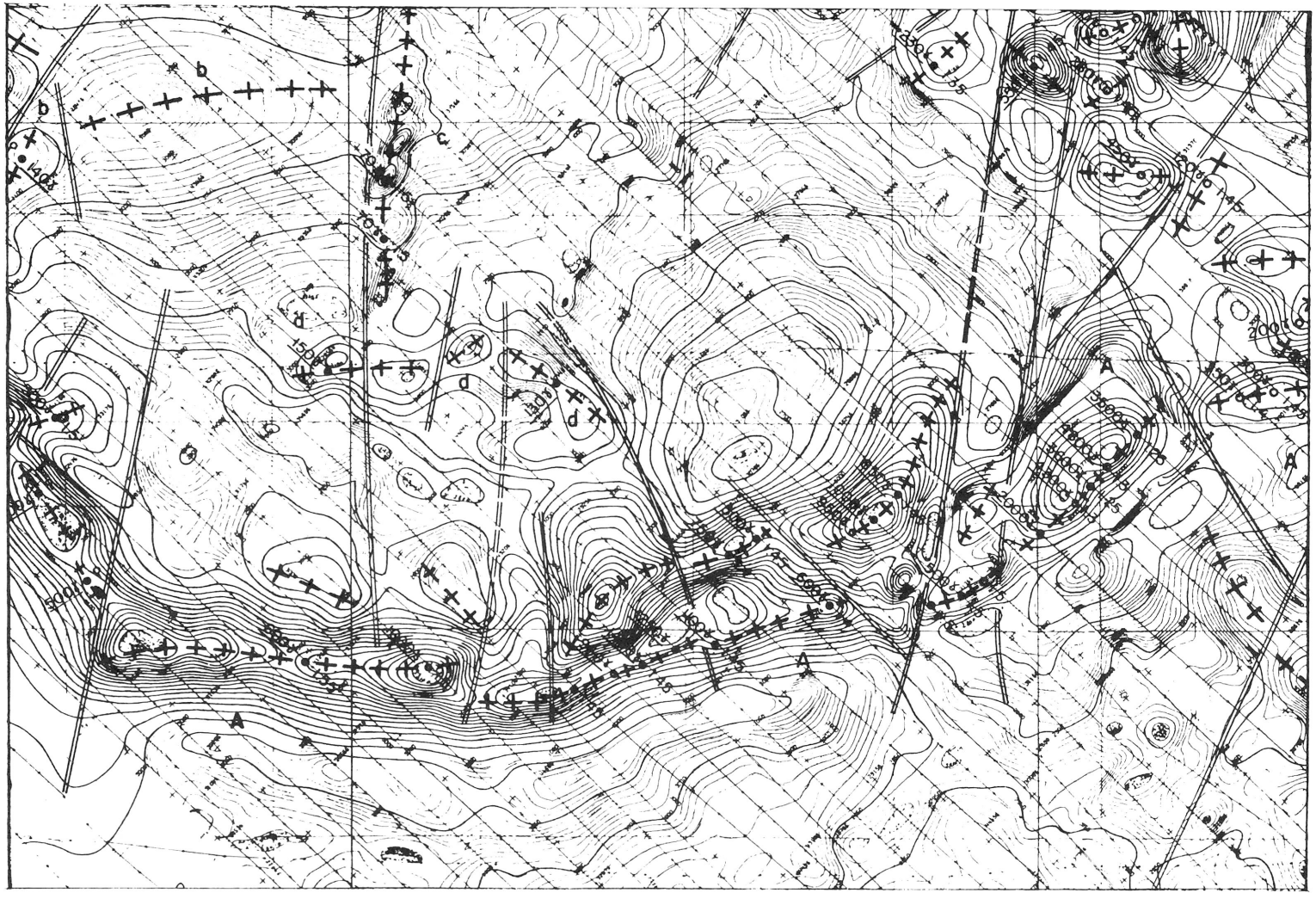

Figure 13. Example of automatic isogam map produced for mineral survey.

Blank page

Page blanche

DISTRIBUTION PATTERN OF SEDIMENTS ON THE CONTINENTAL SHELVES OF WESTERN INDONESIA

By
K. O. Emery
Woods Hole Oceanographic Institution
(with a map, in pocket on back cover)

ABSTRACT

A new chart shows the distribution patterns of mud, sand-and-mud, sand, gravel, rock, and coral bottoms in western Indonesia. It was compiled from about 33,000 notations of bottom materials provided by field plots of lead-line soundings made prior to about 1930 by hydrographers of several maritime nations. The compilation reveals the distribution of relict sands, recent muds, many rock outcrops, and large coral reefs that serve as peripheral dams on the shelf. The chart has value in guiding explorations for tin through its presentation of rock outcrops and nearby sands, and in geophysical explorations for oil and gas through its mapping of mud areas that provide less interference than do other kinds of bottom materials in continuous seismic reflection surveys.

The western Indonesian region contains one of the largest shallow sea floors of the world, occupying a broad sweep around the western and southern sides of Borneo with a length of 2,300 km and a breadth of 300 to 600 km. Only the 1,700-km part southeast of Malaysia is considered here. This part is bordered by land masses on both sides, Borneo on the northeast, and Sumatra and Java on the southwest and south. Two submerged river systems on the shelf (G. A. F. Molengraaff in Kuenen, 1950, pp. 482–484) probably date from Pleistocene times of glacially lowered sea levels. The channels are incised only a few meters into the surface of the shelf at depths of 20 to 120 meters, the latter being also the approximate depth of the shelf-break. Locally, the channels have been filled and obscured by sediments that have been moved by tidal currents and probably also by currents associated with the monsoon (eastward in winter, westward in summer, according to Myers, 1945).

Detailed investigations of sediments have been made only in parts of the region. Van Baren and Kiel (1950) studied the transparent heavy minerals west of Borneo, as an extension of an earlier examination of the patterns of grain size and content of calcium carbonate. The mineralogical results showed derivation of the sediments from both Borneo and Sumatra and the Malay Peninsula, according to Keller and Richards (1967). At the opposite end of the region (southeast of Borneo) a few samples were collected from the shelf by the Siboga Expedition of 1929–1930 and briefly described by Neeb (1943), but the main effort of this expedition was the study of deep basins in the East Indies.

Recent years have witnessed the growth of much interest in the offshore mineral resources of western Indonesia, mainly oil, gas, and tin. The oil and gas is in deeply buried strata of the shelf and the tin is in near-surface sediments. Search for both kinds of resources can be aided by knowledge of the general distribution pattern of surface sediments. The few detailed

studies of the sediments can be supplemented by much qualitative information in the form of chart notations of bottom materials obtained during lead-line surveys that were made mainly prior to 1930. When the tallowed lead was retrieved aboard ship, a notation was made of the kind of material sticking to it. The information was recorded next to the sounding on the field plotting sheets. More recent surveys have utilized echo sounding methods that provide little information about bottom materials as by-products of the main work.

During World War II information was needed about the composition of the shallow sea floor in areas frequented by enemy ships, and many bottom sediment charts were compiled for the Asian region. After the war the charts were declassified, and considerable geological information was deduced from them (Shepard, Emery, and Gould, 1949). For western Indonesia about 33,000 bottom notations on British, Dutch, Japanese, and the United States field sheets served as the basis for constructing seven bottom sediment charts. Five were printed in color on regular navigational charts H.O. 3112, H.O. 3117, H.O. 3747, B.A. 1653, and B.A. 3637, but two others compiled for navigational charts H.O. 1170 and H.O. 3001 that covered a larger region than these five were not printed owing to termination of hostilities in that region.

In order to contribute to the knowledge of bottom sediments of the Indonesian region, the author compiled the five printed charts (that are now out of print) and the two manuscript charts into a single chart that accompanies this report. This chart includes the Java Sea, the Bali Sea, the Flores Sea, Makassar Straits, and part of the South China Sea. The shelf within this chart has an estimated area of 770,000 sq. km, yielding an average of one bottom notation per 23 sq. km. The distribution of bottom notations, however, varies by a factor of about 20, being densest near Malacca Strait (between Sumatra and the Malay Peninsula), and in nearshore belts elsewhere, and least where the topography is deep and smooth.

Only a few broad categories of bottom materials are reported on the field sheets and compiled on the chart. Finest grained of these is **mud**, silt and clay (median diameter is usually finer than 0.05 mm) that generally forms a soft smooth bottom. **Sand-and-mud** is mainly fine sand and silt having a firm to soft smooth bottom. **Sand** consists of detrital or calcareous organic grains (median diameter is generally 0.5 to 2 mm) underlying a bottom that may be smooth to rippled and commonly contains some intermingled shells. **Gravel** is composed of rock fragments as pebbles or cobbles commonly including many broken shells (median diameter is usually 20 to 200 mm). Its surface is more irregular than the surface of finer sediments. **Rock** bottom consists of bedrock outcrops and boulders near outcrops. It is nearly always very irregular. **Coral** bottom is composed of large masses or reefs of calcareous material mainly of massive calcareous algae and coral.

Examination of the chart shows that mud is the predominant bottom material on the shallow sea floor of the region. Almost exclusively it occupies the central areas farthest from land, but it also borders most of the coastal region, particularly off the mouths of rivers. Sand-and-mud and sand are next most abundant, commonly occurring in large irregular patches 50 to 100 km offshore, but also present off projecting coastal points between the mouths of rivers. This pattern suggests that the areas of sand-and-mud and of sand depict relict topography and sediments inherited from Pleistocene times of low sea levels. Later contributions of mud have buried the older sediments off the mouths of the rivers that supply most of the mud and in the central deeper parts of the continental shelf where mud bottom is less disturbed by water movements than at intermediate depths. Other areas of sand, plus gravel and locally rock bottoms, occur in the straits where tidal and other currents prevent the deposition of finer sediments. Examples are Malacca Strait (between the Malay Peninsula and Sumatra), the broad shallow straits on both sides of Billiton Island, Sunda Strait

(between Sumatra and Java) where the great eruption of Krakatao in 1883 also contributed much scoria and ash, and the straits between the small islands of the chain east of Java. Narrow belts of sand, gravel, and rock also fringe the small islands east of Java, because their small rivers probably contribute little mud, and the insular shelves are narrow and steep enough to permit currents to carry finer sediments beyond the shelves into deeper water. A last kind of sand bottom fringes the reefs on both sides of Makassar Straits; this sand probably consists almost exclusively of calcareous debris from the reefs. Rock bottom occurs atop many small submerged hills throughout the region because the hills are incompletely eroded outcrops whose slopes are steep enough to prevent accumulation of sands and finer sediments. Many of the hills have a cap of coral, which in the western part of the chart is almost restricted to such hills. In the eastern part, however, coral occurs in very large patches and in reefs that rise high above the level of the shelf. These reefs, in fact, serve as effective dams that trap muds and cause the shelf to be built upward by deposition of clastic sediments. Examination of the charts, thus, discloses many interesting geological processes.

The various kinds of bottom materials have different significances in the exploration for tin and for oil and gas. Economic placer deposits of tin are most apt to be present near rock bottom, if the rock is tin bearing and the tin mineral (cassiterite) has been released by long intense weathering of the matrix followed by residual concentration of the tin during eluvial or short stream erosion (Emery and Noakes, 1968). Concentrations of tin may also underlie sand bottom near rock outcrops. Large deposits are unlikely to be found in mud (except perhaps beneath sand that in turn underlies the mud), mud-and-sand, gravel, or coral.

The significance of the bottom materials in oil and gas exploration is at least two-fold. Where rock is present, the outcrop may justify investigation to learn the type and age of rock to aid in geological mapping of structure and stratigraphy. The second point has to do with continuous seismic reflection profiling to learn the structure beneath the shelf surface. Traverses across mud bottom are most successful because the mud is more transparent to sound than are the other bottom materials. Sand is relatively opaque to sound and it is such a good reflector that subbottom reflections recorded during traverses across it are commonly obscured by multiple bottom reflections. Similarly, areas of gravel, rock, and coral bottom tend to scatter the incident sound so much that little information about structure at depth can be obtained.

In summary, the areas that are most favorable for tin (bedrock and nearby sand) are least favorable for seismic profiling for oil and gas at depth, and the best areas for the latter are ones of mud bottom which are among the least favorable for tin. The accompanying bottom sediment chart should be considered only a general guide helpful when supplemented by geological maps in choosing areas for detailed geophysical exploration for mineral resources.

REFERENCES

Emery, K. O., and L. C. Noakes, (1968) Economic placer deposits of the continental shelf: Economic Commission for Asia and the Far East, Committee for Co-ordination of Joint Prospecting for Mineral Resources in Asian Offshore Areas, Bangkok, Thailand, Tech. Bull. vol. 1, pp. 95–111.

Keller, G. H., and Adrian F. Richards, (1967) Sediments of the Malacca Strait, Southeast Asia: Jour. Sedimentary Petrology, vol. 37, pp. 102–127.

Kuenen, P. H., (1950) Marine Geology, John Wiley & Sons, Inc., New York, 568 pp.

Myers, E. H., (1945) Recent studies of sediments in the Java Sea and their significance in relation to stratigraphic and petroleum geology: in Pieter Honig and Frans Verdoorn (editors), Science and Scientists in the Netherlands Indies: Board for the Netherlands Indies, Surinam and Curacao, New York, pp. 265–269.

Neeb, G. A., (1943) The composition and distribution of the samples: The Snellius-Expedition, E. J. Brill, Leiden, vol. 5, pt. 3, sect. 2, 268 pp.

Shepard, F. P., K. O. Emery, and H. R. Gould, (1949) Distribution of sediments on East Asiatic continental shelf: Allan Hancock Foundation Publ., Univ. Southern California, Los Angeles, Occ. Paper No. 9, 64 pp.

van Baren, F. A., and H. Kiel, (1950) Contribution to the sedimentary petrology of the Sunda Shelf: Jour. Sedimentary Petrology, vol. 20, pp. 185–213.

NOTE ON THE GEOLOGY OF THE REPUBLIC OF SINGAPORE

By
M. Mainguy, Entreprise de Recherches et d'Activités Petrolières, Paris, France
(with figures 1 and 2)

The territory of the Republic of Singapore and the adjacent waters form part of the Sunda Shelf, which includes the Gulf of Siam, part of the South China Sea and the waters between Borneo, Java and Sumatra in western Indonesia. The shelf is comprised of sediments folded during Cimmerian times and intruded in many places by acidic or intermediate igneous rocks (referred to here collectively as "granites"); these have produced varying degrees of metamorphism in the sediments. The age of these granites is recognized as a crucial question from the point of view of general geology as well as for applied geology and it is now known from recent work, including that done for the Geological Survey of Malaysia in the United Kingdom and studies made for North Viet-Nam by geologists of the Soviet Union, that many of the granites are of a considerably younger age than was formerly believed. The presence of the granitic intrusions is favourable from the standpoint of metallic mineralization, especially tin, but unfavourable as far as petroleum is concerned.

In company with Dr. R.D. Hill, professor of geography at the University of Singapore, and while I was assigned with ECAFE as Regional Adviser on Offshore Prospecting (Geology), the known outcrops on the islands that make up the Republic of Singapore were visited. These outcrops consist of a granitic core, forming the highest hills on the main island, together with a sequence of clastic rocks which are similar to the "upper sandstones" of Cambodia and Viet-Nam but which are strongly metamorphosed on Singapore Island. Within the granites are found rocks known locally as "blue stones"; these appear as inclusions of carbonaceous metasediments incompletely digested by the granite. A bore-hole was drilled west of the city of Singapore through rocks which were referred to as "granite" but which are very probably the "blue stone" type, as a laboratory in Europe identified the rock as a "carbonaceous schist." Permian or Permo-Triassic limestones similar to those found in Thailand, Cambodia and Viet-Nam may possibly be present a short distance away from the island, but no outcrops are known. This could lend support to the theory that the deeps recorded in the Strait of Singapore (see figure 1) were formed at least partly by the solution of limestone (van Bemmelen, 1947 and later R.D. Hill, 1968).

Little is known in detail about the geology of Singapore. The most recent study, by Mrs. Alexander in 1952, is very brief. Much more detail could be obtained at this time as construction and excavation are going ahead very rapidly in Singapore; there are at present a great number of fresh outcrops which will soon disappear.

Singapore's location makes it a key to understanding the regional geology, and a knowledge of the submerged former drainage channels would throw valuable light on recent movements that could have led to the formation of the Tertiary basins, which still hold out the best hope for petroleum prospects.

In the western part of the island, the outcrops of the Mesozoic sequence are traversed by faults that fortunately stand out in the morphology as it is already almost impossible to see

most of them in the field. Their trends are indicated quite clearly in the submarine morphology (figure 1) and it is for this reason that Dr. Hill (1968), while not ruling out completely the possibility that limestone solution played some part in the formation of the deeps, is more inclined to assign a tectonic origin to them–a view that one is very tempted to share.

The eastern end of the island is composed of a mass of old alluvial deposits, which are rather coarse on the whole but their total thickness is not known; it is possible that these could be a valuable potential source of fresh water. These deposits extend eastwards under the sea. (On the accompanying map (figure 1), part of this extension is unfortunately hidden by the legend but it nevertheless remains quite clear).

The source of the alluvium lies to the west in the River Skudai, which flows eastwards over a sill barring the Johore Strait, and partly also to the east, no doubt, in the River Johore, which flows between Pulau Ubin and Pulau Tekong. The latter river does not flow out eastwards in the direction of the South China Sea but moves westwards to join the River Kampar from Sumatra and flows into the Malacca Strait towards the Andaman Sea, after passing over the two previously mentioned deeps that are very probably of tectonic origin. No doubt there is a sill joining the southeastern tip of the Malay Peninsula to the Animbas and Natuna Islands. The underwater hydrographic chart drawn by Kuenen (1950, p. 482) shows the submerged river channels coming down from Sumatra on each side of Bangka Island and passing into the South China Sea between Natuna and Borneo, whereas the Kampar, and no doubt the Inderagiri too, turn to the northwest, towards the Andaman Sea (figure 2).

These few observations are too fragmentary to be of immediate application in furthering knowledge of the region's petroleum prospects, which chiefly depend on the distribution of the younger rocks. It seems to be well established that the Malay Peninsula plunges eastwards under a recent basin (Mio-Pliocene and perhaps Pleistocene), the structure, extent and continuity of which are poorly known; it is not impossible, however, that slumping has occurred on the west coast and has given rise to the formation of young sedimentary basins that are almost completely masked by the sea. Some support for such a hypothesis is to be found in the interpretation of an aeromagnetic profile (Project MAGNET) which indicates a substantial deepening off the west coast of the Peninsula, and in the results of some seismic work in the Andaman Sea; the latter was unfortunately confined to the area beyond the continental shelf but, even so, it shows the existence of relatively deep sedimentary basins there (Weeks, 1967). The west coast of Malaysia and Thailand could be of some interest, and a knowledge of the geological structure of Singapore, from which the submarine morphology could be interpreted, could provide some useful information in this connexion.

REFERENCES

Bemmelen, R.W. van, 1947. The Geology of Indonesia. The Hague, Netherlands.

Hill, R.D., 1968. The Singapore Deeps. *Malayan Nature Journal*, 21/2, Kuala Lumpur, Feb. 1968.

Kuenen, P.H., 1950. Marine Geology. John Wiley and Sons, New York, 568 pp.

Mainguy, M., 1968. Regional Geology and Prospects for Mineral Resources on the northern part of the Sunda Shelf. *CCOP Technical Bulletin*, vol. 1, 1968, pp. 129–142, 2 maps.

Weeks, L. Austin, *et alia*, 1967. Island arc system in the Andaman Sea, *Bull. Amer. Assoc. Petrol. Geol.*, vol. 51 (9).

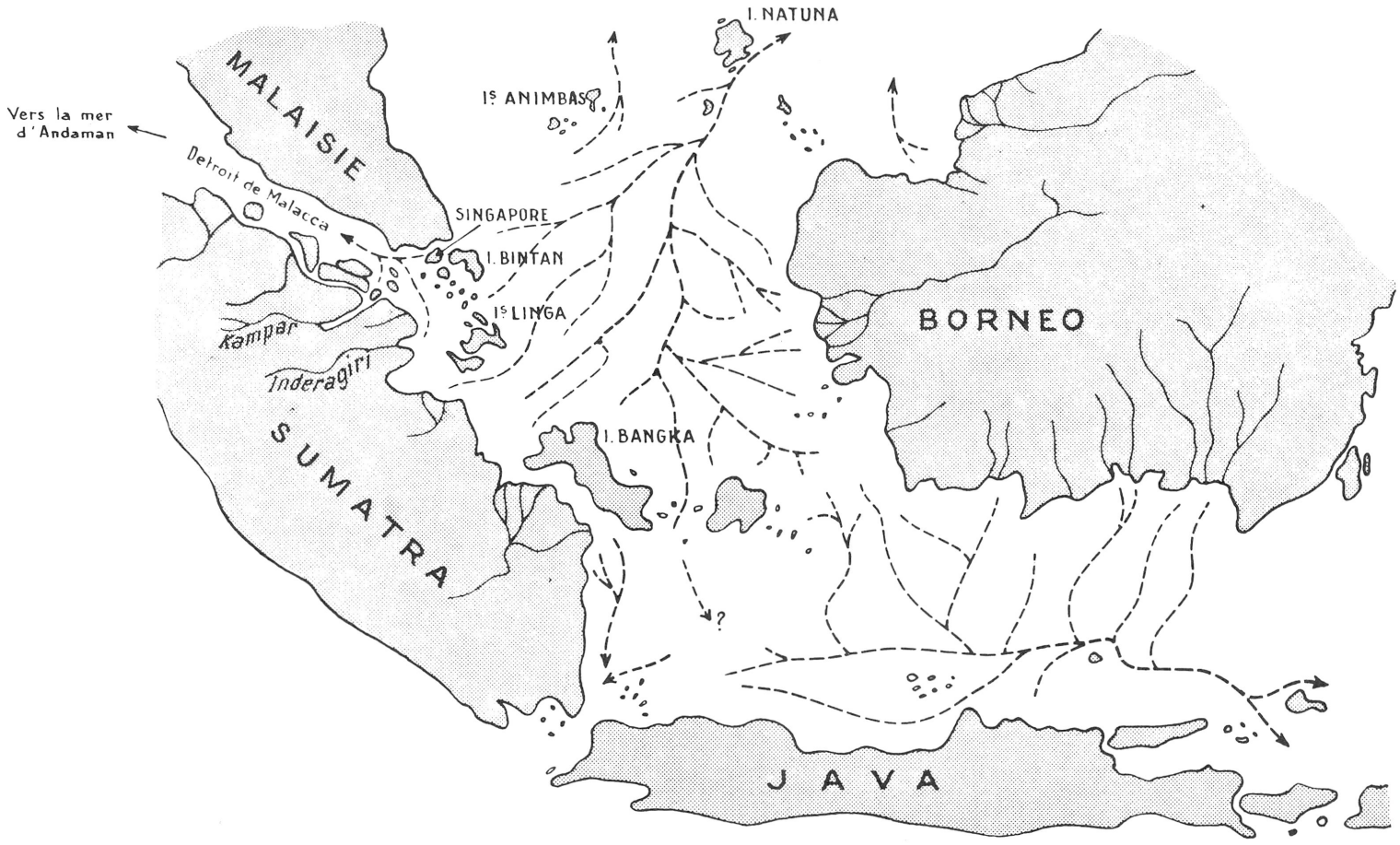

Figure 2. Submerged river channels of the Sunda Shelf.

Blank page

Page blanche

DEVELOPMENT AND STATUS OF PALEONTOLOGICAL RESEARCH IN THE PHILIPPINES

Benjamin A. Gonzales
Philippine Bureau of Mines

INTRODUCTION

Paleontological research in the Philippines may be considered to be still at its earlier stage of development. Despite the fact that studies on Philippine fossil faunas have been started decades ago by foreign specialists who made random collections from various localities in the country, the science has not developed with the same celerity and in such desirable manner as it did in other countries. Several factors are responsible for this lag, among the more important ones being: (1) There was not as much and as early need for its local application as probably there was in other countries hence, whatever studies were made during the early years were more of academically motivated rather than for economic reasons. (2) Most of the early workers were foreigners who came to the country not purposely to study the local faunal sequences but did so mostly by chance in connection with their studies in some other phase of the geological work either in this country or in other nearby regions. Results of their paleontological investigations were mostly not available to the few local geological practitioners and, therefore, did not inspire or motivate further studies. (3) Teaching of the science in local schools was started only very recently hence, there was not as much widespread awareness to it as probably there was in other countries.

However, intensified studies along the different phases of the work carried out during the past several years in connection with economic investigations or for academic reasons have given very satisfactory and encouraging results and have contributed immensely to the better understanding of the local faunal history and development.

HISTORICAL DEVELOPMENT

The first recorded study on Philippine fossil fauna was made more than a century ago in 1862 by Ferdinand von Richtofen who recognized Tertiary orbitoids (he referred to them as Nummulites) from Binangonan Peninsula in Luzon. Remarkable contributions were subsequently made by Felix Karrer (1878) on the Tertiary smaller Foraminifera from Western Luzon; Karl Martin (1896) on the Miocene and Pliocene molluscan faunas of Luzon and Mindanao and; by Warren D. Smith (1906, 1913, 1915) who made several contributions on the occurrence of Philippine orbitoid species and other invertebrate fossils and who, for the first time, put into systematic basis recorded knowledge on Philippine Paleontology and Stratigraphy.

In 1919, H. Yabe published the first of a series of papers by Japanese workers on the distribution of Philippine species of *Lepidocyclina*. Subsequent works by the same investiga-

tor in collaboration with S. Hanzawa (1925, 1929) on the genera *Camerina* and *Discocyclina* provided much information on the then not too much known significance of the three genera in Philippine stratigraphic paleontology. Between 1920 and 1937, several outstanding contributions were made. Notable were by: Roy E. Dickerson (1921, 1928) on the fauna of the Vigo Group and on the distribution of marine fossils in the Philippines; Warren D. Smith (1924) who made a comprehensive review of all then available information on Philippine paleontology and stratigraphy and; Leopoldo A. Faustino (1926) who studied the stratigraphy and paleontology of Philippine coal measures and made initial correlations of Philippine Tertiary sedimentary sequences with those of the other areas in the Indo-Pacific Region using fossil faunas.

The first extensive and systematic study of Philippine Upper Mesozoic and Tertiary paleontology, particularly Foraminifera and Mollusca, was made immediately prior to World War II during the comprehensive study of Philippine geology in connection with the government-sponsored search for oil. During that survey, specific fossil types for the two fossil groups were selected, identified and provisionally compared with formally described and illustrated species from nearby regions. These types then served as guides in the setting-up of standard biostratigraphic sections for the Philippine Tertiary sequences. In order to provide the stratigraphers and geologists a system to use within the country, a classification of the local stages by the use of letters, so-called "letter classification," was provisionally set up for possible future comparison or correlation with the classical European stages but, more specifically with the letter-system established by Van der Vlerk (1927) for the East Indies. The Philippine Tertiary, therefore, was subdivided into six stages, viz., Tertiary U–Z, in ascending order, with some having finer zonal subdivisions (e.g. Tert. upper Z, Tert. Lower W, etc.). Much was hoped to be done by the workers after the initial phase of that survey was completed however, the outbreak of the Pacific war prevented them from undertaking the more detailed studies, especially the formal typological comparison they have contemplated at the onset of their work. A large volume of the fossil materials and records that were accumulated during that survey were either destroyed or lost during the war years hence, the Filipino geologists who were trained in paleontological work during the survey and who took over from the foreign specialists after the hostilities had to virtually start again from scratch and re-work what had been accomplished during the past years.

During the ensuing years and until 1955, the paleontologists of the Bureau of Mines who were then practically the only group engaged in paleontological work in the country carried out extensive studies mainly on foraminiferal faunas. Although they were hampered by the lack of vital reference materials and necessary facilities, the group nonetheless, accomplished much. Their painstaking studies especially on the stratigraphic ranges and systematic classification of Philippine foraminiferal species, led to the establishment of a more solid foundation for the local foraminiferal biostratigraphy and shed much light to the then rather confused status of Philippine stratigraphy and paleontology as a whole. For purposes of uniformity in usage and in order that stratigraphic and paleontologic correlations with other areas in the Indo-Pacific Province may be carried out with more success and less difficulty, the letter-stage classification as suggested and used by Corby, et al during the petroleum survey was modified (Teves, 1954) to conform more closely with that used in the East Indian region. Thus, Corby's Tert. U–Z letter-stage system was transformed to the more widely used Tert. a-h classification of the East Indies.

In 1956, renewed enthusiasm and the ensuing intensified activities in the search for petroleum in the country, brought about much more extensive and expertly studies of Philippine fossil faunas. In order to cope with the needs of modern oil exploration, the paleontologists in the country and those that were brought in by foreign exploration companies widened their scope of investigations. They turned to the more specialized phases of the work including those involving biofacies and paleo-environmental analyses, correlations, and such investigations related to the differentiation of morphogenetic stages of foraminiferal evolutionary series which proved very useful in the determination or timing of diastrophic breaks that are, sometimes, vaguely discernible in the field. Fossils and the paleontologists, at that time, played very active roles in the critical appraisal of the petroleum potentialities of the basin areas in the country. Intra- and extra-basinal correlations of economically important horizons were successfully carried out and greatly facilitated the finding of oil and (or) the rapid evaluation of the overall economic outlook of each prospective region.

For many years and until the early part of the active oil exploration period the larger Foraminifera and benthonic smaller Foraminifera stratigraphy provided a workable framework for many areas. However, large portions of the major sedimentary basins in the country where most of the oil exploration work were undertaken, are underlain by thick sedimentary formations in which the larger Foraminifera are either completely lacking or are very scarce. Among the ubiquitous benthonic smaller Foraminifera group, several stratigraphically valuable species were discerned but, due to the fact that the group, as a whole, is strongly facies-bound, they did not provide good markers which could be satisfactorily used for inter-basinal and regional correlations especially for the Lower and Middle Tertiary sections.

The importance of the evolutionary development of the planktonic Foraminifera for time-stratigraphy gradually came to be realized. It soon became clear that most, if not all, of the major stages in their evolution are locally represented but it took a few more years to work out initial zonations which could be used with some confidence, at least, in certain regions.

A generalized Cenozoic planktonic zonation, somewhat similar to that recognized in equivalent marine strata in other tropical areas of the world, was proposed for use in at least two basin areas in the Philippines (Bandy, 1962). Under the proposed scheme, the composite Tertiary sequence is divided into planktonic zones each based on either one or a combination of such criteria as assemblage associations, tops or bottoms of occurrences, or greatest abundance of particular species or groups in the assemblages. Thus twelve (12) such units starting with the Upper Oligocene (Chattian) *Globigerina concina ciperoensis* Zone through the Middle Pliocene association characterized by *Sphaeroidinella dehiscens dehiscens* were distinguished. Another scheme which is basically that proposed for Trinidad and Venezuela with few additions and which was supposedly applicable for use in the entire country was later suggested (Amato, 1965) however, this was under strong criticism mainly because it was based entirely on planktonic Foraminifera. Considering the fact that highly fossiliferous Tertiary limestones containing large Foraminifera abound in the Philippines, controversial opinions regarding their significance in the local time-stratigraphic classification have been aroused and have led to discussions on the merits of that proposal.

While most of the stratigraphic and paleontologic information contributed by oil exploration companies utilized the local letter-alphabet scale, a few workers used the classicial

European standards. Although the latter would be the most ideal scale to use, there was no united opinion as to the exact correlations of its stage boundaries with those in the letter-stage classification particularly for the Miocene and younger intervals. Furthermore, its usage in local biostratigraphy was considered still questionable inasmuch as no direct comparison between the faunas of the stages defined in Europe and those characteristic of Philippine sedimentary sequences had been made, and considering the accepted opinion that the Indo-Pacific fauna, of which the Philippine group forms a part, evolved independently and somewhat differently sometime during the Tertiary.

Nonetheless, relatively much more information on Philippine foraminiferal faunas were gathered, recorded and published during that short but active exploration period than what have been collected or reported during the previous several years.

Paleontological research after the decline in exploration activities was pursued with more zeal principally by the Paleontology Laboratory of the Bureau of Mines. Previous efforts were sustained and were aimed towards the establishment of faunal controls (foraminiferal zones) for the different basin areas; re-definition and refinement of known stratigraphic ranges of foraminiferal species in the light of new and more conclusive evidence based on properly measured control sections and; determination of morphogenetic and phyllogenetic characters among the representatives of both small and large foraminiferal species.

Research work once more gained headway in 1963 with the finding of a carboniferous cyathopsid coral in a boulder within Miocene-Pliocene conglomerate in southeastern Mindoro (Easton and Melendres, 1963, 1964). This particular horn coral which was identified as of the genus *Gshelia* although it also closely resembles *Caninia* in many aspects, is the first Paleozoic fossil reported from the Philippines. The discovery instigated further investigation of the Pre-Tertiary sediments in the region and in nearby island groups and led to the finding, later, of Permian fusulinids belonging to the *Neoschwagerina-Paraschwagerina-Verbeekina* group (Andal, 1966).

Although mention has been made in earlier reports, Paleocene has not been positively established in the Philippines until 1964 when re-examination of previously dated Eocene limestone through thin sections (Villavicencio and Andal, 1964) revealed the presence of *Distichoplax biserialis* (Dietrich) an alga-like form (Pia, 1935) allocated by Lemoine (1960) to Pterobranchia and which is restricted to Ta, or even to Paleocene, in North Borneo (Keij, 1962). The noted occurrence of this species in several localities definitely established the presence of Paleocene in the country and therefore, necessitated a further revision in the local time, time-rock classification, to wit: Tert. a which formerly was assigned to the Lower (?) Eocene was further subdivided into a lower (Tert. a_1) and an upper (Tert. a_2) part whereby the lower (Tert. a_1) portion tentatively represents the Paleocene.

This particular discovery stirred further interest in the previously dated "Undiagnostic" or Tert. a (? Oligocene to Lower Miocene) clastics below the *Distochoplax*-bearing limestones in southern Palawan and led to the recognition (Samaniego, 1964) of the planktonic species *Globorotalia velascoensis* (Cushman) a form considered restricted and(or) diagnostic for Paleocene in other tropical areas of the world. Thus, the conclusion on the definite existence of Paleocene in the Philippines based on the occurrence of *Distichoplax* was further confirmed by such additional data.

PRESENT STATUS

Today, the Paleontology Laboratory of the Bureau of Mines constitutes the biggest single group of workers who are actively engaged in continuing research on Philippine fossil materials. Although still limited in its studies to only two taxonomic classes (Foraminifera and Mollusca) the laboratory is working simultaneously on several projects of importance which, eventually, will lead to the fuller understanding of the systematics, evolutionary lineages, and stratigraphic distribution of, at least, the foraminiferal faunas in Philippine biostratigraphy. Sustained studies more especially among the planktonics have lately made possible more precise and finer subdivisions of the time-stratigraphic framework and have led to the recognition of, more or less, definite or characteristic fossil associations within particular intervals in the local Tertiary succession. Thus, with the application of either or both small or large foraminiferal combinations, it is now possible to determine with more centainty than before, specific intervals within the Tertiary and even venture on their possible correlations with similar sequence outside the country.

The letter-stage subdivisions for the Tertiary now in use together with some of the characteristic fossil associations used in their recognition are as follows:

Tertiary a_1 (Paleocene)—Deep-water planktonic assemblages are characterized by the restricted occurrence of *Globorotalia velascoensis, G. aequa*, and *Globigerina triloculinoides*. Among the larger Foraminifera associated in general with reef limestones and, seldomly, with coal measures the genus *Miscellanea* and the species *Alveolina primaeva* in addition to *Distichoplax biserialis* are mentioned.

Tertiary a_2 (Lower (?) Eocene)—Primitive forms of *Discocyclina* and *Nummulites* (e.g., *Nummulites globulosa*) and species of the genus *Assilina* represent the faunal facies found in limestones. Among the planktonic species, *Globorotalia aragonensis* and *Halkyardia* make their initial appearance but range through the Upper Eocene (Tert. b) and probably even younger.

Tertiary b (Upper (?) Eocene)—Large lenticular *Nummulites*, e.g., *N. gizehensis, N. boninensis* and *N. aturicus* in association with species of *Pellatispira* and *Fabiana* are typical forms found in limestone deposits. Restricted occurrences of *Hantkenina alabamensis, Globorotalia centralis*, and *G. cerro-azulensis* are criteria used in the recognition.

The top of Tertiary b forms an important stratigraphic horizon in the Philippines as it marks the level where the Eocene *Globorotalia* strain and such genera as *Pellatispira, Discocyclina, Biplanispira,* and *Hantkenina* disappear from the fauna.

Tertiary c-d (Oligocene)—Oligocene planktonic assemblages are characterized by *Globigerina oligocaenica, G. ciperoensis ciperoensis*, and *Globorotalia opima opima*. In limestone sections, the reticulate *Nummulites fichteli* and *N. vascus* usually associated with the orbitoid *Lepidocyclina (P.) planata* are important forms. A distinctive feature is the absence of *Globigerinoides* species in the assemblages.

In the Philippines, the Oligocene-Miocene boundary problem has not yet been satisfactorily resolved hence, the interval in the letter-classification corresponding to Tertiary e_{1-3} is vaguely termed "Oligo-Miocene." Although the fossil criteria has not been conclusively established, evidence seemingly suggest that the interval

corresponds to the upper portion of the local Oligocene represented by a fauna somewhat different and older than what is presently considered as representative of Tertiary e_{4-5} (Lower Miocene) but possibly younger (e.g., absence of *Globigerina oligocaenica*) than that of the Tertiary d assemblage.

Tertiary e_{4-5} (Lower Miocene)—Large forminiferal assemblages are typified by the abundant occurrence of Eulepidinas associated with *Cycloclypeus communis, Borelis pygmaems*, and species of *Spiroclypleus* and *Miogypsinoides*. Species of *Nephrolepidina* occur rarely. Planktonic forms associated with the deep-water clastic facies of rocks include *Globigerinoides bisphaericus, Porticulasphaera glomerosa curva,* and *Globigerina altiapertura.*

Evidently, in this interval the Neogene strain of Globorotalia emerged, evolving into the *Globorotalia menardii* and *Globorotalia fohsi* lineages in the younger sections. Occurring almost simultaneously is the significant development of species referable to *Globigerinoides* which, similarly and rapidly, evolved into the *Globigerinoides triloba-Orbulina universa* group in the younger intervals.

Tertiary f_1–f_2 (Middle Miocene)—Outstanding features among the pelagic assemblages which distinguish the interval from the older and which could aptly serve as bases for subdividing the local Middle Miocene into at least two parts are: the first appearance of *Orbulina universa* at or very near the base of Tertiary f_1; and the gradual development of keeled Globorotalias as shown by the transition in the *G. fohsi* and *G. praemenardii* lineages.

Among the near-shore benthonic assemblages of the type found in limestones, the abundant occurrence of Nephrolepidinas and Miogypsinas and the complete absence of Eulepidinas are significant. *Cycloclypeus transiens* and species of *Flosculinella* are associated forms.

A handicap in biostratigraphic classification and more so in correlations is the presence of an almost wholly arenaceous small foraminiferal fauna in several areas and in moderately thick formations. This particular association containing a restricted number of species of *Ammobaculites, Cyclammina, Trochamina*, and *Bathysiphon* is found mostly associated with fine silts and probably represents a deep-water facies.

Tertiary f_3 (Upper Miocene)—Small foraminiferal associations though abundantly represented lack stratigraphically restricted forms. Recognition therefore depends either on lowest or highest stratigraphic occurrence of certain species within particular horizons in the interval, assemblage associations, negative evidence, or a combination of two or all factors. Among the newcomers *Globorotalia crassaformis, G. tumida*, and *Sphaeroidinella dehiscens immatura* are mentioned. Typical *Globorotalia praemenardii, G. fohsi robusta*, and possibly *Globoquadrina dehiscens* make their last appearance.

In limestone sections, *Miogypsina kotoi* and species of *Tribliolepidina* are recognized.

Tertiary g–h (Pliocene)—Orbitoid Foraminifera is absent. *Cycloclypeus carpenteri, Operculinoides reticulata,* and species of *Alveolinella* occur commonly but persist

to the Recent. Among the pelagic forms *Sphaeroidinella dehiscens dehiscens* and *Globorotalia truncatulinoides* make their initial appearance and, in addition to *Pulleniatina obliquiloculata*, constitute the characteristic forms.

In several widely scattered areas monotonous but rich assemblages containing diversified forms of *Nonion, Elpidium*, and *Rotalia* generally associated with coarse clastic sediments are found.

Pleistocene—Quaternary deposits of generally shallowwater origin are distinguished by the presence of *Calcarina spengleri, Marginopora vertebralis,* and species of *Baculogypsinoides*. Similarly with Pliocene, rich molluscan faunas are found and together with the abundantly represented benthonic smaller Foraminifera are of much help in biostratigraphic studies.

Detailed investigations conducted lately on the Philippine Cretaceous has indicated at least two subdivisions, each represented by a distinct fauna which, more or less, correlate with those found in synchronous strata elsewhere in the world.

Lower Cretaceous assemblages considered correlative with those described from the Albian and Aptian in other regions include such species as *Cuneolina hensonii, C. pavonia,* and *C. parva*, in addition to small forms of *Orbitolina* and the algae *Lithocodium*. A distinctive feature is the absence of planktonic species.

Turonian—Maestrichtian equivalents are characteristically rich in planktonics, the most typical of which probably is the genus *Globotruncana* represented by several species. Large foraminiferal associations include *Kathina jamaicensis* and forms referable to *Pseudorbitoides* and *Omphalocycleus*.

Until about a few years ago, stratigraphic correlation work in the Philippines depended mainly on the benthonic Foraminifera. The work thus have been limited within individual basins and the results, at that, have not quite been satisfactory owing largely to the fact that vertical and lateral facies are generally rapid. Attempts were made to correlate the Philippine Tertiary subdivisions with those of the classical European stages but failed primarily because the Philippine fauna like those of the other areas in the Indo-Pacific Province has characteristics of its own.

However, recent biostratigraphic studies conducted in the major basinal areas have shown that correlation within and between these areas could be carried out more accurately with the use of planktonics. Thus faunal zones based on their stratigraphic occurrences in properly measured and systematically sampled control sections are established in the individual regions and compared. Minor adjustments in some instances had to be made between the allocated time ranges of certain elements in both small and large Foraminifera groups and, as the case may be, in the stratigraphic position of some formations but, a reasonably reliable correlation between the larger Foraminifera and the planktonic zonation is always obtained.

Amassed information have, by large, indicated the feasibility of establishing one zonation standard for the whole country which, even as now, appears to closely correlate with those set up in the other tropical areas of the world. For example, with the planktonic data at hand it is now possible to state, with some reservations, that the Philippine Tertiary e_{4-5} correlates,

at least in part, with the Aquitanian; Tertiary f_1_f_2 with the Burdigalian and; Tertiary f_3 partly with the Vindobonian as described by Blow (1959) in Venezuela.

Table 1 shows the time range of some characteristic fossils in the Philippine Tertiary.

REFERENCES

Andal, P.P., 1966, A report on the discovery of fusulinids in the Philippines: The Philippine Geologist, vol. 20, no. 1, pp. 14–22.

Amato, F.L., 1965, Stratigraphic Paleontology in the Philippines: The Philippine Geologist, vol. 19, no. 1, pp. 1–24.

Bandy, O.L., 1962, Cenozoic planktonic foraminiferal zonation and basinal development for the Philippines: The Philippine Geologist, vol. 16, no. 3, pp. 12–34.

Blow, W.H., 1959, Age, correlation and biostratigraphy of the upper Tocuyo (San Lorenzo) and Pozon formations, Eastern Falcon, Venezuela: Bull. Amer. Pal., vol. 39, no. 178, pp. 67–251.

Corby, G.W., et al 1951, Geology and oil possibilities of the Philippines: Phil. Bur. of Mines Tech. Bull. No. 21.

Easton, W.H. and Melendres, Jr. M.M., 1963, First Paleozoic fossil from Philippine Archipelago: Bull. Amer. Assoc. Pet. Geol., vol. 47, no. 10, pp. 1871–1886.

Samaniego, R.M., 1964, The occurrence of *Globorotalia velascoensis* in the Philippines: The Philippine Geologist, vol. 18, no. 3, pp. 65–74.

Teves, J.S., 1954, Indonesian Tertiary alphabet symbols for use in the Philippines: The Philippine Geologist, vol. 8, no. 3, pp. 67–70.

Villavicencio, M.L., and Andal, P.P., 1964, *Distichoplax biserialis* (Dietrich) in the Philippines: The Philippine Geologist, vol. 18, no. 4, pp. 103–113.

Table 1. Time range of some characteristic fossils in the Philippine Tertiary.

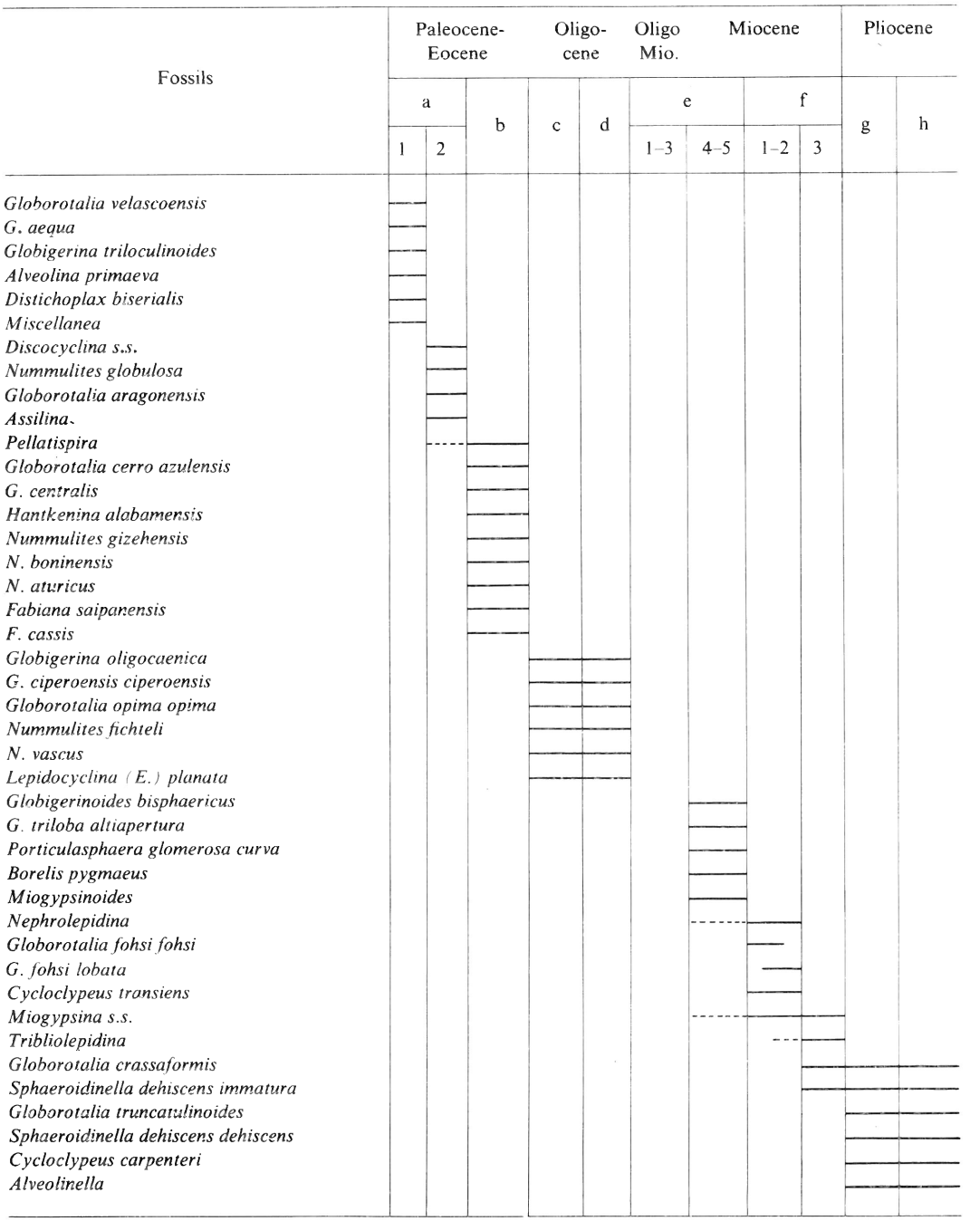

Blank page

Page blanche

A PETROGRAPHIC STUDY OF THE MESOZOIC AND CENOZOIC ROCK FORMATIONS IN THE TUNGLIANG WELL TL-1 OF THE PENGHU ISLANDS, TAIWAN, CHINA

By
J. T. Chou
Chinese Petroleum Corporation
(with tables 1–3, and figures 1–22)

ABSTRACT

A petrographic study of the Mesozoic and Cenozoic rocks in the Tungliang Well TL–1, Paisha, Penghu Islands, was made, based on 16 core samples and 50 rock thin sections.

The rocks below 503.5 m depth, possibly of Mesozoic age, comprise hydrothermally altered arkose, subarkose, sandstone, siltstone, and porphyrite or basaltic rock. The hydrothermally formed minerals present in these rocks indicate that these rocks were hydrothermally altered, representing the later stage of the farther facies of a contact metamorphism. Between 592 m and 695 m depth, the hydrothermal alteration gradually becomes stronger with increase of depth. The siltstones, sandstones, and arkoses between 725 m and 898 m depth are affected by hydrothermal veins. The ages of these rocks are still unknown because no fossils have been found in them, but they are petrographically similar to the so-called Mesozoic rocks in the Paochung Well PC–1, which are well correlated with the Mesozoic formations (containing the Aptian Ammonite and Mollusca fauna) in the Peikang Well PK–2 and PK–3, western Taiwan.

The Cenozoic rocks above 503.5 m depth in Well TL–1 consist of limestone, sandstone, graywacke, subgraywacke, mudstone, and claystone, of Miocene age, and of hypersthene-augite dolerite, augite-bearing-hypersthene basalt, basaltic tuff, sandstone, shale, mudstone or claystone, of Pliocene and Pleistocene age. The limestone between 500 m and 503.5 m depth contains *Miogypsina*, and lies unconformably above the so-called Mesozoic formations.

The so-called Mesozoic rocks are quite different lithologically from those of the Cenozoic. The Mesozoic rocks are relatively indurated, cherty, and hydrothermally altered. Their apparent specific gravities are higher than 2.5, and their effective porosities are lower than 7 per cent. On the contrary, the Cenozoic rocks are relatively friable, higher in effective porosity (77 %), and entirely free from hydrothermal alteration.

The Cenozoic sand grains are more rounded than the Mesozoic ones. The average sphericity of the Cenozoic sand grains is 0.75 and that of the Mesozoic ones is 0.73. In Well PC–1, the Tertiary sand grains are also more rounded than the Mesozoic ones. The average sphericity of the Tertiary sand grains in PC–1 is 0.80, and that of the Mesozoic ones is 0.75. The average sphericity of the sand grains in Well PC–1 is higher than that of the sand grains in Well TL–1. This may indicate that the sediments in Well TL–1 are closer to the source area.

The dolerite and basalt, occurring between 116 m and 305 m depth, were probably intruded and extruded during Plio-Pleistocene time and belong to the Penghu basaltic stage.

Published with the Permission of the Chinese Petroleum Corporation.

INTRODUCTION

As a first step in oil exploration in the Taiwan Strait, the Chinese Petroleum Corporation (CPC) drilled a stratigraphic test well on the Penghu Islands (the Pescadores) in 1966 in order to know the thickness, lithology, geologic structure and the age of the sedimentary rocks under the Strait.

The drilling of the Tungliang stratigraphic test well (called the Tungliang TL–1) was commenced on October 15 and suspended on December 7, 1966. The well is located about 850 m northeast of the village of Tungliang (Fig. 1) on land 5.78 m above sea level. It was drilled to a total depth of 899 m but neither oil nor gas was found.

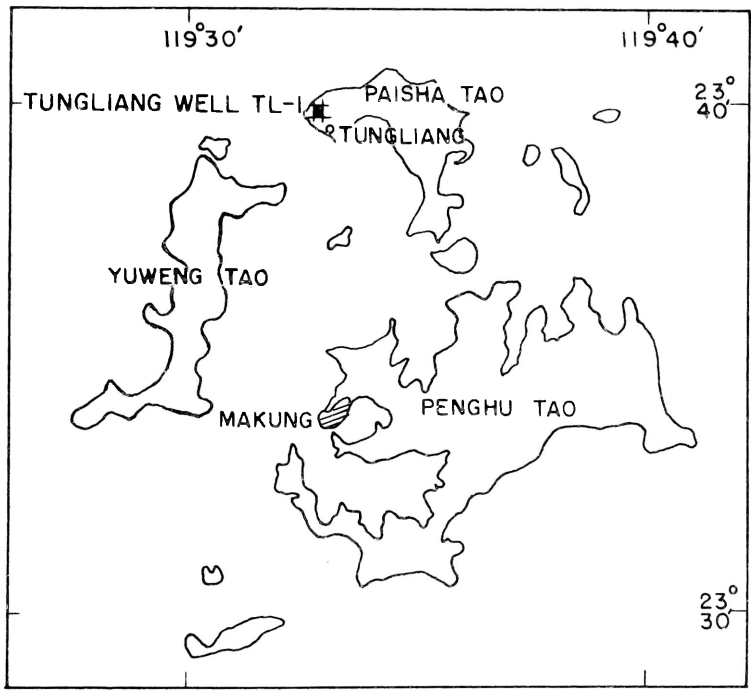

Figure 1. Map showing the location of the Tungliang well TL–1 of the Penghu Islands, Taiwan, China.

This well not only furnishes important information on the subsurface geology in the Penghu region, but also clarifies the geologic relations between the Penghu region and the Peikang region.

Based on Pan's regional gravimetric study (1967), Huang's foraminiferal study (1967), and the writer's petrographic study, a stratigraphic profile between the Tungliang Well TL–1 and the Paochung Well PC–1 was drawn (Fig. 2). The Paochung Well, located two kilometres north of Paochung, Yunlinhsien, was drilled to the total depth of 1989.82 m by CPC in 1959, and the Mesozoic formations were encountered below 1688 m depth.

According to Huang's study (1967), the upper part of the subsurface formations in Well TL–1 is believed to range from Miocene to Pleistocene in age, but the suggested Mesozoic age of the lower part is possibly subject to change because no fossils have been found in this part.

Table 1. Mineralogical constituents of the Mesozoic and Cenozoic igneous rocks of the Tungliang Well TL–1 of the Penghu Islands.

Depth (m)	Figure No.	Geological age	Classification of rocks	Mineralogical constituents																	
				Labradorite	Tremolite (mono amphiboles)	Augite	Hypersthene	Diopside (clino-pyroxenes)	Pigeonite	Chlorite	Serpentine	Magnetite	Pyrrhotite	Chalcedony	Zeolites (analcite)	Biotite	Muscovite	Calcite	Calcareous cement	Plagioclase	Glass
Well TL–1 116–116.4	22	Pliocene Pleistocene	Augite-bearing hypersthene basalt (Zeolitized)			R	R			VR		R		C	VR			R	R	C	VR
302–305	20	Pliocene and Pleistocene	Hypersthene-augite dolerite	C		R	R		R	C	VR	VR									
695–695.15d	4	Mesozoic or (Paleocene)	Porphyrite or basaltic rock, hydrother—mally altered		C			R					C			VR	VR	P		C	

C: Common, R: Rare, VR: Very rare, P: Present

Table 2. Mineralogical constituents of the Mesozoic and Cenozoic sedimentary rocks of the Tungliang Well TL–1 of the Penghu Islands.

Depth (m)	Figure No.	Geological age	Classification of rocks	Roundness	Sphericity	Mineralogical constituents (Volume percent)																		
						Quartz	Chert	Feldspars	Rock fragments	Iron ores	Pyrrhotite	Rutile	Glauconite	Chlorite	Zeolites	Zircon	Epidote Diopside Actinolite	Carbonaceous cement	Calcite	Calcareous cement	Siliceous cement (cherty)	Muscovite or Sericite (matrix)	Biotite (matrix)	Argillaceous (clayey) matrix
Well TL–1 202–207	21	Pliocene and Pleistocene	Arenaceous shale or arenaceous mudstone			54	2.0	1.0	5.0	8.0		1.0	18.0			0.2		5.0				3.0		2.8
403–407	19	Miocene	Subgraywacke, v.f.g., lt. gy.	Suba.-Subr.	0.75	60	8.0	2.5	6.5	1.0			3.0	5.0						8.0		1.0		5.0
500	18	Miocene	Limestone rich in Miogypsina	Suba.-Subr.	0.75	6	3.5	1.0		1.0			0.5						80.0	8.0				
503.8	17	Miocene	Silty sandstone subgraywacke, v.f.g.	An.-Suba.	0.75	38	35.0	1.0	5.0	3.0											7.0	6.0		5.0
592–592.55	16	Mesozoic or Paleocene	Cherty silty subarkose	An.-Suba.	0.73	39	28.0	6.0	3.0	1.5	1.0			1.5						2.0	11.0	2.5	4.5	
631.8–632a	15	Mesozoic or Paleocene	Cherty siltstone			52			5.0	1.0						0.5					9.5	10.0	22.0	
631.8–632c	14	Mesozoic or Paleocene	Cherty siltstone		0.73	74			2.0	2.0											6.0	12.0		4.0
660–660.35a	13	Mesozoic or Paleocene	Silty subarkose, hydrothermally altered	An.-Suba.	0.73	46	10.0	8.0	2.0	2.0	2.0				2.0		9.0		5.0	5.0	3.0	3.0	3.0	
725.7–726.4c	12	Mesozoic or Paleocene	Arenaceous siltstone, hydrothermally altered	An.-Suba.	0.73	70.9		2.0	2.0	3.0		2.0				0.1					6.0	9.0	5.0	
763.9–765.3a.c.		Mesozoic or Paleocene	Arenaceous siltstone, hydrothermally altered	An.-Suba.	0.73	71.3	3.0	2.0	1.0	1.5	2.0					0.2				8.0		10.0	1.0	
763.9–765.3b.d.e.	11	Mesozoic or Paleocene	Arenaceous siltstone, hydrothermally altered	An.-Suba.	0.73	60.5	2.0	2.5	0.5	1.0	3.0									2.0	5.0	3.5	20.0	
797–797.7a.b.c.	10	Mesozoic or Paleocene	Arenaceous Sericitic siltstone	An.-Suba.	0.73	73				2.0		0.1				0.1					2.0	22.8		
797–797.7d	9	Mesozoic or	Silty sandstone graywacke, v.f.g.	An.-Suba.	0.71	56	7.0	1.0	15.0	0.5			0.5						2.0	1.0		1.0		16.0
830–831.1a	8	Mesozoic or Paleocene	Cherty siltstone	Suba.	0.73	65			3.0	3.0											9.0	15.0	5.0	
830–831.1b	7	Mesozoic or Paleocene	Sericitic siltstone	Suba.	0.73	46			3.0	3.0						0.1					4.9	43.0		
864.2–865.1a	6	Mesozoic or Paleocene	Silty arkose	An.-Suba.	0.73	55		17.0	2.0	1.0				10.0					3.0		2.0	10.0		
898–898.2a	5	Mesozoic or Paleocene	Arkose, hydrothermally altered	An.-Suba.	0.73	64.5		12.5	2.0		2.0			1.0			14.0		2.0		2.0			

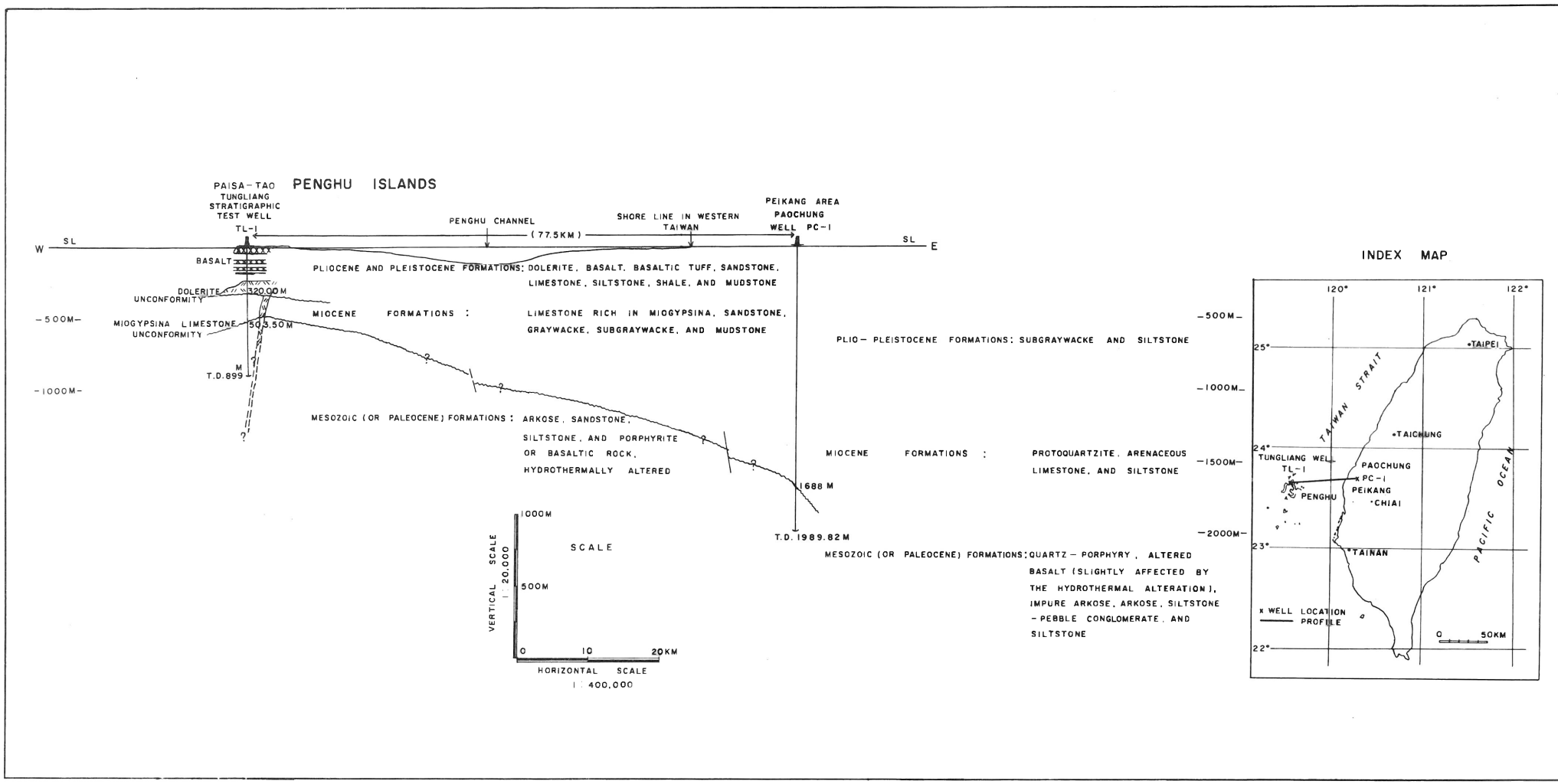

Figure 2. Stratigraphic profile between the Tungliang well TL–1 and the Paochung well PC–1.

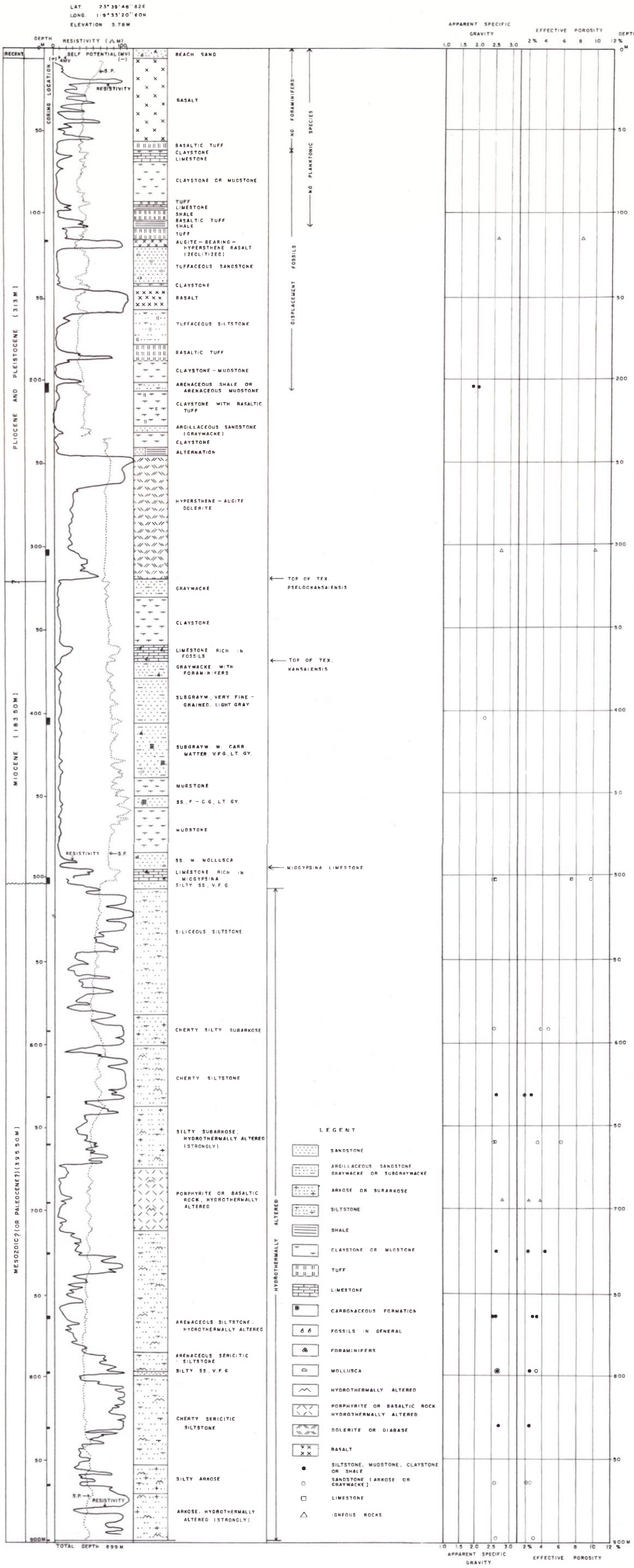

Figure 3. Columnar section of the Tungliang well TL–1.

The petrographic study of the Mesozoic and Cenozoic rocks in the Tungliang Well TL–1 was based on 16 core samples and 50 rock thin sections. The results of the mineralogical analysis and the measurements of apparent specific gravity and effective porosity of the rocks are given in Tables 1, 2, and 3. The columnar section of the rock formations is presented in Figure 3.

PETROGRAPHY

The grain sizes of the particles were determined on Wentworth's scale. The rocks were defined according to Moorhouse's (1959) and Pettijohn's (1957) classifications.

The mineralogical constituents of the porphyrite or basaltic rock and the other igneous rocks in the Tungliang Well TL–1 are shown in Table 1 and those of the sedimentary rocks in Table 2.

Table 3. Apparent specific gravities and effective porosities of the rocks in Well TL–1.

Depth (m)	Classification	Apparent specific gravity	Effective porosity (%)
116—116.45	Augite-bearing hypersthene basalt	2.57	8.41
202—207A	Arenaceous mudstone	1.88	—
202—207B	Arenaceous shale	2.02	—
302—305	Hypersthene–augite dolerite	2.73	10.19
403—407	Subgraywacke, very fine-grained, light gray	2.23	—
500—503.8A	Limestone rich in *Miogypsina*	2.51	7.31
500—503.8B	Silty sandstone, very fine-grained	2.54	9.65
592—592.55A	Cherty silty subarkose	2.55	4.65
592—592.55B	Cherty silty subarkose	2.55	3.74
631.8—632A	Cherty siltstone	2.61	2.62
631.8—632B	Cherty siltstone	2.60	1.86
660—660.35A	Silty subarkose, hydrothermally altered	2.52	6.18
660—660.35B	Silty subarkose, hydrothermally altered	2.57	3.54
695—695.15A	Porphyrite or basaltic rock, hydrothermally altered	2.76	3.89
695—695.15B	Porphyrite or basaltic rock, hydrothermally altered	2.79	2.25
725.7—726.4A	Arenaceous siltstone, hydrothermally altered	2.62	2.26
725.7—726.4B	Arenaceous siltstone, hydrothermally altered	2.63	4.27
764.1 A	Arenaceous siltstone, hydrothermally altered	2.54	3.30
764.1 B	Arenaceous siltstone, hydrothermally altered	2.60	2.96
797—797.7B	Arenaceous sericitic siltstone	2.65	2.44
797—797.7A	Silty sandstone (graywacke?), very fine-grained	2.65	3.23
830—831.1	Cherty sericitic siltstone	2.71	2.44
864.2—865.1A	Silty arkose	2.59	2.14
864.2—865.1B	Silty arkose	2.57	2.50
898—898.2	Arkose, hydrothermally altered	2.64	3.03

Rocks of the Mesozoic Formations

The so-called Mesozoic rocks, occurring below 503.5 m depth, include arkose, subarkose, siltstone, sandstone, and porphyrite or basaltic rock. These are quite similar to the so-called Mesozoic rocks in Well PC–1 drilled on the coastal plain in western Taiwan. Most of these rocks in Well TL–1 are characterized by the appearance of hydrothermally formed minerals such as epidote, diopside, actinolite, chlorite, calcite, pyrite, pyrrhotite, biotite, muscovite, sericite, etc. Especially, the arkose is strongly affected by hydrothermal solution between 898 m and 898.2 m depth and between 660 m and 660.35 m depth. This phenomenon may represent the later stage or the farther facies of a contact metamorphism.

Porphyrite or basaltic rock, hydrothermally altered: This rock (Fig. 4) occurs at the depth of 695 m. It is gray to greenish gray in color, and composed mainly of plagioclase, tremolite, diopside and pyrrhotite, with small amounts of biotite, muscovite, and calcite. The rock is characterized by abundant prismatic or fibrous tremolite crystals which are colorless to pale green. It is also characterized by the abundant pyrrhotite grains. The plagioclase is probably represented by the calcic plagioclase. The diopside is colorless to pale green. The abundant grains of tremolite, diopside, and pyrrhotite indicate that the rock was hydrothermally altered, representing the later stage or the farther facies of a contact metamorphism. The apparent specific gravity of the porphyrite ranges from 2.76 to 2.79, and the effective porosity ranges from 2.25 to 3.89 per cent.

Arkose, hydrothermally altered: This arkose (Fig. 5) occurs at the depth of 898 m, the bottom of the well. It is gray to dark gray in color. The sand grains are angular to subangular in shape and silt to coarse in size, the mean sphericity being 0.73. The arkose is composed mainly of quartz, orthoclase, and plagioclase, with small amounts of rock fragments, calcite, pyrrhotite, epidote, diopside, actinolite, and chlorite. It is characterized by more grains of epidote, diopside, actinolite and chlorite, indicating that the arkose must have been hydrothermally altered, and may represent the later stage or the farther facies of a contact metamorphism. The apparent specific gravity is 2.64, and the effective porosity is 3.03 per cent.

Silty arkose: Silty arkose (Fig. 6) was found between 864.2 m and 865.1 m depth. It is light gray to gray in color and quite hard. The sand grains are angular to subangular in shape and silt to coarse in size, the mean sphercity being 0.73. The arkose consists mainly of quartz, feldspars (mostly orthoclase) and chlorite. Small amounts of iron ores, muscovite, rock fragments, and calcite are also present. The matrix consists mainly of sericite and the cement is siliceous. The anhedral chlorite is pale green and shows an abnormal blue interference color, being probably penninite. It is associated with iron ores and is formed by hydrothermal alteration of aluminous minerals. The apparent specific gravity of the silty arkose ranges from 2.57 to 2.59 and the effective porosity ranges from 2.14 to 2.50 per cent.

Sericitic siltstone: This siltstone (Fig. 7), at *b* in the core from between 830 m and 831.1 m depth, is gray to dark gray in color. The particles are mostly silty and subangular in shape, the mean sphericity being 0.73. The siltstone is composed principally of quartz silt. Small amounts of muscovite, iron ores, and rock fragments, and a very small amount of euhedral zircon crystals, are also present. The matrix consists predominantly of sericite, and the

cement is siliceous. The siltstone is characterized by the very abundant minute shredded sericite. The sericite is a secondary mineral formed by hydrothermal alteration of silicates, especially the feldspars. Therefore, the siltstone was affected by hydrothermal solution. The sericitic siltstone has an apparent specific gravity of 2.71 and an effective porosity of 2.44 per cent.

Cherty siltstone: This siltstone (Fig. 8), at *a* in the core from between 830 m and 831.1 m depth, is also gray to dark gray in color. The particles are silty and subangular in shape, the mean sphericity being 0.73. The siltstone is composed mainly of quartz silt, with small amounts of iron ores and rock fragments. The matrix consists of sericite and biotite, and the cement is siliceous. The siltstone is charaterized by the abundant minute shredded sericite and biotite, indicating that it may have been hydrothermally altered. The apparent specific gravity of the cherty siltstone is 2.71, and the effective porosity is also 2.44 per cent.

Silty sandstone (graywacke?), very fine-grained: This sandstone (Fig. 9), at *d* in the core sample from between 797 m and 797.7 m depth, is gray in color and cherty. The sand grains are silt to medium in size and angular to subangular in shape, the mean sphericity being 0.71. The sandstone consists mainly of quartz, chert and rock fragments, with accessory sericite, iron ores, feldspars, glauconite, and calcite. The matrix is argillaceous and the cement is calcareous. The sandstone has an apparent specific gravity of 2.65 and an effective porosity of 3.23 per cent.

Arenaceous sericitic siltstone: This siltstone (Fig. 10), at *a*, *b* and *c* in the core from between 797 m and 797.7 m depth, is also gray in color and cherty. The particles are silt to very fine in size and angular to subangular in shape, the mean sphericity being 0.73. The siltstone is composed principally of quartz, with accessory iron ores and a very small amount of zircon and rutile. The matrix consists of muscovite-sericite, and the cement is siliceous. The muscovite-sericite is platy, shredded, and widespread. The presence of abundant muscovite-sericite grains indicates that the siltstone was altered by hydrothermal solution. The siltstone has an apparent specific gravity of 2.65 and an effective porosity of 2.44 per cent.

Arenaceous siltstone: This siltstone (Fig. 11), at *b*, *d* and *e* in the core from between 76g.9 m and 765.3 m depth, is gray in color and arenaceous. The particles are silt to medium in size and angular to subangular in shape, the mean sphericity being 0.73. The siltstone is composed chiefly of quartz grains, with small amounts of feldspars (chiefly orthoclase), pyrrhotite, chert, iron ores and rock fragments. The matrix consists of platy or wavy shredded biotite and sericite, and the cement is siliceous and calcareous. The biotite is yellow to greenish brown in color and strongly pleochroic. The siltstone is characterized by the biotite and the angular to subangular, very fine- to medium-grained quartz and the orthoclase. The presence of abundant biotite indicates that the siltstone was somewhat altered by thermal solution. The apparent specific gravity of the siltstone is 2.60, and the effective porosity is 2.96 per cent.

Similar siltstone at *a* and *c* in the core from between 763.9 m and 765.3 m depth is also gray in color and arenaceous. The particles range from silt to coarse in size and angular to subangular in shape, the mean sphericity being 0.73. The siltstone is composed principally of quartz, with small amounts of chert, biotite, feldspars, iron ores, pyrrhotite, rock fragments and zircon. The matrix consists of sericite, and the cement is siliceous. The siltstone was hydrothermally altered. The apparent specific gravity is 2.54, and the effective porosity is 3.3 per cent.

Similar siltstone (Fig. 12) at *c* and *d* in the core from between 725.7 m and 726.4 m depth is light gray to gray in color, arenaceous and cherty. The particles are angular to subangular in shape, the mean sphericity being 0.73. The siltstone is composed mainly of quartz silt. Small amounts of plagioclase, rock fragments, iron ores, zircon and rutile are also present. The matrix consists of biotite and sericite, and the cement is siliceous. The siltstone was hydrothermally altered. The apparent specific gravity ranges from 2.62 to 2.63, and the effective porosity ranges from 2.26 to 4.27 per cent.

Silty subarkose, hydrothermally altered: This subarkose (Fig. 13), at *a* in the core from between 660 m and 660.35 m depth, is gray is color. The sand grains are angular to subangular in shape, the mean sphericity being 0.73. The subarkose is composed chiefly of quartz, chert, and feldspars. Small amounts of rock fragments, iron ores, pyrrhotite, calcite, zeolites, actinolite, epidote, chlorite, chalcedony, and diopside are also present. The matrix consists of sericite and biotite and the cement is calcareous and siliceous. The sericite and chlorite are distributed throughout the subarkose. The presence of actinolite, diopside, epidote, chlorite, chalcedony, zeolites, pyrrhotite, and sericite indicates that the subarkose was hydrothermally altered, representing the later stage or the farther facies of a contact metamorphism. The calcite was replaced by pyrrhotite and zeolites. The zeolites have low refractive indices and lack of color in thin section. They are isometric, so that they are probably either analcite or faujasite. The apparent specific gravity of this silty subarkose ranges from 2.52 to 2.57, and the effective porosity ranges from 3.54 to 6.18 per cent.

Cherty siltstone: This siltstone (Fig. 14), at *c* in the core from between 631.8 m and 632 m depth, is gray in color and shows conchoidal fracture. The particles are mainly silt in size. The siltstone is composed principally of quartz silt, with small amounts of iron ores and rock fragments. The matrix is both argillaceous and sericitic, and the cement is siliceous. The siltstone is slightly altered by thermal solution. The apparent specific gravity is 2.60, and the effective porosity is 1.86 per cent.

Similar siltstone (Fig. 15), at *a* in the core from between 631.8 m and 632 m depth, is brownish gray to gray in color and also shows conchoidal fracture. It is made up predominantly of siltsized quartz and rock fragments, and spotted by iron ores and zircon. The matrix consists of biotite and sericite and the cement is siliceous. The siltstone was hydrothermally altered. The apparent specific gravity is 2.61, and the effective porosity is 2.62 per cent.

Cherty silty subarkose: This subarkose (Fig. 16), between 592 m and 592.55 m depth, is light gray to gray in color, cherty and silty. The sand grains are silt to coarse in size and angular to subangular in shape, the mean sphericity being 0.73. The subarkose is moderately poorly sorted. It consists mainly of quartz and chert, with small amounts of pyrrhotite, feldspars, rock fragments, iron ores and chlorite. The matrix consists of biotite and muscovite-sericite, and the cement is calcareous. The chlorite is platy, micaceous and pale green in color, and shows abnormal blue interference color; it is probably penninite. The apparent specific gravity of the subarkose is 2.55, and the effective p*f*irosity ranges from 3.74 to 4.65 per cent.

Rocks of the Cenozoic Formations

The Cenozic rocks, occurring above 503.5 m depth, include limestone, sandstone, graywacke, subgraywacke, mudstone and claystone of Miocene age, and hypersthene-augite

dolerite, augite-bearing-hypersthene basalt, basaltic tuff, sandstone, shale, mudstone or claystone, of Pliocene and Pleistocene age.

Silty sandstone, very fine-grained: This sandstone (Fig. 17) at 503.8 m depth is light gray to grayish white in color and silty. The sand grains are silt to fine in size and angular to subangular in shape, the mean sphericity being 0.75. The sandstone is composed mainly of quartz and chert, with small amounts of rock fragments, iron ores, and feldspars. The chert is the more abundant constituent. The matrix is argillaceous and sericitic, and the cement is siliceous. The rock fragments are shale and slate. The apparent specific gravity of this sandstone is 2.54 and the effective porosity is 9.65 per cent. The sandstone covers unconformably the Mesozoic formations.

Limestone rich in Miogypsina: The limestone (Fig. 18) between 500 and 503.5 m depth is light gray to grayish white in color; it is composed chiefly of *Miogypsina* sp., molluscan fragments, coralline algae, and some echinoid spines, with small amounts of very fine- to medium-grained quartz, chert, feldspars, glauconite and magnetite. The mineral grains are cemented by recrystallized calcite. The quartz grains are subangular to subrounded, the mean sphericity being 0.75. The glauconite is very small in amount. The apparent specific gravity of the limestone is 2.51 and the effective porosity is 7.31 per cent. Based on biostratigraphic considerations, this limestone may be equivalent to the Miocene molluscan limestone in the Peikang Well PK–3 (Huang, 1967). The limestone lies unconformably above the Mesozoic formations.

Subgraywacke, very fine-grained, light gray: The subgraywacke (Fig. 19) between 403 m and 407 m depth is light gray in color and silt-sized to medium-grained. The sand grains are subangular to subrounded in shape and the average sphericity is 0.75. The subgraywacke consists mainly of quartz, with small amounts of chert, rock fragments, chlorite, glauconite, feldspars (orthoclase and plagioclase), iron ores and sericite; chlorite and glauconite are the more common accessories. The matrix is argillaceous and the cement is calcareous. The apparent specific gravity of the subgraywacke is 2.23.

Hypersthene-augite dolerite: This dolerite (Fig. 20) between 302 m and 305 m depth is greenish black in color and shows a doleritic texture. The dolerite is composed mainly of calcic plagioclase, pyroxenes and chlorite, with accessory magnetite, serpentine or olivine. The plagioclase is labradorite; it is usually lath-shaped and well twined. The albite twinning is in rather narrow lamellae and is frequently combined with Carlsbad twins. The pyroxenes usually occupy an interstitial position to plagioclase. The common pyroxenes in the dolerite are augite, hypersthene, and pigeonite; these pyroxenes occur both as groundmass minerals and as phenocrysts. The augite is generally pale green in color and may probably be altered to chlorite. The hypersthene is also pale green in color and shows parallel extinction as measured from the trace of prismatic cleavage in thin sections cut parallel to the *c* axis. The pigeonite is colorless to pale green in color, and the maximum extinction angle varies from 22° to 45°. The chlorite is abundant as a secondary mineral; it is probably altered from the pyroxenes. The magnetite is a widespread accessory in the dolerite. The apparent specific gravity of the dolerite is 2.73.

Arenaceous shale or arenaceous mudstone: This shale or mudstone (Fig. 21) between 202 m to 207 m depth is composed principally of silt to very fine-grained quartz and glauconite,

with small amounts of iron ores, rock fragments, sericite, chert, feldspars, rutile and zircon in an argillaceous and carbonaceous matrix. The glauconite is predominantly present as grains in the matrix. The iron ores are mainly magnetite and limonite. The apparent specific gravity of the arenaceous shale is 2.02, and that of the arenaceous mudstone is 1.88.

Augite-bearing hypersthene basalt: This basalt (Fig. 22) between 116 m and 116.45 m depth is dark gray in color and has abundant vesicles. A great variety of minerals is found in the amygdules. All vesicles are filled with secondary minerals; the most abundant are calcite, zeolites (probably analcite) and silica minerals (including chalcedony and quartz). The plagioclases are tiny and lath-shaped, and occur in the calcic and glassy groundmass. Magnetite is a common accessory mineral. Augite also occurs commonly in the groundmass. There are large euhedral hypersthene phenocrysts; these are faintly pleochroic with typical pleochroism as follows: X=pink; Y=yellow; Z=green. They show parallel extinction as measured from trace of prismatic cleavage in sections cut parallel to the c axis. Some of the larger grained hypersthene phenocrysts are zoned. The chalcedony is present in the groundmass with plagioclase, calcite, glass, augite and chlorite. The chlorite was probably derived from aluminous minerals such as pyroxenes and amphiboles. The apparent specific gravity of the basalt is 2.57, and the effective porosity is 8.41 per cent.

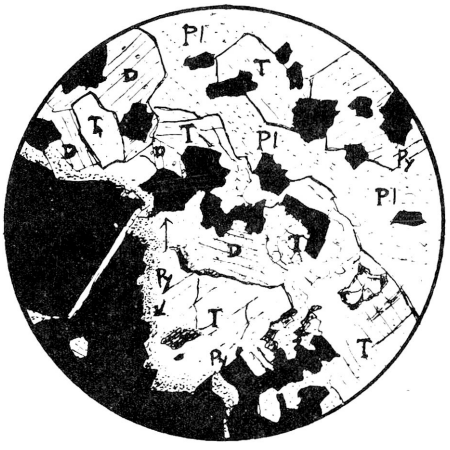

Fig. 4. Porphyrite or basaltic rock, hydrothermally altered, Mesozoic, Well TL-1 (695 – 695.15 m, d). Tremolite (T), diopside (D), pyrrhotite (Py), and laths of plagioclase (Pl) occur in micaceous groundmass. Lower polarizing prism only. (× 60.)

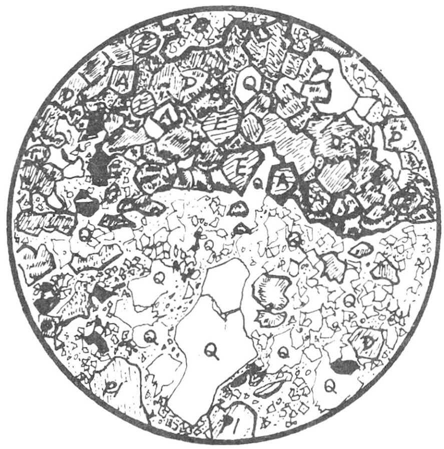

Fig. 5. Arkose, hydrothermally altered, Mesozoic, Well TL-1 (898 – 898.2 m, a). Angular to subangular grains of quartz (Q), orthoclase (Or), and plagioclase (Pl), with small amounts of rock fragments, calcite, pyrrhotite (Py), epidote (E), diopside (D), actinolite (A), and Chlorite (Ch), cemented by silica (chert and quartz). Lower polarizing prism only. (X 60.)

Fig. 6. Silty arkose, Mesozoic, Well TL-1 (864.2 – 865.1 m, a.) Angular to subangular grains of quartz (Q) and feldspars (F), with small amount of iron ores (I), muscovite (Mu), rock fragments, Chlorite (Ch), and calcite in sericitic matrix and siliceous cement. Lower polarizing prism only. (X 60.)

Fig. 7. Sericitic siltstone, Mesozoic, Well TL-1 (830-831.1 m, b). Subangular particles of quartz (Q), silt, with small amounts of muscovite (Mu), iron ores (I), rock fragments (R), and a very small amount of zircon in a sericitic matrix(S)cemented by siliceous matters(chert). Lower polarizing prism only. (X 60.)

Fig. 8. Cherty siltstone, Mesozoic, Well TL-1 (830-831.1 m, a). Subangular particles of quartz (Q) silt in a matrix of sericite (S) and biotite (B), with accessory iron ores (I) and rock fragments, cemented by siliceous matters (chert). Lower polarizing prism only. (X 180.)

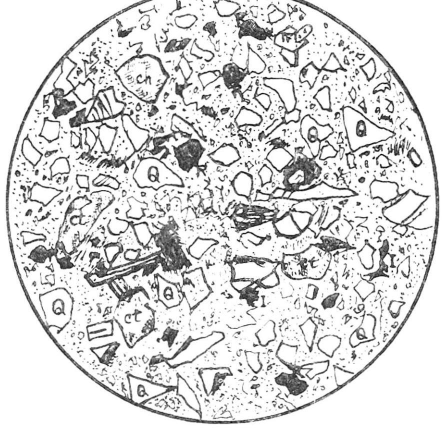

Fig. 9. Silty sandstone (graywacke ?), very fine-grained, Mesozoic, Well TL-1 (797 – 797.7 m, d). Angular to subangular grained quartz (Q), chert (Ct), and rock fragments (R), in argillaceous matrix, with accessory sericite, iron ores (I), feldspars, and glauconite, cemented by carbonate. Lower polarizing prism only. (X 60.)

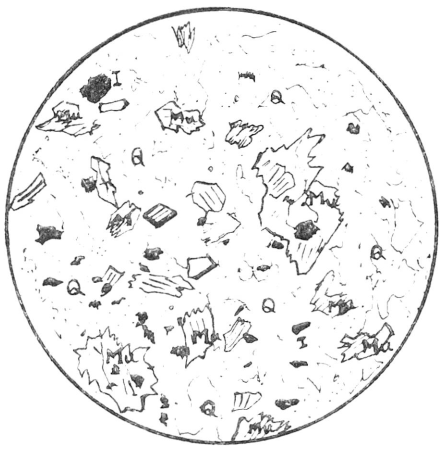

Fig. 10. Arenaceous sericitic siltstone, Mesozoic, Well TL-1 (797 – 797.7 m, a. b, and c). Angular to subangular particles of quartz (Q) in a matrix of muscovite (Mu) – sericite, with accessory iron ores (I), rutile, and zircon, cemented by silica. Lower polarizing prism only. (X 180.)

Fig. 11. Arenaceous siltstone, Mesozoic, Well TL-1 (763.9 - 765.3 m, b, d, and e). Angular to subangular grained quartz (Q) silt in a matrix of biotite (B), and sericite, with accessory chert, rock fragments, iron ores (I), feldspars, and pyrrhotite, cemented by silica and carbonate. Lower polarizing prism only. (X 180.)

Fig. 12. Arenaceous siltstone, Mesozoic, Well TL-1 (725.7 - 726.4 m, c). Angular to subangular grained quartz (Q) silt in a matrix of sericite (S) and biotite (B), with small amounts of accessory plagioclase (Pl), rock fragments, zircon, iron ores (I), and rutile (Ru), cemented by siliceous matters. Lower polarizing prism only. (X 180.)

Fig. 13. Silty subarkose, hydrothermally altered, Mesozoic; Well TL-1 (660 – 660.35 m, a). Angular to subangular grained quartz (Q) and feldspars in a matrix of sericite, with accessory rock fragments, iron ores, biotite, pyrrhotite, calcite (Ca), zeolites (Z), actinolite, epidote (E), chlorite (Ch), Chalcedony, and diopside, cemented by carbonate, chert (Ct), and quartz. Lower polarizing prism only. (X 60.)

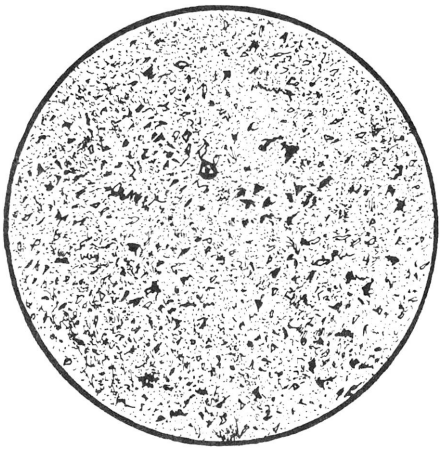

Fig. 14. Cherty siltstone, Mesozoic, Well TL-1 (631.8 – 632 m, c). Angular to subangular grained quartz silt in argillaceous and sericitic matrix, with accessory iron ores and rock fragments, cemented by silica (chert). Lower polarizing prism only. (X 60.)

Fig. 15. Cherty siltstone, Mesozoic, Well TL-1 (631.8-632 m, a). Angular to subangular grained quartz (Q) silt and rock fragments (R) in a matrix of biotite (B), sericite (S), and muscovite, with accessory iron ores and zircon, cemented by silica (chert). Lower polarizing prism only (X 60.)

Fig. 16. Cherty silty subarkose, Mesozoic, Well TL-1 (592 - 592.55 m, a and b). Angular to subangular quartz (Q) grains and chert (Ct) grains in a matrix of biotite (B) and muscovite-sericite (S), with accessory pyrrhotite (Py), feldspars (F), rock fragments, and glauconite, cemented by silica (chert) and carbonate. Lower polarizing prism only. (X 60.)

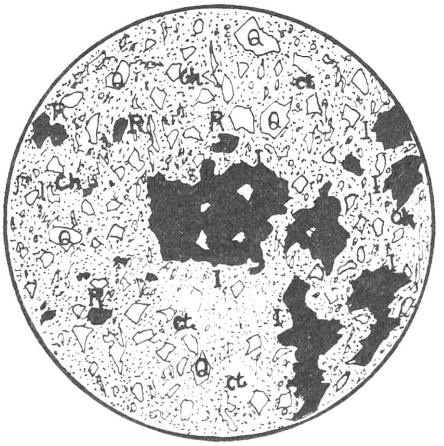

Fig. 17. Silty sandstone, very fine-grained, Miocene, Well TL-1 (503.8 m). Angular to subangular grains of quartz (Q), chert (Ct), and rock fragments (R) in argillaceous and sericitic matrix, with accessory iron ores (I) and feldspars, cemented by silica (quartz). Lower polarizing prism only. (X 60.)

Fig. 18. Limestone rich in Miogypsina, Miocene, Well TL-1 (500 m). Miogypsina sp., Mollusca fragments, and quartz (Q) grains are cemented by recrystallized calcite (Ca). Accessories are chert, feldspars, glauconite, and magnetite. Lower polarizing prism only. (X 60.)

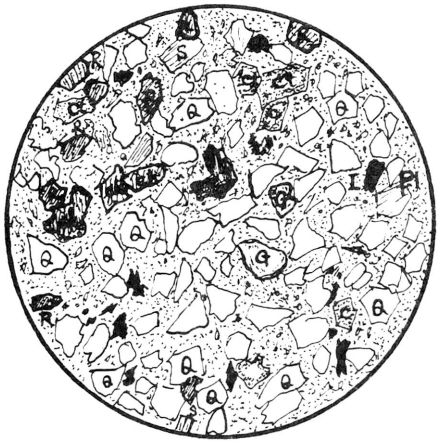

Fig. 19. Subgraywacke, very fine-grained, light gray, Miocene, Well TL-1 (403 – 407 m). Subangular to subrounded grains of quartz (Q) in argillaceous matrix, with accessory chert (Ct), rock fragments (R), sericite (S), glauconite (G), orthoclase, plagioclase (Pl), iron ores (I), and chlorite (Ch), cemented by carbonate. Low polarizing prism only. (X 60.)

Fig. 20. Hypersthene-augite dolerite, Pliocene and Peistocene, Well TL-1 (302-305 m). Augite (Au), hypersthene (Hy), and pigeonite occur both as groundmass minerals and as phenocrysts. These pyroxenes occupy an interstitial position to plagioclase (labradorite, La), which is lath-shaped and well twined. The chlorite (Ch) is abundant as a secondary mineral. Lower polarizing prism only. (X 60.)

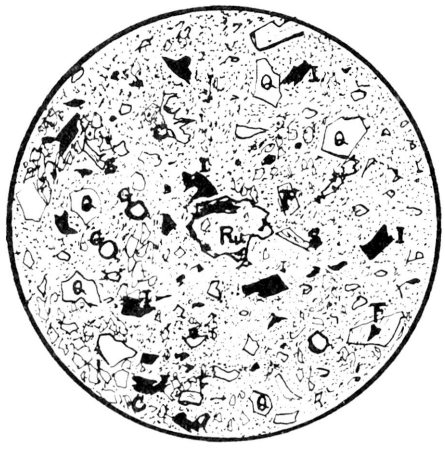

Fig. 21. Arenaceous shale or arenaceous mudstone, Pliocene and Pleistocene, Well TL-1 (202 – 207 m). Subangular, silt sized to very fine-grained quartz (Q) in argillaceous matrix, with accessory rock fragments, chert, sericite (S), iron ores (I), glauconite (G), feldspars (F), Rutile (Ru), and zircon, cemented by carbonaceous matters (C). Lower polarizing prism only. (X 60.)

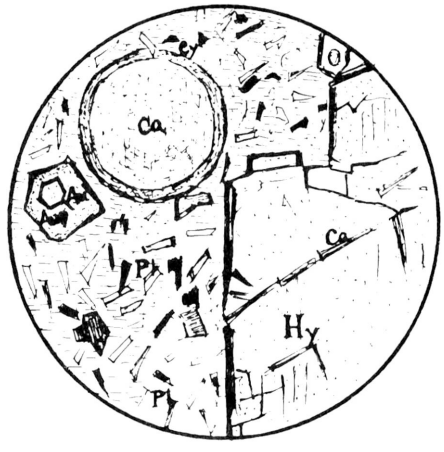

Fig. 22. Augite-bearing hypersthene basalt, Pliocene and Pleistocene, Well TL-1 (116 – 116.4 m). Large euhedral hypersthene (Hy) phenocrysts in a groundmass of tiny lath-shaped plagioclase (Pl), augite (Au), and glass. Vesicles are filled with calcite (Ca), zeolites, chalcedony (Cy), and quartz. These are cemented by carbonate. Accessories are augite (Au) and magnetite. Lower polarizing prism only. (X 60.)

STRATIGRAPHIC CORRELATION

Based on the writer's petrographic study and Huang's foraminiferal studies of the sediments in Well TLH1 (1967) and PK–3 (1968), as well as Lee's petrographic study of the Mesozoic and Cenozoic rocks in Well PC–1 (1962), a stratigraphic correlation is made between these two wells. Figure 2 shows the stratigraphic profile between Well TL–1 and Well PC–1.

The rocks below 503.5 m depth in Well TL–1, possibly of Mesozoic age, include arkose, subarkose, sandstone, siltsone and porphyrite or basaltic rock. Although no fossils have been found from these rocks, they are quite similar to the so-called Mesozoic rocks in Well PC–1. The formations below 503.5 m depth in Well TL–1 are considered to be Aptian because they are petrographically and stratigraphically well correlated to the so-called Mesozoic formations of Well PC–1 (Lee, 1962), which in turn correspond with the sediments containing Aptian ammonite and molluscan faunas (Huang, 1967; Lin, 1961; Matsumoto *et al.*, 1965) in Well PK–2 and PK–3. Huang (1968) found the Paleocene planktonic species, *Globigerina spiralis, Globigerina triloculinoides*, and *Globorotalia pseudobulloides*, in the cores of the arenaceous siltstone below 1963 m depth in Well PK–3. He pointed out that the Aptian ammonite and molluscan fauna associated with these Paleocene planktonic foraminifera may be attributed to reworking. Therefore, the sediments below 503.5 m depth in Well TL–1 may be Paleocene in age.

The Miocene limestone rich in *Miogypsina*, between 500 m and 503.5 m depth in Well TL–1, was not encountered in Well PC–1. Based on biostratigraphic considerations, this limestone may be correlated to the Molluscan Limestone in Well PK–3 (Huang, 1967).

Both the hypersthene-augite dolerite, between 302 m and 305 m depth, and the augite-bearing hypersthene basalt, between 116 m and 116.45 m depth, may belong to the Penghu basalts which were intruded and extruded during Plio-Pleistocene time (Lin, 1967; Lin *et al.*, 1948; Yen, 1950, 1953a, 1953b, 1954, 1956, 1957, and 1958).

CONCLUSIONS

The rocks below 503.5 m depth in Well TL–1 include hydrothermally altered arkose, subarkose, sandstone, siltstone and porphyrite or basaltic rock. Although no fossils have been found in these rocks, they are considered to be of Aptian age because they are petrographically and stratigraphically well correlated to the so-called Mesozoic formations in Well PC–1, which in turn correspond with the sediments containing an Aptian ammonite and molluscan fauna in the Peikang Wells PK–2 and PK–3.

The hydrothermally formed minerals present in the so-called Mesozoic rocks indicate that these rocks were hydrothermally altered, representing the later stage or farther facies of a contact metamorphism. The dolerite and basalt between 116 m and 305 m depth were probably intruded and extruded during the Plio-Pleistocene and belong to the Penghu basaltic stage.

The so-called Mesozoic formations in Well TL–1 are quite different lithologically from the Cenozoic formations. The Mesozoic rocks are relatively indurated, cherty, and hydrothermally altered. Their apparent specific gravities are higher than 2.5 and their effective porosities are lower than 7 per cent. On the contrary, the Cenozoic rocks are relatively friable, higher in effective porosity (>7 %), and entirely free from hydrothermal alteration.

The Cenozoic sand grains are more rounded than those of the Mesozoic. The average

sphericity of the Cenozoic sand grains is 0.75 and that of the Mesozoic ones is 0.73. In Well PC–1 the Tertiary sand grains are also more rounded than the Mesozoic ones. The average sphericity of the Tertiary sand grains is 0.80, and that of the Mesozoic ones is 0.75. The average sphericity of sand grains in Well PC–1 is higher than that of the sand grains in Well TL–1. This may indicate that the sediments in Well TL–1 are closer to the source area.

There is a distinct difference between the assemblages of small foraminifera in the tertiary sediments of the Penghu region and the Peikang region. The foraminiferal fauna in the Tertiary sediments of the Penghu regions is of shallower facies than that in the Peikang region.

ACKNOWLEDGMENTS

The writer is deeply grateful to Dr. T. P. Yen of the Geological Survey of Taiwan for his valuable guidance and critical reading of the manuscript. Thanks are also due to Mr. C. C. Liu, Mr. C. Chou, Miss C. H. Lo, and Miss C. H. Lee for their assistance in the laboratory.

REFERENCES

Huang, Tunyow. 1967. Foraminiferal study of the Tungliang Well TL–1 of the Penghu Islands: **Petroleum Geol. Taiwan**, no. 5, p. 131–149, 4 pls., 4 figs.

——, 1968. Some Paleocene planktonic foraminiferids from Well PK–3, Peikang, Yunlin, Taiwan: **(Unpublished report, CPC file)**.

——, and Lee, P. J., 1962.—Stratigraphy of the Kuanyin well, Taoyuan, and its relation to that of the Peikang well, Yunlin, Taiwan: **Petroleum Geol. Taiwan**, v. 1, p. 67–74, 1 fig., 2 tabs.

Huang, L. S., and Liu, S. P., 1967. Subsurface geological report on the Tungliang TL–1 stratigraphic test well, Penghu: **(Unpublished report, CPC file, in Chinese)**.

Lee, P. J., 1962. Mesozoic and Cenozoic rocks of the Paochung Well, Yunlin, Taiwan: **Petroleum Geol. Taiwan**, v. 1, p. 75–86, 6 figs., 2 tabs.

Lin, C. C., 1961. On the occurrence of Jurassic Ammonite newly found in Taiwan, China: **Acta Geol. Taiwanica**, no. 9, p. 79–81, 1 pl.

——, 1967. Geology of the islets around the Island of Taiwan (in Chinese): **Quart. Jour. Bank of Taiwan**, v. 18, no. 4, p. 229–256, 5 figs., 2 tabs.

Lin, C. C., **et al.**, 1948. Geology and mineral resources of the Penghu Islands (in Chinese): **Taiwan Mining Industry**, v. 9, nos. 3–4, p. 26–38.

Matsumoto, T., **et al.**, 1965. Some Molluscan fossils from buried Cretaceous of Western Taiwan: **Petroleum Geol. Taiwan**, no. 4, p. 1–24, 2 figs.

Moorhouse, W. W., 1959. The study of rocks in thin section: Harper & Brothers, New York, 493 p.

Pan, Y. S., 1967. The regional gravity of the Penghu Islands, Taiwan, China: **Petroleum Geol. Taiwan**, no. 5, p. 117–129, 6 figs.

Pettijohn, F. J., 1957. Sedimentary rocks: Harper and Brothers, New York, 718 p.

Wahlstrom, E. E., 1955. Petrographic Mineralogy: John Wiley & Sons, Inc., New York, Chapman & Hall, Ltd., London, 391 p.

Yen, T. P., 1950. Neogene and Quaternary basalt in Taiwan: **Quart. Jour. Taiwan Museum**, v. 3, p. 33–54.

——, 1953a. Hypersthene bearing pigeonite augite basalt from Tientaishan, Penghu: **Formosan Science**, v. 7, p. 31–34.

——, 1953b. On the occurrence of pigeonite in the Penghu basalts: **Ditto**, v. 7, p. 66–70.

——, 1954. Igneous activity in Taiwan: **Ditto**, v. 8, p. 97–98.

——, 1956. Neogene basaltic activity in western Taiwan and its stratigraphic significance: **Ditto**, v. 10, p. 23–26.

——, 1957. The occurrence of tholeiitic basalt in the eastern Asiatic Cenozoic alkaline province: **Ditto**, v. 11, p. 1–6.

——, 1958. Cenozoic volcanic activity in Taiwan: **Taiwan Mining Industry**, v. 10, nos. 1–2, p. 1–39, 6 figs., 11 tabs.

Blank page

Page blanche

OUTLINE OF EXPLORATION FOR OFFSHORE EXTENSIONS OF COAL FIELDS IN JAPAN

By
Shigemoto Tokunaga, Geological Survey of Japan
(with one figure and five tables)
(Submitted as document I&NR/R.96 at fifth session of CCOP)

Geologic Features of Offshore Coal Fields

The coal fields of Japan are scattered from Hokkaido in the north to Kyushu in the south and the geologic age of these fields ranges from Triassic to late Tertiary. Anthracite, bituminous coal and lignite are produced and also coking coal and non-coking coal are mined. The geological ages of the main coal-bearing formations in Japan are listed in table 1; from this it is seen that the more important coal fields are of older Tertiary age.

The economically important coal fields in Japan are Ishikari, Kushiro, Joban, Ube, Omine, Chikuho, Fukuoka, Miike, Sasebo, Sakito-Matsushima and Amakusa. Most of the important coal fields, except Ishikari and Omine, are situated near the coast and the coal-bearing strata extend from the land into some offshore areas.

Table 1. Geologic age of Japanese coal fields.

Geologic age	Name of coal field	Name of prefecture
Miocene	Gifu-Aichi (Lignite)	Gifu & Aichi pref., Honshu
	Sendai (Lignite)	Miyagi, Honshu
	Mogami	Yamagata, Honshu
	Tempoku	Hokkaido
	Sasebo[1)]	Nagasaki, Kyushu
Oligocene	Kushiro[1)]	Hokkaido
	Joban[1)]	Fukushima, Honshu
	Fukuoka	Fukuoka, Kyushu
	Chikuho	Fukuoka, Kyushu
	Kokura[1)]	Fukuoka, Kyushu
	Karatsu	Saga, Kyushu
	Sakito-Matsushima[1)]	Nagasaki, Kyushu
Eocene	Ishikari	Hokkaido
	Ube[1)]	Yamaguchi, Honshu
	Miike[1)]	Kumamoto, Kyushu
	Takashima[1)]	Nagasaki, Kyushu
	Amakusa[1)]	Kumamoto, Kyushu
Triassic	Omine	Yamaguchi, Honshu

1) Offshore field or field developed on land with extension into adjoining offshore area.

The Paleozoic formations in Japan are mainly composed of marine sediments; however, the rarer terrestrial deposits in some places include thin coal seams, but they are not important economically. In the Triassic formations some lacustrine deposits occur in tectonic zones of southwest Japan. The coal-bearing formations in the Omine and Nariwa coal fields show the same depositional conditions and the typical Triassic flora, which is well represented in Japan, is found in the roof of coal seams. The anthracite from the Omine region was produced by intense folding and volcanic activities which took place after the Triassic period. Coal seams of Mesozoic age also occur in Jurassic and Cretaceous marine sedimentary rocks in very restricted areas.

The boundary between Cretaceous and Tertiary offers very important and interesting geologic problems in Japan. Paleocene sedimentary rocks have not yet been found in Japan, but the possibility of the presence of Paleocene formations is inferred from studies of foraminifera and other fossils in the eastern part of the Kushiro coal field and the "Akazaki Formation" in coal fields of western Kyushu.

The Paleogene coal fields are situated mainly in the middle and eastern parts of Hokkaido, along the Pacific coast of Honshu and in northwestern Kyushu. The exploitation of the offshore extensions of these coal fields is carried out both from land and from islands. In the Kushiro, Miike, Ube, and Amakusa coal fields, vertical or oblique shafts are sunk on land, and in the Sakito-Matsushima and Takashima coal fields, they are sunk on islands. The distribution of these offshore workings is shown in figure 1.

Procedures for exploration of offshore coal fields in Japan

The first step in exploration for offshore coal fields in Japan is to look for outcrops of coal seams in the coastal regions and to extend the galleries from fields being exploited on land to follow the coal seams and determine their extent in the adjoining offshore area.

Most of the important coal fields in Japan are located near the coastal areas, as previously mentioned; consequently, both the geologic and geophysical surveys are effective for the exploration of offshore areas.

The procedures for exploration differ somewhat depending on the geophysical features of the sediments and the structures in which the coal seams are present in the areas concerned. Generally, the first steps to be taken would include (a) geologic survey in the coastal area; (b) geologic and topographic surveys of the sea bottom by divers; and (c) dredging in the offshore area. The second stage would include (a) detailed geologic surveys and (b) geophysical surveys by the magnetic method, gravity method, seismic method (reflection and refraction) and sonic method (sparker, echo sounder, gas exploder). The results of these surveys would then be followed up by drilling and well logging; these would include drilling from floating barges or drilling vessels, electric and radioctivity logging, thermal measurements and well shooting.

The seismic survey is carried out in cases where the strata are gently dipping or folding is rather gentle, and sonic survey is effective where the basement rocks under the sea bottom are composed of granite or hard Paleozoic rocks. The floating barge is used frequently in shallow water, as in the Ariake area, while drilling vessels are used in deeper waters as, for example, in the Takashima coal field area.

A drilling vessel was first used in the area offshore from Kushiro City, Hokkaido, and wells were drilled down to as much as 860 m below the sea bottom. At Kushiro, geologic survey of the sea bottom was carried out by divers using the aqua-lung; this was found to be very effective for finding faults and sand dykes. The iron-pipe type of drilling was also

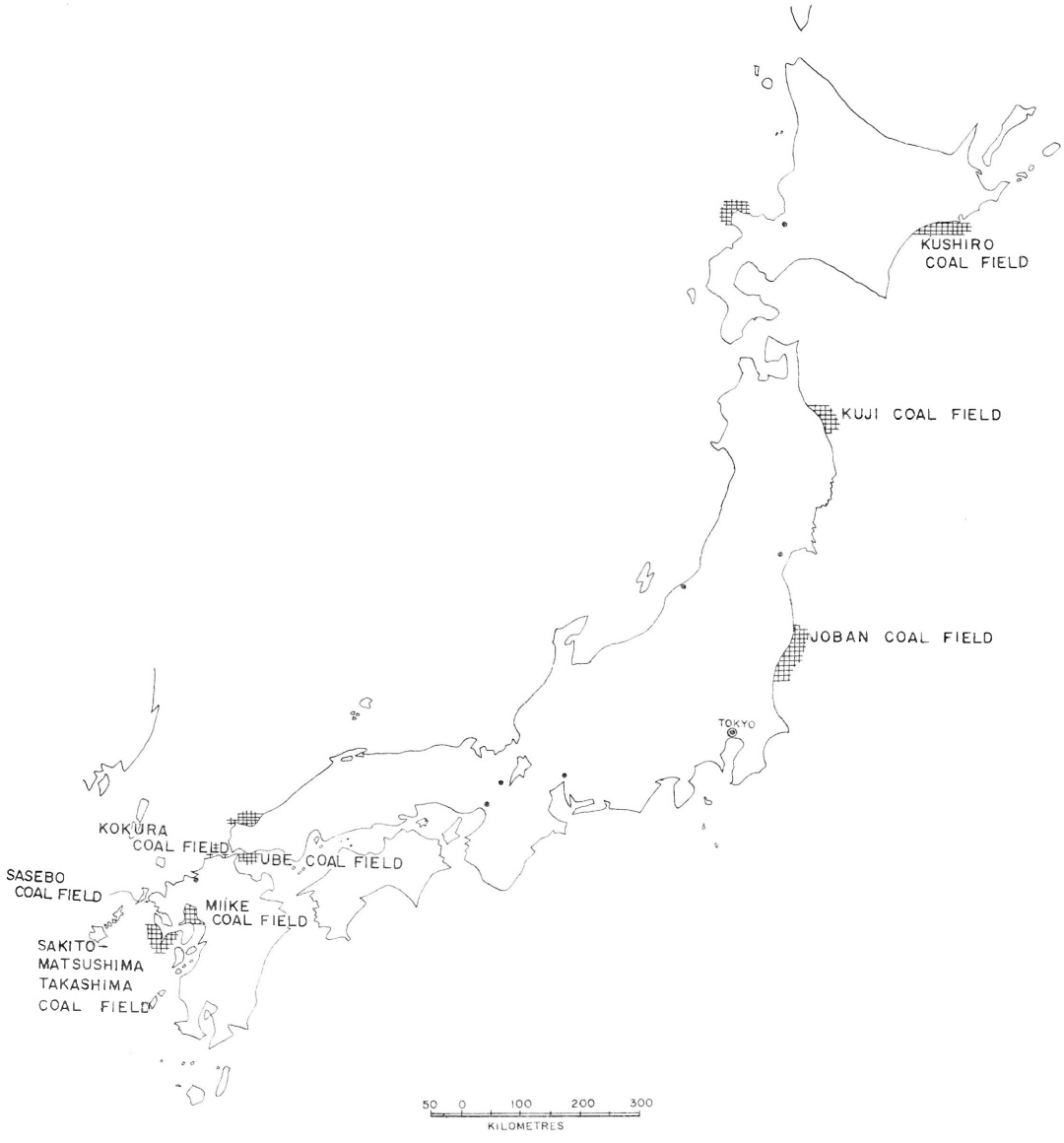

Figure 1. Offshore coal fields in Japan.

Table 2. Procedures of exploration in offshore coal fields.
(Source: Resources Council, Science and Technology Agency, 1966, Geological Survey of Japan 1968; compiled by Coal Section, Geological Survey of Japan).

Coal mine	1959	1960	1961	1962	1963	1964	1965	1966	1967
Taiheiyo (Kushiro)	SD SS		SS	D	D	D DV	DV	DF	DV
Ube (Ube)	SA DF	SA DF	RL GC DF	SA DF RL GC	SS RL DF				
Ariake (Miike)	DF	SA DF	SA DF	DF	DF				
Miike (Miike)	DF	SR	DF SE SA SS	DF	DF	DF	DF SS	DF SS WS	DF SS WS
Tobishima (Sasebo)	SS								
Takeshita (Sasebo)			D	D	D				
Fukishima (Sasebo)		DV							
Sakito (Sakito-)	SE SF					SS			
(Matsushima)	SD	SS				DL MS			
Oshima (Sakito-)	WS MS	SE SS					SS	DL WS	
(Matsushima)			SR						
Ikeshima (Sakito-)	MS SD	SS SR						SA	
(Matsushima)									
Iojima (Takashima)		SS GS MS		DF					
Futago (Takashima)	SD	SD SA	SD			DL	SS		
Hashima		SE SS							
Shiki (Amakusa)		SS			DF SS				
Horinosako (Amakusa)			SS						
Takenosako (Amakusa)			SS SR		SS SR				

Abbreviation: SD, survey by diver; D, dredging; SS, sonic survey by sparker; SR, sonic survey by "Rass"; GC, geochemical survey; RL, radioactive well logging; MS, magnetic survey; GS, gravity survey; SE, seismic reflection survey; SA, seismic refraction survey; DF, drilling from floating barge; DV, drilling vessel DL, drilling on land; WS, well shooting.

done after these surveys and much useful information was obtained.

At the Ube coal field, the velocity of seismic waves of strata underlying the sea bottom was obtained by geophysical prospecting, and fractured or fault zones in the offshore area were located and mapped. Up to the present, drilling has been carried out at 200 locations on the north side of the fractured zone, 35 in the zone itself and 30 on the south side of the zone. Radioactive well logging carried out in this field, was the first application of this technique in coal exploration and it proved to be useful for correlation of strata in this area.

In the Ariake district of the Miike coal field, more than 10 seismic surveys were made and about 100 holes were drilled over the field; in the main part of the field, the presence of the Paleogene coal bearing formation was determined by drilling from a floating barge and the seismic wave velocity of each stratum was clarified by reflection and refraction methods.

The magnetic method is most effective where volcanic rocks crop out on the sea bottom, as was proved in the Sakiio and Matsushima coal fields.

Some examples of procedures in offshore areas are shown in table 2.

In the past few years, some geophysical prospecting and drilling has been done in an offshore area of northwest Kyushu under the sponsorship of the Japanese Government. One well was drilled to a depth of 1,500 metres at Kanise, north of Oshima Island, in 1966 and the first offshore well was drilled in the northern part of the Takashima coal field to a depth of about 750 m below the sea bottom. In 1968, a few wells will be drilled at the northern part of Futago-shima.

Present status of offshore coal fields

Exploitation of coal in offshore areas of Japan began in 1860 at the Takashima coal field and, at the present time, twenty-two mines are being worked in offshore areas: one at Kushiro; two at Ube; one at Miike; five at Sasebo; three at Sakito-Matsushima; three at Takashima; and seven at Amakusa. The coal output from offshore areas was almost ten million tons in 1963; this amounts to 20.6 per cent of the total output of coal in Japan, as shown in table 3.

Table 3. Coal reserves and output in offshore coal fields.
(Source: Resources Council, Science and Technology Agency, 1966; compiled by Coal Section, Geological Survey of Japan).

Name of coal field	Coal reserves in offshore coal fields (1000 t)	Output from offshore coal fields (1000 t/year)	Remarks
Kushiro	308,197	1,498	Bituminous coal
Ube	409,333	934	Bituminous coal
Ariake	406,806	0	
Miike	946,176	3,425	Bituminous & coking coal
Sasebo	130,740	716	Bituminous & coking coal
Sakito-Matsushima	643,561	1,575	Bituminous & coking coal
Takashima	330,325	1,615	Bituminous & coking coal
Amakusa	57,662	228	Anthracite coal
Total	3,232,800 (in 1967)	9,991 (in 1963)	
Total in all coal fields of Japan	20,245,786 (in 1955)	51,098 (in 1963)	

The deepest working area lies 700 m below sea-level at the Hashima mine, in the Takashima coal field area; in other coal mines, the galleries in offshore areas lie at depths of 200 to 500 m. The distances between the working areas and the shore-lines became progressively greater and the level gallery at Ube, although closed recently, had been extended as far as seven thousand metres from the shore.

The greatest water depth above the offshore extension of Takashima coal field is more than fifty metres at the working area. In the Ube coal field area, however, the water depth is only fifteen metres at the working area, although it is farther away from the shore-line, while

at the Miike coal field, the area above the offshore workings is above water at low tide. The water depths and distances from the shore-lines are shown in table 5. The reserves of coal in offshore areas are estimated to be about three thousand million tons and they constitute 21.3 per cent of the total reserves of coal in Japan.

Table 4. Workable coal seams in offshore coal fields.

Name of coal field	Name of coal mine	Coal bearing formation	Coal seam	Thickness of coal seam (m)	Thickness of coal seam including partings (m)
Kushiro	Taiheiyo	Harutori	Main seam	2.70	2.76
Ube	Ube	Okinoyama	Itsudan	1.30	1.50
Miike	Miike	Inari	Main seam	3.03	3.37
Sakito-Matsushima	Sakito	Sakito	15 Shaku	3.10	3.76
	Oshima	Sakito	Main seam	2.75	4.71
Takashima	Iojima	Hashima	10 Shaku	3.60	3.60
	Futago	Hashima	18 Shaku	4.00	4.20
	Hashima	Hashima	1 Jyo	2.70	2.70
Amakusa	Shiki	Toishi	4 Shaku	1.07	1.20
	Uonuki	Toishi	5 Shaku	1.50	1.50

Table 5. Depth and distance from shore of working areas in offshore coal fields. (Source: Resources Council, Science and Technology Agency; compiled by Coal Section, Geological Survey of Japan).

Name of coal mine and coal pit	Depth of working area below sea level (m)	Depth of water at working area (m)	Distance from shore at working area (m)	Distance from shore at deepest working face (m)
Taiheiyo (Kushiro C.F.)	−200—−493	30	1,200—3,300	4,200
Ube (Ube C.F.)	− 95—−360	15	750—7,000	7,000
Ariake (Miike C.F.)	—	10	—	—
Miike (Miike C.F.)	−100—−700	0—10	2,800—5,600	5,600
Sakito (Sakito Matsushima C.F.)	−124—−130	33	100— 900	1,600
Oshima (Sakito-Matsushima C.F.)	−584—−590	10—15	100— 250	900
Ikeshima (Sakito-Matsushima C.F.)	−290—−390	30—65	250—1,300	1,500
Futagoshima (Takashima C.F.)	−290—−900	30—80	2,500—3,500	4,200
Hashima (Takashima C.F.)	−880—−940	45—55	650— 700	2,130
Shiki (Amakusa C.F.)	−180—−250	0—41	0— 100	200

昭和 44 年 4 月 30 日 印刷

昭和 44 年 5 月 5 日 発行

工業技術院地質調査所

印刷者 小 宮 山 一 雄

印刷所 小宮山印刷工業株式会社

Annexed 2 Plates
to
Regional gravity survey of
Luzon Island, Philippines
By
Bureau of Mines, Department of Agriculture
and Natural Resources, the Philippines

.....

Annexed 1 Plate
to
Distribution pattern of sediments
on the continental shelves of western Indonesia
By
K. O. Emery
Woods Hole Oceanographic Institution